ΕΘΝΙΚΟ ΜΕΤΣΟΒΙΟ ΠΟΛΥΤΕΧΝΕΙΟ

Σχολή Μηχανολόγων Μηχανικών
Τομέας Μηχανολογικών Κατασκευών &
Αυτομάτου Ελέγχου
Εργαστήριο Αυτομάτου Ελέγχου

Διπλωματική Εργασία

Βέλτιστη Επιλογή Σημείων Κράτησης για Συνεργατικά Υποθαλάσσια Οχήματα με Βραχίονα

Σπυρίδων Γ. Τάραντος

Επιβλέπων καθηγητής: Κωνσταντίνος Ι. Κυριακόπουλος

Αθήνα, Ελλάδα, Οκτώβριος 2017

National Technical University of Athens
School of Mechanical Engineering
Section of Mechanical Design & Automatic Control
Control Systems Lab

Diploma Thesis

Optimal Grasp Points Selection for Cooperative Underwater Vehicle - Manipulator Systems

Spyridon G. Tarantos

Supervisor: Prof. Kostas J. Kyriakopoylos

Athens, Greece, October 2017

Optimal Grasp Points Selection for Cooperative Underwater Vehicle - Manipulator Systems

Spyridon G. Tarantos

Athens, October 2017

Ελληνική Περίληψη

Στην ενότητα αυτή παρατίθεται μια εκτεταμένη περίληψη της διπλωματικής στην ελληνική γλώσσα. Η συγκεκριμένη διπλωματική εργασία περιέχει πληθώρα εξειδικευμένης ορολογίας η οποία δεν τυγχάνει επιτυχημένης μετάφρασης στην ελληνική γλώσσα, γεγονός το οποίο ενδεχομένως να παραπλανήσει και να κουράσει τον αναγνώστη. Για το λόγο αυτό κρίθηκε ότι η συγγραφή του κυρίως κειμένου στην αγγλική γλώσσα θα ευνοήσει την απόδοση του περιεχομένου και θα αποτρέψει πιθανή παρανόηση των όρων από τον αναγνώστη.

Εισαγωγή Η ρομποτική αποτελεί ένα αντικείμενο μελέτης με μεγάλο ενδιαφέρον, καθώς χρησιμοποιείται όχι μόνο σε εξεζητημένες εφαρμογές, αλλά και στη καθημερινή ζωή. Γενικά, θα μπορούσαμε να περιγράψουμε τη ρομποτική ως τη μελέτη μηχανών που μπορούν να αντικαταστήσουν τους ανθρώπους στην εκτέλεση μιας διαδικασίας, όσον αφορά τόσο τη σωματική εργασία όσο και τη λήψη των αποφάσεων.

Γενικά, υπάρχουν πολλά είδη ρομπότ ανάλογα με την αποστολή που πρέπει να φέρουν σε πέρας. Σε περίπτωση που για την αποστολή απαιτείται ευκινησία και επιδεξιότητα χρησιμοποιούνται κινητά ρομπότ με βραχίονα (mobile manipulator systems) τα οποία αποτελούνται από μια κινητή βάση και έναν ή περισσότερους βραχίονες. Ανάλογα με τον τύπο της κινητής βάσης μπορούμε να κατηγοριοποιήσουμε τα mobile manipulator systems σε εδάφους, αέρος και υποβρύχια. Στα πλαίσια αυτής της διπλωματικής θα ασχοληθούμε με τα υποβρύχια.

Η ανάγκη για χρήση υποβρύχιων ρομπότ έγκειται στο γεγονός ότι ο άνθρωπος δεν μπορεί να πλησιάσει αφιλόξενες περιοχές όπως είναι τα βάθη της θάλασσας, αλλά ακόμα και στη περίπτωση που είναι σε θέση να το κάνει δεν θα μπορούσε να φέρει σε πέρας χρονοβόρες εργασίες εκεί. Γενικά, τα υποβρύχια ρομπότ χρησιμοποιούνται σε πληθώρα εφαρμογών. Στα πλαίσια της συγκεκριμένης διπλωματικής θα εξεταστεί η χρήση τους σε μια εφαρμογή συλλογής και εναπόθεσης κατά την οποία τα ρομπότ πιάνουν ένα αντικείμενο το μεταφέρουν και το τοποθετούν σε μια τελική θέση. Τα υποβρύχια ρομπότ με τα οποία θα ασχοληθούμε ονομάζονται υποθαλάσσια οχήματα με βραχίονα (Underwater Vehicle – Manipulator Systems, UVMS).

Σημειώνεται ότι πολύ συχνά ένα ρομπότ δεν είναι ικανό να εκτελέσει μια εργασία μόνο του. Σε αυτές τις περιπτώσεις απαιτείται συνεργασία περισσοτέρων. Με τον τρόπο αυτό στην περίπτωση της μεταφοράς ενός αντικειμένου, η οποία είναι η εφαρμογή που μας ενδιαφέρει, η συνεργασία των ρομπότ οδηγεί στην αύξηση του μεγέθους και του βάρους του μεταφερόμενου αντικειμένου, καθώς και σε διευκόλυνση της εκτέλεσης απαιτητικών ελιγμών.

Διατύπωση του Προβλήματος – Προσέγγιση της Λύσης Το πρόβλημα με το οποίο ασχολείται αυτή η διπλωματική είναι η συνεργασία υποθαλάσσιων οχημάτων με βραχίονα για μια εφαρμογή συλλογής και εναπόθεσης ενός αντικειμένου, κατά την οποία τα ρομπότ πρέπει να πλησιάσουν ένα αντικείμενο να το πιάσουν και να το μεταφέρουν από μία αρχική τοποθεσία σε μια τελική. Πιο συγκεκριμένα ασχολείται με το στάδιο της προσέγγισης του αντικειμένου από τα ρομπότ και ειδικότερα με την λήψη της απόφασης για το σε ποιά σημεία του αντικειμένου θα πρέπει να πιάσουν οι ακροδέκτες των βραχιόνων των ρομπότ. Η απόφαση αυτή είναι μείζονος σημασίας, καθώς κατάλληλη επιλογή σημείων κράτησης μπορεί να οδηγήσει σε καλύτερη απόδοση του συνεργατικού συστήματος (ρομπότ και αντικείμενο) με μικρότερη κατανάλωση ενέργειας και άρα μεγαλύτερη αυτονομία, ενώ αντίθετα, λανθασμένη επιλογή τέτοιων σημείων μπορεί να οδηγήσει σε αδυναμία του συστήματος να εκτελέσει τις απαιτούμενες ενέργειες, ενδεχόμενη καταστροφή του εξοπλισμού και γενικά αποτυχία της όλης επιχείρησης.

Γενικά, για την επιλογή σημείων κράτησης χρησιμοποιούνται κατάλληλα μέτρα (grasp quality measures). Αυτά είναι δύο ειδών: μέτρα στα οποία λαμβάνεται υπόψη η εκτελούμενη διεργασία και μέτρα ανεξάρτητα με αυτή. Στην εφαρμογή που μελετάμε ενδέχεται να μην μπορούμε να προβλέψουμε τις επιμέρους ενέργειες που θα πρέπει να εκτελέσουν τα ρομπότ. Κατά συνέπεια η χρήση μέτρων που λαμβάνουν υπόψη τις ενέργειες αυτές θα ήταν ανούσια. Έτσι, προτείνεται η χρήση μέτρων που δεν θα λαμβάνουν υπόψη τις επιμέρους ενέργειες που θα πρέπει να εκτελέσουν τα ρομπότ αλλά που εξασφαλίζουν ότι όποια και αν είναι η ενέργεια που θα προκύψει να εκτελέσουν, τα σημεία κράτησης θα πρέπει να επιτρέπουν στο σύστημα να την εκτελέσει με τη μικρότερη δυνατή κατανάλωση ενέργειας.

Στα πλαίσια αυτής της διπλωματικής προτείνονται δύο τέτοια μέτρα, τα οποία εξάγονται από την ανάλυση του ελλειψοειδούς δυναμικής δυνατότητας χειρισμού (Dynamic Manipulability Ellipsoid) του συστήματος. Το πρώτο μέτρο στοχεύει στη μεγιστοποίηση του όγκου του ελλειψοειδούς εξασφαλίζοντας παράλληλα ένα κάτω όριο στην μικρότερη απόδοση του συστήματος, όσον αφορά την προκαλούμενη επιτάχυνση στο αντικείμενο. Το δεύτερο μέτρο είναι η μικρότερη απόσταση στο χώρο των μεταφορικών και περιστροφικών επιταχύνσεων, όπως προκύπτουν από την αποσύνθεση του ελλειψοειδούς.

Μοντελοποίηση του Συνεργατικού συστήματος Προκειμένου να δημιουργήσουμε το ελλειψοειδές δυναμικής δυνατότητας χειρισμού του συστήματος, απαραίτητη είναι η μοντελοποίηση του συνεργατικού συστήματος ρομπότ – αντικειμένου. Αρχικά, ορίζεται η κινηματική του υποβρυχίου ρομπότ, η οποία προκύπτει από την κινηματική της βάσης (υποβρύχιου οχήματος) σε συνδυασμό με τη κινηματική του βραχίονα. Στη συνέχεια, ορίζονται οι εξισώσεις κίνησης του ρομπότ όταν αυτό βρίσκεται σε αλληλεπίδραση με το περιβάλλον του, καθώς στη περίπτωσή μας ασκεί δύναμη και ροπή στο αντικείμενο.

Επόμενο βήμα είναι η μοντελοποίηση του αντικειμένου το οποίο τα ρομπότ θα μεταφέρουν. Για το λόγο αυτό ορίζεται η δυναμική του αντικειμένου όταν αυτό κινείται σε ρευστό.

Συνδυάζοντας τις εξισώσεις κίνησης των M ρομπότ και του αντικειμένου προκύπτουν οι εξισώσεις κίνησης του συνεργατικού συστήματος, δηλαδή των M ρομπότ που συγκρατούν το αντικείμενο και του αντικειμένου.

Με κατάλληλες πράξεις μπορούμε να φέρουμε τις εξισώσεις αυτές σε μορφή κατά την οποία να συνδέεται η είσοδος ελέγχου στους κινητήρες των ρομπότ με την προκαλούμενη επιτάχυνση στο αντικείμενο. Έχουμε, λοιπόν, τη συσχέτιση των εισόδων ελέγχου των κινητήρων με την επιτάχυνση στο κέντρο βάρους του αντικειμένου. Η συσχέτιση αυτή θα χρησιμοποιηθεί για τη κατασκευή του dynamic manipulability ellipsoid του συστήματος.

Επιλογή Βέλτιστων Σημείων Κράτησης Όπως αναφέρθηκε προηγουμένως, η επιλογή των βέλτιστων σημείων κράτησης μπορεί να βοηθήσει στο να εκμεταλλευτούμε στο έπακρο τις δυνατότητες που παρέχει η συνεργασία των ρομπότ, όσον αφορά τη διαχείριση του αντικειμένου. Για την επιλογή των σημείων αυτών είναι απαραίτητο να υιοθετηθεί μία ποσότητα η οποία θα αντανακλά τις ανάγκες του συστήματος και το γενικό στόχο τον οποίο θέλουμε να επιτύχουμε. Χρησιμοποιώντας τη ποσότητα αυτή μπορούμε να αξιολογήσουμε τα υποψήφια σετ των σημείων κράτησης και να επιλέξουμε το βέλτιστο. Οι ποσότητες αυτές είναι τα μέτρα για την επιλογή των σημείων κράτησης (grasp quality measures).

Με βάση τη βιβλιογραφία, για την επιλογή σημείων κράτησης χρησιμοποιούνται συνήθως μέτρα που λαμβάνουν υπόψη τις εργασίες που θα ακολουθήσουν. Αυτή η πρακτική είναι επιθυμητή και προτείνεται στις περιπτώσεις που γνωρίζουμε τις εργασίες που πρέπει να εκτελέσουν τα ρομπότ. Υπάρχουν όμως περιπτώσεις που δεν μπορούμε να γνωρίζουμε εκ των προτέρων την ακριβή πορεία που πρέπει να ακολουθήσουν τα ρομπότ και κατά συνέπεια τις επιμέρους εργασίες που πρέπει να εκτελέσουν. Ειδικά στην περίπτωση που το περιβάλλον είναι αδόμητο, η πορεία πρέπει να ορίζεται από τα ίδια τα ρομπότ κατά τη διάρκεια της επιχείρησης, με τις πληροφορίες που λαμβάνουν από τους αισθητήρες τους. Ακόμα και στην περίπτωση που το περιβάλλον είναι απολύτως γνωστό, το σύστημα ενδέχεται να βρεθεί αντιμέτωπο με απροσδόκητες καταστάσεις, όπως κινούμενα εμπόδια, των οποίων η πορεία δεν θα μπορούσε να προβλεφθεί εκ των προτέρων. Σε τέτοιες περιπτώσεις, οι επιμέρους ενέργειες που θα πρέπει να εκτελέσουν τα ρομπότ θα πρέπει να ορίζονται κατά τη διάρκεια της επιχείρησης. Για την αντιμετώπιση αυτού του προβλήματος θα μπορούσε να γίνει αλλαγή των σημείων κράτησης κατά τη διάρκεια της επιχείρησης. Έτσι όταν θα προέκυπτε κάποια κατάσταση που δεν είχε προβλεφθεί εκ των προτέρων τα ρομπότ θα έπρεπε να ξαναπιάσουν το αντικείμενο σε νέα σημεία για να ικανοποιήσουν τις νέες ανάγκες του συστήματος. Παρ' όλα αυτά, η συγκεκριμένη λύση δεν είναι προτιμητέα, καθώς απαιτεί πολύ χρόνο και πολλούς ελιγμούς από τα ίδια τα ρομπότ, τα οποία καθ' όλη τη διάρκεια αυτή καταναλώνουν ενέργεια η οποία, δεδομένου ότι είναι αυτόνομα, είναι περιορισμένη.

Για τους παραπάνω λόγους, θα χρησιμοποιηθούν μέτρα που δε σχετίζονται με τις επιμέρους ενέργειες που θα εκτελέσουν τα ρομπότ, αλλά επιτρέπουν την εκτέλεση οποιασδήποτε ενέργειας και αν απαιτηθεί με την κατανάλωση της ελάχιστης δυνατής ενέργειας.

Στην πλαίσια της εργασίας αυτής, ως ενέργεια του συστήματος θα εννοείται η πρόκληση επιτάχυνσης στο κέντρο βάρους του μεταφερόμενου αντικειμένου, ενώ ως απόδοση του συστήματος θα νοείται η ικανότητα του συστήματος να επιταχύνει το αντικείμενο σε μια δεδομένη κατεύθυνση για δεδομένη προσδιδόμενη ποσότητα ενέργειας. Όπως αναφέρθηκε προηγουμένως, τα προτεινόμενα μέτρα προέρχονται από την ανάλυση του dynamic manipulability ellipsoid (DME) του συστήματος. Το DME παρέχει μία συσχέτιση μεταξύ του χώρου που αντιστοιχεί στη καταναλισκόμενη ενέργεια, ο οποίος στη περίπτωσή μας είναι ο χώρος των εισόδων ελέγχου, με το χώρο των προκαλούμενων επιταχύνσεων στο αντικείμενο. Για τον υπολογισμό του DME θεωρούμε ότι το διάνυσμα των εισόδων ελέγχου κείτεται σε μία μοναδιαία σφαίρα. Χρησιμοποιώντας τις εξισώσεις κίνησης του συνεργατικού συστήματος προκύπτει η εξίσωση του ελλειψοειδούς.

Προτεινόμενα Μέτρα Δεδομένου ότι μεγιστοποιώντας το μέγεθος του DME, μεγιστοποιείται και η επιτάχυνση που θα μπορούσε να επιτύχει το σύστημα δυνητικά, για πεπερασμένη ποσότητα καταναλισκόμενης ενέργειας, τα προτεινόμενα μέτρα στοχεύουν στη μεγιστοποίηση του μεγέθους του ελλειψοειδούς με διαφορετικό, όμως, τρόπο το καθένα.

Το πρώτο προτεινόμενο μέτρο στοχεύει στη μεγιστοποίηση του όγκου το DME θέτοντας παράλληλα ένα κάτω όριο στην ελάχιστη απόδοση του συστήματος, όσον αφορά την προκαλούμενη επιτάχυνση. Γενικά, με τη μέθοδο αυτή δε διαχωρίζεται η «καθαρή» επιτάχυνση του συστήματος, από αυτή που προκαλείται από το ίδιο βάρος του. Επίσης, ο τρόπος με τον οποίο μεγιστοποιείται ο όγκος είναι αυθαίρετος, δηλαδή δεν μπορούμε να επέμβουμε στις διευθύνσεις στις οποίες θα μεγεθυνθεί το ελλειψοειδές. Για το λόγο αυτό ενδέχεται ο κίνδυνος να επιλεγούν σημεία που ναι μεν εξασφαλίζουν τη μεγιστοποίηση του όγκου του ελλειψοειδούς, αλλά το σύστημα να μην είναι σε θέση να σηκώσει το βάρος του ή ακόμα και αν το σηκώσει να μην μπορεί να επιταχυνθεί σε ορισμένες κατευθύνεις εξαιτίας αυτού. Για να αποφευχθεί ο παραπάνω κίνδυνος προτείνεται το συγκεκριμένο μέτρο να συνοδεύεται από ένα περιορισμό, που λαμβάνοντας υπόψη την επίδραση του βάρους να ορίζει ένα κάτω όριο στην επίδοση του συστήματος.

Το προηγούμενο μέτρο δεν λαμβάνει υπόψη τη διαφορετική τάξη μεγέθους των δύο επιταχύνσεων, της μεταφορικής και της περιστροφικής, με αποτέλεσμα η λύση να επηρεάζεται κυρίως από την επιτάχυνση με τη μεγαλύτερη. Με αφορμή την παραπάνω παρατήρηση, προτείνεται το δεύτερο μέτρο το οποίο στοχεύει στη μεγιστοποίηση των ελαχίστων αποστάσεων στο χώρο των μεταφορικών και περιστροφικών επιταχύνσεων, όπως προκύπτουν από την αποσύνθεση του DME. Το DME μετατοπίζεται έτσι ώστε να λαμβάνεται υπόψη η επίδραση του βάρους του συστήματος, με αποτέλεσμα ο χώρος των επιταχύνσεων να περιλαμβάνει μόνο τη «καθαρή» επιτάχυνση που προκαλείται στο κέντρο βάρους του αντικειμένου. Στη συνέχεια, για κάθε κατεύθυνση της μεταφορικής και της περιστροφικής επιτάχυνσης μετράται η απόσταση του ορίου του ελλειψοειδούς από το κέντρο του. Η απόσταση αυτή αποτελεί το μέτρο της επιτάχυνσης στη κατεύθυνση αυτή. Με επανάληψη αυτής της διαδικασίας σε κάθε κατεύθυνση δημιουργούνται οι χώροι των περιστροφικών και μεταφορικών επιταχύνσεων. Με τον τρόπο αυτό μπορεί να υπολογιστεί η μικρότερη απόσταση από το κέντρο μέχρι το όριο του χώρου για τον κάθε χώρο επιτάχυνσης. Το σταθμισμένο άθροισμα των δύο αυτών αποστάσεων αποτελεί το προτεινόμενο μέτρο.

Σχήματα Βελτιστοποίησης Για την επιλογή των σημείων κράτησης απαραίτητη είναι η χρήση ενός σχήματος βελτιστοποίησης. Δεδομένου ότι το DME του συστήματος δεν επηρεάζεται μόνο από τη θέση του σημείου κράτησης αλλά και διαμόρφωση του ρομπότ, δηλαδή τη θέση του και τη θέση των αρθρώσεων του βραχίονα, σαν μεταβλητές απόφασης θα χρησιμοποιηθούν οι θέσεις των σημείων κράτησης και οι μεταβλητές που ορίζουν τη διαμόρφωση των ρομπότ.

Ως αντικειμενική συνάρτηση θα χρησιμοποιηθούν τα προτεινόμενα μέτρα τα οποία θέλουμε να μεγιστοποιηθούν. Ως περιορισμοί ορίζονται τα όρια των μεταβλητών που ορίζουν τη διαμόρφωση των ρομπότ, η συνθήκη κατά την οποία η θέση του i-οστου σημείου κράτησης θα πρέπει να ταυτίζεται με τη θέση του ακροδέκτη του i-οστού ρομπότ, η συνθήκη κατά την οποία ο προσανατολισμός του ακροδέκτη του i-οστού ρομπότ θα πρέπει να ταυτίζεται με τον επιτρεπόμενο προσανατολισμό στο i-οστό σημείο κράτησης, όπως επιβάλλεται από τη γεωμετρία του αντικειμένου και τέλος ένας περιορισμός που εξασφαλίζει ότι τα σημεία κράτησης έχουν επιλεγεί έτσι ώστε τα ρομπότ να μη συγκρούονται μεταξύ τους. Επιπλέον, για το πρώτο προτεινόμενο μέτρο, αυτό της μεγιστοποίησης του όγκου του ελλειψοειδούς, θα πρέπει να χρησιμοποιηθεί και ο περιορισμός που ορίζει το κατώτατο όριο στη επίδοση του συστήματος, όσον αφορά την προκαλούμενη επιτάχυνση στο αντικείμενο.

Προσομοιώσεις-Αποτελέσματα Τα παραπάνω σχήματα βελτιστοποίησης επιλύθηκαν με τη χρήση MATLAB. Τα σενάρια τα οποία δοκιμάστηκαν περιελάμβαναν τις περιπτώσεις όπου 2, 3 και 4 υποβρύχια ρομπότ χρησιμοποιούνται για να πιάσουν μια ράβδο και μια πλάκα με κυκλική, ορθογώνια παραλληλόγραμμη, τετράγωνη και ελλειπτική πλευρά. Από τις εν λόγω προσομοιώσεις προέκυψαν ενδιαφέροντα αποτελέσματα ως προς την αποτελεσματικότητα του κάθε μέτρου αλλά και ως προς την καταλληλότητά τους για διάφορες εφαρμογές.

Όσον αφορά το πρώτο προτεινόμενο μέτρο, δηλαδή αυτό που μεγιστοποιεί τον όγκο του DME. Με μια πρώτη ματιά τα αποτελέσματα φαίνονται διαισθητικά σωστά, δηλαδή ομοιάζουν με τα σημεία που θα επιλέγαμε να πιάσουμε ένα αντικείμενο αυθόρμητα. Βασικό χαρακτηριστικό αυτής της μεθόδου είναι ότι δίνει αποτελέσματα σε χρόνο μικρότερο του ενός λεπτού, ανάλογα βέβαια με τη μορφή του αντικειμένου και με τη θέση των αρχικών σημείων. Αυτό το γεγονός κάνει το μέτρο κατάλληλο για χρήση σε περιπτώσεις όπου η απόφαση για τα σημεία κράτησης πρέπει να παρθεί πολύ γρήγορα. Μια τέτοια περίπτωση θα μπορούσε να είναι αύτη κατά την οποία δεν γνωρίζουμε την ακριβή μορφή του αντικειμένου ή την ύπαρξη εμποδίων που δυσκολεύουν τη συγκράτηση του αντικειμένου από συγκεκριμένα σημεία, εκ των προτέρων. Σε αυτές τις περιπτώσεις, η αναγνώριση του αντικειμένου θα πρέπει να γίνει από τα ίδια τα ρομπότ κατά τη διάρκεια της αποστολής. Κατά συνέπεια, η απόφαση για τα σημεία κράτησης θα πρέπει να παρθεί και αυτή κατά τη διάρκεια της αποστολής, θέτοντας περιορισμό στον χρόνο που αυτή θα πρέπει να διαρκέσει, καθώς εκείνη τη στιγμή τα ρομπότ καταναλώνουν τη δική τους ενέργεια. Μιλώντας γενικά για το συγκεκριμένο μέτρο, αυτό επιτυγχάνει τη μεγιστοποίηση του όγκου του DME. Με αυτό τον τρόπο το DME μεγεθύνεται σε κάθε κατεύθυνση και κατά συνέπεια μεγεθύνονται η μεταφορική, η περιστροφική επιτάχυνση και ο συνδυασμός τους. Ο τρόπος με τον οποίο μεγιστοποιείται αυτός ο όγκος είναι αυθαίρετος και έτσι δεν εξασφαλίζεται ότι το μέτρο της επιτάχυνσης μεγιστοποιείται σε κάθε κατεύθυνση. Επιπλέον, αυτή η μέθοδος δε διαχωρίζει τη μεταφορική από τη περιστροφική επιτάχυνση, οι οποίες ενδέχεται να έχουν διαφορετική τάξη μεγέθους με αποτέλεσμα η επιτάχυνση με τη μεγαλύτερη τάξη μεγέθους να επηρεάζει περισσότερο τη λύση. Επίσης, η συγκεκριμένη μέθοδος δε λαμβάνει υπόψη την επίδραση του βάρους του συστήματος, παρ' όλα αυτά με τη χρήση του προτεινόμενου περιορισμού εξασφαλίζει την αποφυγή ανεπιθύμητων καταστάσεων στις οποίες θα μπορούσε να οδηγήσει αυτό το γεγονός. Τέλος, σημειώνεται ότι η χρήση των μεταβλητών της διαμόρφωσης των ρομπότ στις μεταβλητές απόφασης ενδέχεται να οδηγήσουν σε μεγαλύτερη μεταβολή του όγκου από ότι η μεταβολή της θέσης των σημείων κράτησης, γεγονός που θα οδηγούσε σε αποτελέσματα που θα αντιστοιχούσαν στη βέλτιστη διαμόρφωση των ρομπότ και όχι στα βέλτιστα σημεία κράτησης.

Όσον αφορά στο δεύτερο προτεινόμενο μέτρο, δηλαδή αυτό που μεγιστοποιεί την ελάχιστη απόσταση στο χώρο των μεταφορικών και περιστροφικών επιταχύνσεων, και αυτό με μια πρώτη ματιά δίνει αποτελέσματα που φαίνονται διαισθητικά σωστά. Γενικά, αυτή η μέθοδος στοχεύει στη μεγιστοποίηση της χειρότερης απόδοσης του συστήματος. Ένα μεγάλο πλεονέκτημα της μεθόδου είναι η αποσύνθεση του χώρου των επιταχύνσεων στους επιμέρους χώρους των μεταφορικών και περιστροφικών επιταχύνσεων με αποτέλεσμα η διαφορά των τάξεων μεγέθους να μην επηρεάζει τη λύση. Η αποσύνθεση του χώρου των επιταχύνσεων είναι χρονοβόρος και οδηγεί στο μεγάλο μειονέκτημα της μεθόδου που είναι ο χρόνος λήψης της απόφασης. Αυτός φτάνει και τα 50 λεπτά ανάλογα με το σχήμα του αντικειμένου και τα αρχικά σημεία, καθιστώντας την ακατάλληλη για την επιλογή σημείων κράτησης κατά τη διάρκεια της επιχείρησης. Παρ' όλα αυτά, η μέθοδος είναι κατάλληλη σε περιπτώσεις που η μορφή και η θέση του αντικειμένου είναι γνωστά εκ των προτέρων οπότε και η απόφαση μπορεί να παρθεί πριν από την έναρξη της επιχείρησης. Μεγάλο πλεονέκτημα του συγκεκριμένου μέτρου είναι ότι λαμβάνει υπόψη την επίδραση του βάρους του συστήματος δίνοντας πιο αξιόπιστα αποτελέσματα.

Εν συνεχεία, γίνεται μια σύγκριση μεταξύ των δύο προτεινόμενων μέτρων . Γενικά, τα δύο μέτρα οδηγούν σε διαφορετικά σημεία κράτησης και αυτό οφείλεται στο διαφορετικό τρόπο με τον οποίο μεγιστοποιείται το ελλειψοειδές. Όπως προκύπτει από τη σύγκριση, το πρώτο μέτρο παρέχει το μεγαλύτερο μέγιστο μέτρο επιτάχυνσης ενώ το δεύτερο μέτρο τη καλύτερη μικρότερη απόδοση.

Προτάσεις για Περαιτέρω Έρευνα Γενικά, η επιλογή των σημείων κράτησης προσφέρεται για περεταίρω έρευνα. Τα μέτρα που προτείνονται στη παρούσα διπλωματική εργασία επιδέχονται βελτιώσεων κυρίως σε θέματα που αφορούν τις υποθέσεις που έγιναν για την εξαγωγή τους. Επίσης, βελτιώσεις επιδέχονται και τα μέτρα αυτά καθαυτά, όπως η ενσωμάτωση της επίδρασης του βάρους στο πρώτο και ένας πιο γρήγορος τρόπος αποσύνθεσης του χώρου των επιταχύνσεων στο δεύτερο. Τέλος, όσον αφορά τη συνολική επιχείρηση της συλλογής και εναπόθεσης του αντικειμένου, προτείνεται η ενασχόληση με τη φάση της προσέγγισης του αντικειμένου από την ομάδα των ρομπότ.

Abstract

In recent years, robotics have become an increasing field of study with rapid growth. This mainly happens due to their applicability in everyday life. A great characteristic of robotics is their ability to give access to areas where humans would not be able to reach or even if they would, they would not be able to execute long lasting operations, there. An area like this is the ocean, where many long duration operations are taking place, making the use of robots necessary. This thesis focuses in the use of Underwater Vehicle - Manipulator Systems (UVMS), that are usually suitable for operations like these. The application that is studied is a cooperative pick-and-place operation in which a team of UVMSs have to reach an object, grasp it and transfer it from its initial location to a final one.

More specifically, this work is dedicated to the selection of the grasp points where the UVMSs' end-effectors have to grasp at in order to lift, manipulate and transfer an object from its initial location to a final one. A main characteristic, of applications like this, is that the environment, where the robots have to execute their tasks, is unstructured and likely unexplored. But even if we know the exact environment's structure a priori, it is possible to contains moving obstacles with unpredicted motion that might interrupt predefined tasks. For these reasons, in this work, for the evaluation and the selection of the grasp points, non-task specific grasp quality measures are used. As a result, the quality measures do not aim to an optimal execution of a set of predefine posterior tasks, but to the system's (UVMSs and manipulated object) ability to execute each task, that might arise during the operation, in the best possible way.

In this work, two novel non-task specific quality measures for the selection of optimal grasp points on an object in a cooperative pick-and-place operation by a team of UVMSs, are presented. These measures are extracted from the analysis of the system's dynamic manipulability ellipsoid (DME). The system's DME is used as a mapping from the system's control input space to the system's acceleration space connecting the consuming energy by the UVMSs' actuators with the provoked acceleration on the manipulated object. As a result the two proposed measures aim in the maximization of the system's ability to accelerate the object by also minimizing the consuming energy for this purpose. Each measure achieves this goal in a different way.

The first proposed measure is the volume of the system's DME. This measure aims in the maximization of the DME in every direction. Generally, this measure does not take into account the acceleration produced by the system's weight, for this reason it is proposed to be used combined with a constraint that, based in this acceleration, guarantees a bound in the system's minimum performance, as concerns the acceleration of the object's center of gravity. As concerns the second measure, this is the minimum distance in the translational and rotational acceleration space, as arise from the decomposition of the system's dynamic manipulability ellipsoid.This measure provides grasp points that guarantee the maximum possible minimum system's performance as concerns the acceleration of the object's center of gravity. More specifically, it is guaranteed that the system will be able to accelerate the object in the most difficult translational and rotational direction in the best way, i.e. higher magnitude with lower energy consumption.

In order to select the grasp points, the proposed grasp quality measures have

to be embodied in an optimization scheme, whose objective function will be this very measure. For this reason, two optimization schemes were created for the purpose of this thesis, one for each measure. As constraints are established the limitations imposed be the UVMSs, i.e. joint limits and actuators' maximum torque, and the shape of the manipulated object.

Finally, in order to clarify the proposed measures and to verify their efficiency, the optimization schemes were solved for various case studies, i.e. different number of UVMSs and object of varied shapes. The results were analyzed in order to understand the advantages and disadvantages of the proposed measures. A comparison between the proposed measures is taking place in order to illustrate their differences due to the different way that each of the two measures maximizes the system's DME.

Acknowledgments

First of all I would like to thank my supervisor prof. Kostas J. Kyriakopoulos for giving me the opportunity to collaborate with him and his research team. His advices and guidance not only determined the result of this thesis, but also triggered me to deal with aspects of science that I was previously unfamiliar and they will constitute a supply for my future course.

Special thanks to PhD student Shahab Hesmati-alamdari for his guidance, help and cooperation to the implementation of this work. His contribution was decisive.

Furthermore, I would like to thank all the members of the Control Systems Lab and specifically Gearge Karras, Charalambos Bechlioulis, Michael Logothetis, Panos Marantos and Nikos Koukis not only for their contribution to this work, but also for the friendly atmosphere that created in the workplace.

Finally, I would like to thank from the bottom of my heart my family, for the support that provided me in all these years of my studies.

Spyridon G. Tarantos,
Athens, Greece, October 2017

List of Figures

Contents

Chapter 1

Preface

1.1 Introduction

Robotics

Robotics is a field of study that provokes a great interest to engineers and scientists from many disciplines, due to its applicability not only in special operations, like search and rescue in areas suffer from natural disasters, inspections in contaminated areas or exploration of other planets, but also in everyday applications like driving or even vacuum cleaning. As mentioned in [1], robotics are concerned with the study of those machines that can replace human beings in the execution of a task, as regards both physical activity and decision making. A phrase that reveals the evolution of robotics in our society is: "The dream to create machines that are skilled and intelligent has been part of humanity from the beginning of time. This dream is now becoming part of our world's striking reality" [1].

Mobile Manipulators

As long as the main goal of the robots' use is to implement certain procedures or tasks, there are many kinds of robots depending on the application that they are designed for. Generally, robots can be classified in two major categories. To those that have a fixed base, which are called *robot manipulators* and those with a mobile base, which are called *mobile robots.* As concerns the *robot manipulators*, they are characterized by their dexterity while the *mobile robots* are characterized by their mobility. In many applications both of the previously mentioned properties are required for their efficient implementation. For these cases the use of mobile manipulator systems is imposed. The mobile manipulator systems are consisted of a mobile base equipped with one or more manipulators, combining the mobile base's mobility and the manipulators' dexterity. Consequently, a mobile manipulator is able to execute various complex tasks (e.g., lifting an object, open a vane or drilling on a surface) as a fixed base manipulator does, but has also the ability to extend its workspace, due to its mobile base. Thus, common applications in which the use of mobile manipulators is essential are mining, construction, forestry, planetary exploration and the military [2]. Generally, the mobile manipulator systems, depending on their mobile base's type, can be categorized as ground (Fig. 1.1a), aerial (Fig. 1.1b) or underwater (Fig. 1.1c), executing tasks in the field, the air and the ocean respectively. In this work the operation that the mobile robots will have to execute is going to take place in the ocean so we will concentrate to the case of mobile robots whose base is an underwater vehicle.

(a) Unmanned ground mobile manipulator (sourse: ICARUS)

(b) Multi-rotor aerial robot with manipulator (ARCAS project)

(c) UVMS ECA Hytec H2000 (sourse:ROV Innovations)

Figure 1.1: Mobile manipulator systems

Underwater Vehicles - UVMSs

One of the most common reasons why we use robots, and especially mobile robots, is the need to have access in regions that the human is not able to or it would be extremely risky to do it. Even if the human is able to access these areas it would be impossible to execute long lasting operations. Such an inhospitable environment is the deep ocean and this is the reason why the underwater robots are important. The underwater robots is an interesting field of research with great potential and this is the reason why many researchers dealt with them. Indicatively in [3] Fossen presents modeling and control of marine vehicle focusing also in underwater vehicles, while in [4], Antonelli presents modeling and control of underwater robots and especially of UVMSs. Common operations for underwater robots are inspection, maintenance, repair and service work on underwater installations [5]. In this thesis, we will examine the use of underwater vehicles in a pick-and-place operation.

Generally, we refer to underwater vehicles as Unmanned Underwater Vehicles (UUVs) [4] and they are categorized to Remotely Operated Vehicles (ROVs), which are physically linked (with wire) underwater vehicles and Autonomous Underwater Vehicles (AUVs), that do not have the limitations that a wire provides but they have to deal with the autonomy limitations.

In many operations it is required from the underwater robots to execute certain tasks that demand their interaction with their environment. Operations like these could be the lift of an object, the turn of a valve e.t.c.. In order to provide this ability to the robots, they have to be equipped with one or more manipulators. In this case the system is called Underwater Vehicle - Manipulator System (UVMS) [4] and might be autonomous (AUV+Manipulator) or not (ROV+Manipulator).

This work concentrates at the autonomous Underwater Vehicle Manipulator Systems (UVMS) like the one illustrated in Fig. 1.2.

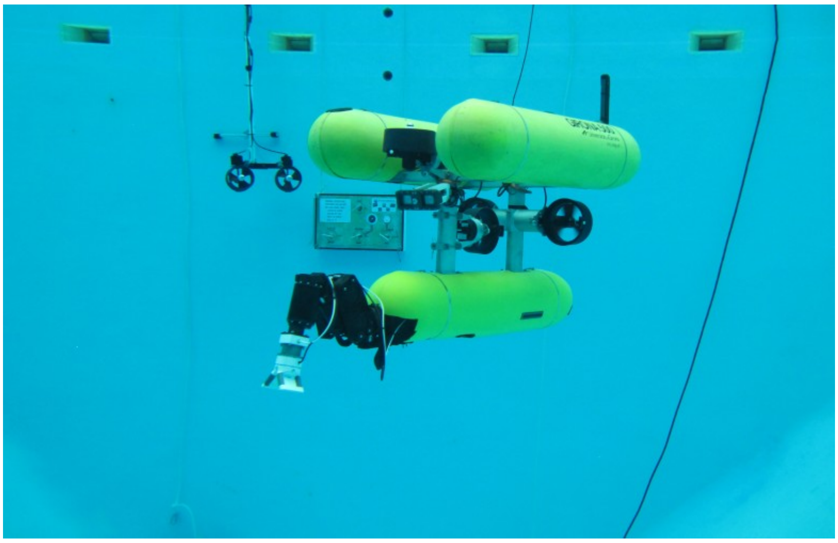

Figure 1.2: UVMS developed for the TRIDENT project (GIRONA 500 AUV + manipulator)

Cooperative Manipulation

Despite the mobile manipulators' advantages, they also have some typical limitations. Some of the most usual are the autonomy range and the actuators' maximum torque. As a result many tasks are difficult or impossible to be executed by a single robot. Such tasks could be the carriage of a heavy or of a long enough object, the assemblance of multiple parts without the use of special fixtures in order to facilitate the grasping or handling of flexible objects. In these cases the robot might be unable to execute the tasks or it is possible to have limited traveling time due to exaggerate energy consumption. These limitations can be compensated more efficiently, if multiple mobile manipulators are cooperatively involved. In this way, a task that would have been doomed to failure in the one-robot case, might be feasible when more robots are employed in cooperative way. As concerns the case of object transportation, in which we are interested in, the cooperative manipulation affects positively in terms of size, weight and shape of the transported object and facilitates, also, intricate moves and maneuvers [6].

1.2 Problem Statement

A common application of mobile manipulators and especially of UVMSs, as concerns this work, is the pick-and-place operation. In cases where the object is heavy enough or in cases where the environment is not hospitable for the human (deep in the ocean, in contaminated areas e.t.c.) the need of robots to execute these tasks is imposed. In this operation, the robots have to reach an object, grasp it and transfer it from an initial location to a final one. In Fig. 1.3 is illustrated the case that two UVMSs have grasped an object and they are carrying it in order to transfer it to a final destination. As concerns the reaching phase, that is illustrate in Fig. 1.4, the robots are reaching the object in order to grasp it, starting from their initial positions. The problem of cooperative reaching an object can be divided into two subproblems. The first is the decision of the positions on the object where the robots will grasp at. The second, is the way that the robots must reach these positions. This work deals with the first problem, the determination of the grasp points.

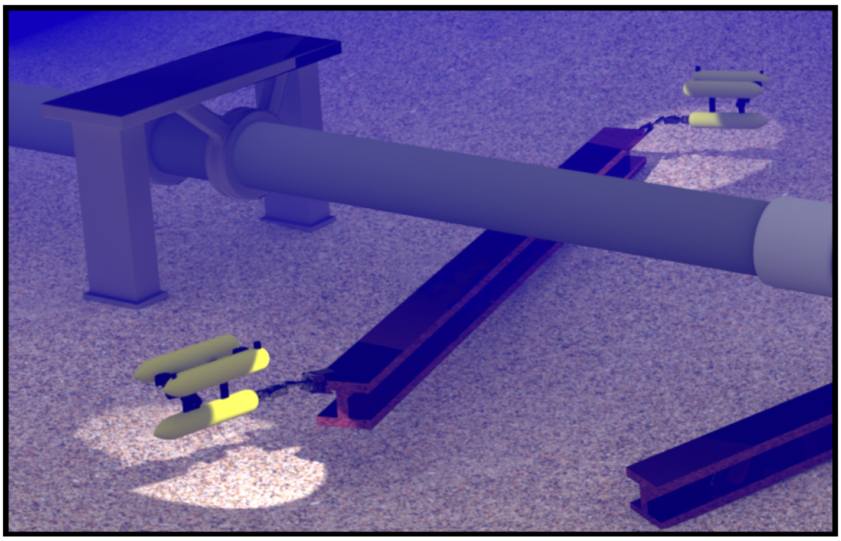

Figure 1.3: UVMSs carrying an object in order to transfer it to a final destination.

The determination of the grasp points is crucial for the rest of the operation (i.e., transportation, manipulation), as long as a correct grasp planning may lead to higher performance for the cooperative system, with lower energy consumption, which would lead to higher autonomy. The achievement of higher autonomy is translated to the robots' ability to stay longer in the water, which is crucial for the efficient execution of long lasting operations. In order to

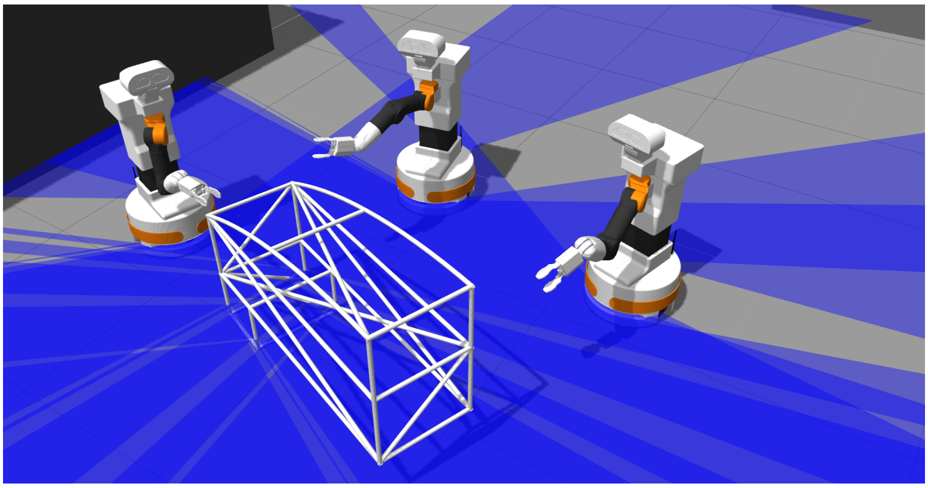

Figure 1.4: Mobile manipulators reaching object for grasping

strengthen the importance of the determination of the grasp points, it is mentioned that an improper grasping could lead to inability of the team to execute the imposed operation successfully, which means inability to transfer the object, possible destruction of the object or of the robotic equipment and generally the complete failure of the whole operation. As can be inferred from the above the proper selection of the grasp points is of great importance and as a result proper grasp quality measures have to be adopted.

There are two kinds of quality measures for the selection of grasp points. The first is the task oriented, which are quality measures that take into account the tasks that the system , robots and object, will have to execute during the operation. On the other hand, there are the quality measure that do not take into account the following tasks, mainly because they are not known a priori. So the selection of the grasp points is not based on them. These measures are called non-task specific.

In many cases, especially when the environment is unstructured, like an area full of ruins after an earthquake, an unexplored terrain or the deep ocean, we are not aware of the exact path that the robots team and the grasp object will have to follow. Consequently, we are not aware of the consecutive tasks that the robots will have to execute a priori. In addition to the unstructured environment, there might be moving obstacles whose motion can not be predicted (e.g., a collapsing floor or a chain moved by ocean currents). Then, the tasks can not be imposed before the start of the operation, as long as the robots will have to collect on-line information about their environment. Each task will have to be planned depending on the informations that the sensors of the robots provide about the surrounding environment's structure and the relative position of the moving obstacles. As can be referred from the above, the grasp quality measures can not be task dependent and as a result non-task specific measures should be used for the evaluation of the potential grasp points. This measures should guarantee that no matter the task that might arise to be executed, the resulting grasp points will permit to the system to execute it with the least possible energy consumption.

So in this work, the determination of the optimal grasp points, in a pick-and-place operation is examined. For this operation we are not aware of the consecutive tasks that might arise, so we are interested in finding proper non-task specific quality measures for the grasp points evaluation.

1.3 Approach of Solution

In this work two non-task specific measures are presented in order to define grasp points that by grasping them, the mobile manipulators can execute every needed task with the least possible energy consumption. For the following analysis, as task will be denoted the acceleration of the object's center of gravity (translational, rotational or combination of them).

The measures will be extracted from the system's dynamic manipulability ellipsoid [7]. The first proposed method aims at the maximization of the system's dynamic manipulability ellipsoid (DME)[7, 8] by also guaranteeing a bound in the system's minimum performance, as concerns the provoked acceleration. This measure maximizes the system's potential acceleration, by maximizing the volume of the system's DME. In order to avoid the possibility that might arise, of the system's inability to accelerate its own weight or to execute a number of tasks, in this work this measure is proposed to be accompany by a constraint that guarantees a lower bound at the system's performance.

The second proposed measure is the minimum distance in the translational and rotational acceleration space. These two spaces are extracted by the decomposition of the system's dynamic manipulability ellipsoid. The minimum distance from the center of one of these two spaces with its bound corresponds to the most difficult acceleration's directions, which means that the system accelerates in this with the minimum magnitude and for maximum energy consumption. The maximization of this measure, and consequently the maximization of these two distances, guarantees that the system will accelerate in the most difficult direction with the best possible way, i.e. higher magnitude with lower energy consumption.

In order to select the grasp points, two optimization schemes will be implemented. Each one of them will have as objective function one of the proposed quality measures. The constraints that are considered for these optimization schemes are the UVMS's joint limits, control input saturations, a minimum distance between the robots (i.e., in order to satisfy collision avoidance) as well as the object's shape.

1.4 Thesis Structure

The structure of this thesis is as follows:

In Chap. 2 the model of the cooperative system, UVMSs and manipulated object, is presented. More specifically, in section 2.1 the UVMS's kinematics and equations of motion are determined. In section 2.2 the dynamics of the manipulated object are presented. Finally, in section 2.3 the UVMSs' equations of motion are combined with these of the manipulated object consisting the dynamics of the cooperative system.

In Chap. 3 the proposed grasp quality measures are presented. A brief outline of the relative to the grasp points selection work is listed in section 3.1, while in section 3.2 the proposed approach for the grasp point selection, that is followed in this thesis, is explained. In 3.3 the general concept of Dynamic Manipulability Ellipsoid (DME) is illustrated and the DME of the cooperative system is determined. Finally, in section 3.4 the proposed grasp quality measures are presented , accompanied with the necessary informations for their comprehension.

In Chap. 4 the optimization schemes for the selection of the grasp points are presented, while in Chap. 5 the results from the application of the optimization schemes in various case studies are presented, accompanied with comments for each proposed measure.

Finally, in Chap. 6 some concluding remarks for the use of the presented methods are listed, followed by proposals for the improvement of the aforementioned measures and for further research.

Chapter 2

Modeling of the Cooperative System

2.1 Reference Frames

In order to determine the equations of motion of the cooperative system, the following reference frames are introduced. These frames are also illustrated in Fig. 2.1 .

Earth-Fixed Frame With $\{I\}$ is denoted the earth-fixed frame $O_I - X_I Y_I X_I$ that will be used as inertial frame.

Vehicle-Fixed Frame With $\{V\}$ is denoted the vehicle-fixed frame $O_V - X_V Y_V X_V$, whose origin is located on the vehicle's center of gravity.

Manipulator's Base frame With $\{0\}$ is denoted the end-effector's base frame $O_0 - X_0 Y_0 X_0$ which is fixed on the vehicle. As $\boldsymbol{P_0}$ is denoted the pose of the manipulator's base frame with respect to the vehicle-fixed frame.

Manipulator's End-Effector frame With $\{ee\}$ is denoted the end-effector's frame $O_{ee} - X_{ee} Y_{ee} Z_{ee}$.

Object-fixed frame With $\{O\}$ is denoted the object-fixed frame $O_o - X_o Y_o Z_o$ whose origin is located at the object's center of gravity

2.2 Modeling of UVMS

2.2.1 Vehicle's Kinematics

In order to describe the position and the orientation of the vehicle in the inertial frame {I}, as can be seen in Fig. 2.1, the following vector is used:

$$\boldsymbol{\eta} = \begin{bmatrix} \boldsymbol{\eta_1}^T & \boldsymbol{\eta_2}^T \end{bmatrix}^T \in \mathbb{R}^6 \tag{2.1}$$

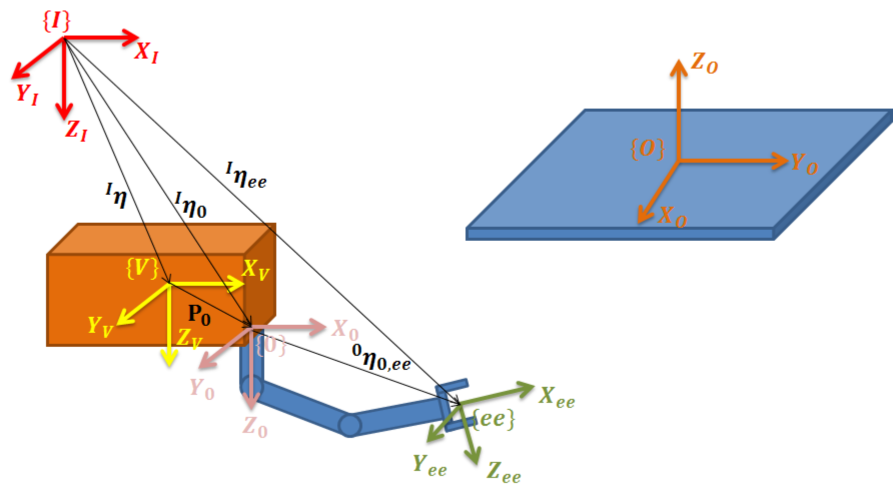

Figure 2.1: In this figure simplified sketches of the UVMS and the object are depicted. There are also presented the reference frames, which are denoted in this section, and some important position vectors.

where $\boldsymbol{\eta_1} = \begin{bmatrix} x_v & y_v & z_v \end{bmatrix}^T \in \mathbb{R}^3$ is the vector of the vehicle's position coordinates and $\boldsymbol{\eta_2} = \begin{bmatrix} \phi_v & \theta_v & \psi_v \end{bmatrix}^T \in \mathbb{R}^3$ is the vector of vehicle's Euler-angle coordinates in the inertial frame {I}. In our case, we use the roll, pitch, yaw angles for the attitude representation.

The time derivative of the vehicle's posture in inertial frame {I}, is denoted as:

$$\dot{\boldsymbol{\eta}} = \begin{bmatrix} \dot{\boldsymbol{\eta}}_1 \\ \dot{\boldsymbol{\eta}}_2 \end{bmatrix} \in \mathbb{R}^6 \tag{2.2}$$

where $\dot{\boldsymbol{\eta}}_1 \in \mathbb{R}^3$ is the time derivative of the vehicle's position coordinates and $\dot{\boldsymbol{\eta}}_2 \in \mathbb{R}^3$ the time derivative of the vehicle's Euler angles coordinates.

With $\boldsymbol{\nu} \in \mathbb{R}^6$ is denoted the vehicle-fixed velocity:

$$\boldsymbol{\nu} = \begin{bmatrix} \boldsymbol{\nu_1} \\ \boldsymbol{\nu_2} \end{bmatrix} \in \mathbb{R}^6 \tag{2.3}$$

As $\boldsymbol{\nu_1} \in \mathbb{R}^3$ is denoted the body-fixed linear velocity, which is the linear velocity of the origin of the vehicle-fixed frame $\{V\}$ with respect to the origin of the inertial frame $\{I\}$, expressed in the vehicle-fixed frame:

$$\boldsymbol{\nu_1} = \begin{bmatrix} u \\ v \\ \omega \end{bmatrix} \in \mathbb{R}^3 \tag{2.4}$$

The body-fixed linear velocity, $\boldsymbol{\nu_1}$, is related with the time derivative of the vehicle's position coordinates, $\dot{\boldsymbol{\eta}}_1$, with the following expresion:

$$\boldsymbol{\nu_1} = {}^{\boldsymbol{V}}\boldsymbol{R_I}\dot{\boldsymbol{\eta}}_1 \tag{2.5}$$

where ${}^{V}\boldsymbol{R_I} \in \mathbb{R}^3$ is the rotation matrix that expresses the transformation from the inertial frame $\{I\}$ to the vehicle-fixed frame $\{V\}$. In nautical field as attitude representation are used the roll, pitch and yaw angles, so the rotation matrix becomes:

$$ {}^{V}\boldsymbol{R_I}(\boldsymbol{\eta_2}) = \begin{bmatrix} c_\psi c_\theta & s_\psi c_\theta & -s_\theta \\ -s_\psi c_\phi + c_\psi s_\theta s_\phi & c_\psi c_\phi + s_\psi s_\theta s_\phi & s_\phi c_\theta \\ s_\psi s_\phi + c_\psi s_\theta c_\phi & -c_\psi s_\phi + s_\psi s_\theta c_\phi & c_\phi c_\theta \end{bmatrix} \in \mathbb{R}^3 \tag{2.6} $$

where, as a matter of convenience, the c_a and s_a are used as short notations for $cos(a)$ and $sin(a)$ respectively.

As $\boldsymbol{\nu_2} \in \mathbb{R}^3$ is denoted the body-fixed angular velocity, which is the angular velocity of the vehicle-fixed frame (body-fixed frame) with respect to the inertial frame, expressed in the vehicle-fixed frame:

$$ \boldsymbol{\nu_2} = \begin{bmatrix} p \\ q \\ r \end{bmatrix} \in \mathbb{R}^3 \tag{2.7} $$

The body-fixed angular velocity, $\boldsymbol{\nu_2}$, is related with the time derivative of the vehicle's Euler angles coordinates, $\dot{\boldsymbol{\eta}}_{\boldsymbol{2}}$, with the following expression:

$$ \boldsymbol{\nu_2} = \boldsymbol{J}_{k,o}(\boldsymbol{\eta_2})\dot{\boldsymbol{\eta}}_{\boldsymbol{2}} \tag{2.8} $$

As $\boldsymbol{J}_{k,o}(\boldsymbol{\eta_2})$ is denoted a proper Jocobian matrix depending on the attitude representation. For the roll, pitch ,yaw angles representation the Jacobian matrix is of the form:

$$ \boldsymbol{J}_{k,o}(\boldsymbol{\eta_2}) = \begin{bmatrix} 1 & 0 & -s_\theta \\ 0 & c_\phi & c_\theta s_\phi \\ 0 & -s_\phi & c_\theta c_\phi \end{bmatrix} \tag{2.9} $$

Combining equations (2.5) and (2.8) we have:

$$ \begin{bmatrix} \boldsymbol{\nu_1} \\ \boldsymbol{\nu_2} \end{bmatrix} = \begin{bmatrix} {}^{V}\boldsymbol{R_I}(\boldsymbol{\eta_2}) & \boldsymbol{O}_{3\times3} \\ \boldsymbol{O}_{3\times3} & \boldsymbol{J}_{k,o}(\boldsymbol{\eta_2}) \end{bmatrix} \begin{bmatrix} \dot{\boldsymbol{\eta}}_{\boldsymbol{1}} \\ \dot{\boldsymbol{\eta}}_{\boldsymbol{2}} \end{bmatrix} \tag{2.10} $$

By denoting the matrix $\boldsymbol{J}_e(\boldsymbol{\eta_2}) \in \mathbb{R}^{6\times6}$ as

$$ \boldsymbol{J}_e(\boldsymbol{\eta_2}) = \begin{bmatrix} {}^{V}\boldsymbol{R_I}(\boldsymbol{\eta_2}) & \boldsymbol{O}_{3\times3} \\ \boldsymbol{O}_{3\times3} & \boldsymbol{J}_{k,o}(\boldsymbol{\eta_2}) \end{bmatrix} \tag{2.11} $$

and by substituting (2.11) to (2.10) we have:

$$ \boldsymbol{\nu} = \boldsymbol{J}_e(\boldsymbol{\eta_2})\dot{\boldsymbol{\eta}} \tag{2.12} $$

The above equation represents the vehicle's differential kinematics.

2.2.2 Manipulator's Kinematics with Mobile Base

Let assume that we have a manipulator of n_m joints. The vector of joints' positions is $\boldsymbol{q} = \begin{bmatrix} q_1 & ... & q_{n_m} \end{bmatrix}^T \in \mathbb{R}^{n_m}$.

We define the end-effector's posture as:

$$ \boldsymbol{\eta_{ee}} = \begin{bmatrix} \boldsymbol{\eta_{ee1}} \\ \boldsymbol{\eta_{ee2}} \end{bmatrix} \in \mathbb{R}^6 \tag{2.13} $$

where $\boldsymbol{\eta_{ee1}} \in \mathbb{R}^3$ is the position of the end-effector in the inertial frame {I} and $\boldsymbol{\eta_{ee2}} \in \mathbb{R}^3$ is the orientation of the end-effector in the inertial frame $\{I\}$. This vector is also illustrated in Fig. 2.1

As it was mentioned before, the base frame of the end-effector, {0} is fixed at the vehicle and in posture in the vehicle-fixed frame $\{V\}$ of $\boldsymbol{P_0} \in \mathbb{R}^6$. As a result the position of the end-effector is a function of the vehicle's position and orientation and of the manipulator's configuration, $\boldsymbol{\eta_{ee1}} = \boldsymbol{k_1}(\boldsymbol{\eta_1}, \boldsymbol{\eta_2}, \boldsymbol{q})$. The orientation of the end-effector is also a function of vehicle's orientation and manipulator's configuration, $\boldsymbol{\eta_{ee2}} = \boldsymbol{k_2}(\boldsymbol{\eta_2}, \boldsymbol{q})$. So the posture of the end-effector can be denoted by the following function:

$$\boldsymbol{\eta_{ee}} = \boldsymbol{k}(\boldsymbol{\eta_1}, \boldsymbol{\eta_2}, \boldsymbol{q}) \tag{2.14}$$

The above equation is the equation of direct kinematics of the UVMS and is extracted by using the Denavit-Hartenberg convention. It depends on the vehicle's and manipulator's structure and differs from robot to robot.

2.2.3 UVMS's Kinematics

For the manipulator's differential kinematics let
$\boldsymbol{\eta_0}$: be the vector of manipulator's base frame position in inertial frame {I}
${}^{\boldsymbol{0}}\boldsymbol{\eta_{0,ee}}$: be the vector connecting the manipulator's base with the end effector, expressed in manipulator's base frame {0}
${}^{\boldsymbol{0}}\boldsymbol{\omega_{0,ee}}$: the end-effector's angular velocity in manipulator's base frame
Let consider the vector ${}^{\boldsymbol{0}}\boldsymbol{v_{ee}} = \begin{bmatrix} {}^{\boldsymbol{0}}\dot{\boldsymbol{\eta}}_{\boldsymbol{0,ee}}^T & {}^{\boldsymbol{0}}\boldsymbol{\omega}_{\boldsymbol{0,ee}}^T \end{bmatrix}^T \in \mathbb{R}^6$ for which holds:

$${}^{\boldsymbol{0}}\boldsymbol{v_{ee}} = \begin{bmatrix} {}^{\boldsymbol{0}}\dot{\boldsymbol{\eta}}_{\boldsymbol{0,ee}} \\ {}^{\boldsymbol{0}}\boldsymbol{\omega_{0,ee}} \end{bmatrix} = \begin{bmatrix} \boldsymbol{J_p} \\ \boldsymbol{J_o} \end{bmatrix} \dot{\boldsymbol{q}} = \boldsymbol{J}\dot{\boldsymbol{q}} \tag{2.15}$$

where $\boldsymbol{J} \in \mathbb{R}^{6\times n_m}$ is the manipulator's geometric Jacobian. The geometric Jacobian can be derived in an easy and systematic way from the manipulators direct kinematics, as derived from Denavit-Hartenberg convention, as mentioned in [9].

$$\boldsymbol{\eta_{ee1}} = \boldsymbol{\eta_0} + {}^{\boldsymbol{I}}\boldsymbol{R_0}\,{}^{\boldsymbol{0}}\boldsymbol{\eta_{0,ee}} \tag{2.16}$$

By differentiating we obtain:

$$\dot{\boldsymbol{\eta}}_{\boldsymbol{ee1}} = \dot{\boldsymbol{\eta}}_{\boldsymbol{0}} + {}^{\boldsymbol{I}}\dot{\boldsymbol{R}}_{\boldsymbol{0}}\,{}^{\boldsymbol{0}}\boldsymbol{\eta_{0,ee}} + {}^{\boldsymbol{I}}\boldsymbol{R_0}\,{}^{\boldsymbol{0}}\dot{\boldsymbol{\eta}}_{\boldsymbol{0,ee}} \tag{2.17}$$

By using the equation ${}^{\boldsymbol{I}}\dot{\boldsymbol{R}}_{\boldsymbol{0}} = {}^{\boldsymbol{I}}\boldsymbol{\omega_0} \times {}^{\boldsymbol{I}}\boldsymbol{R_0}$ we obtain:

$$\dot{\boldsymbol{\eta}}_{\boldsymbol{ee1}} = \dot{\boldsymbol{\eta}}_{\boldsymbol{0}} + {}^{\boldsymbol{I}}\boldsymbol{\omega_0} \times {}^{\boldsymbol{I}}\boldsymbol{R_0}\,{}^{\boldsymbol{0}}\boldsymbol{\eta_{0,ee}} + {}^{\boldsymbol{I}}\boldsymbol{R_0}\,{}^{\boldsymbol{0}}\dot{\boldsymbol{\eta}}_{\boldsymbol{0,ee}} \tag{2.18}$$

$$\dot{\boldsymbol{\eta}}_{\boldsymbol{ee1}} = \dot{\boldsymbol{\eta}}_{\boldsymbol{0}} - \boldsymbol{S}({}^{\boldsymbol{I}}\boldsymbol{R_0}\,{}^{\boldsymbol{0}}\boldsymbol{\eta_{0,ee}})\,{}^{\boldsymbol{I}}\boldsymbol{\omega_0} + {}^{\boldsymbol{I}}\boldsymbol{R_0}\,{}^{\boldsymbol{0}}\dot{\boldsymbol{\eta}}_{\boldsymbol{0,ee}} \tag{2.19}$$

As mentioned in (2.15) ${}^{\boldsymbol{0}}\dot{\boldsymbol{\eta}}_{\boldsymbol{0,ee}} = \boldsymbol{J_p}\dot{\boldsymbol{q}}$ so we obtain:

$$\dot{\boldsymbol{\eta}}_{\boldsymbol{ee1}} = \dot{\boldsymbol{\eta}}_{\boldsymbol{0}} - \boldsymbol{S}({}^{\boldsymbol{I}}\boldsymbol{R_0}\,{}^{\boldsymbol{0}}\boldsymbol{\eta_{0,ee}})\,{}^{\boldsymbol{I}}\boldsymbol{\omega_0} + {}^{\boldsymbol{I}}\boldsymbol{R_0}\boldsymbol{J_p}\dot{\boldsymbol{q}} \tag{2.20}$$

$$\dot{\boldsymbol{\eta}}_{\boldsymbol{ee1}} = \dot{\boldsymbol{\eta}}_{\boldsymbol{0}} - \boldsymbol{S}({}^{\boldsymbol{I}}\boldsymbol{R_0}\,{}^{\boldsymbol{0}}\boldsymbol{\eta_{0,ee}})\,{}^{\boldsymbol{I}}\boldsymbol{\omega_0} + {}^{\boldsymbol{I}}\boldsymbol{J_p}\dot{\boldsymbol{q}} \tag{2.21}$$

If also considered that ${}^{\boldsymbol{I}}\boldsymbol{\omega_0} = {}^{\boldsymbol{I}}\boldsymbol{R_V}\boldsymbol{\nu_2}$ then:

$$\dot{\boldsymbol{\eta}}_{\boldsymbol{ee1}} = \dot{\boldsymbol{\eta}}_{\boldsymbol{0}} - \boldsymbol{S}({}^{\boldsymbol{I}}\boldsymbol{R_0}{}^{\boldsymbol{0}}\boldsymbol{\eta_{0,ee}}){}^{\boldsymbol{I}}\boldsymbol{R_V}\boldsymbol{\nu_2} + {}^{\boldsymbol{I}}\boldsymbol{J_p}\dot{\boldsymbol{q}} \tag{2.22}$$

For the time derivative of the manipulator's base frame position $\dot{\boldsymbol{\eta}}_{\boldsymbol{0}}$ we have:

$$\dot{\boldsymbol{\eta}}_{\boldsymbol{0}} = {}^{\boldsymbol{I}}\boldsymbol{R_V}\boldsymbol{\nu_1} + {}^{\boldsymbol{I}}\boldsymbol{\omega_0} \times {}^{\boldsymbol{I}}\boldsymbol{R_V}{}^{\boldsymbol{V}}\boldsymbol{r_{V,0}} \tag{2.23}$$

$$\dot{\boldsymbol{\eta}}_{\boldsymbol{0}} = {}^{\boldsymbol{I}}\boldsymbol{R_V}\boldsymbol{\nu_1} - \boldsymbol{S}({}^{\boldsymbol{I}}\boldsymbol{R_V}{}^{\boldsymbol{V}}\boldsymbol{r_{V,0}}){}^{\boldsymbol{I}}\boldsymbol{R_V}\boldsymbol{\nu_2} \tag{2.24}$$

where ${}^{\boldsymbol{V}}\boldsymbol{r_{V,0}} \in \mathbb{R}^3$ is the vector connecting the origin of the vehicle-fixed frame with the base of the manipulator expressed in vehicle-fixed frame $\{V\}$.
By substituting (2.24) in (2.22) we have:

$$\dot{\boldsymbol{\eta}}_{\boldsymbol{ee1}} = {}^{\boldsymbol{I}}\boldsymbol{R_V}\boldsymbol{\nu_1} - \boldsymbol{S}({}^{\boldsymbol{I}}\boldsymbol{R_V}{}^{\boldsymbol{V}}\boldsymbol{r_{V,0}}){}^{\boldsymbol{I}}\boldsymbol{R_V}\boldsymbol{\nu_2} - \boldsymbol{S}({}^{\boldsymbol{I}}\boldsymbol{R_0}{}^{\boldsymbol{0}}\boldsymbol{\eta_{0,ee}}){}^{\boldsymbol{I}}\boldsymbol{R_V}\boldsymbol{\nu_2} + {}^{\boldsymbol{I}}\boldsymbol{J_p}\dot{\boldsymbol{q}} \tag{2.25}$$

$$\dot{\boldsymbol{\eta}}_{\boldsymbol{ee1}} = {}^{\boldsymbol{I}}\boldsymbol{R_V}\boldsymbol{\nu_1} - \Big(\boldsymbol{S}({}^{\boldsymbol{I}}\boldsymbol{R_V}{}^{\boldsymbol{V}}\boldsymbol{r_{V,0}}) + \boldsymbol{S}({}^{\boldsymbol{I}}\boldsymbol{R_0}{}^{\boldsymbol{0}}\boldsymbol{\eta_{0,ee}})\Big){}^{\boldsymbol{I}}\boldsymbol{R_V}\boldsymbol{\nu_2} + {}^{\boldsymbol{I}}\boldsymbol{J_p}\dot{\boldsymbol{q}} \tag{2.26}$$

$$\dot{\boldsymbol{\eta}}_{\boldsymbol{ee1}} = \boldsymbol{J_{p,uvms}}\boldsymbol{\zeta} \tag{2.27}$$

where

$$\boldsymbol{J_{p,uvms}} = \begin{bmatrix} {}^{\boldsymbol{I}}\boldsymbol{R_V} & -\Big(\boldsymbol{S}({}^{\boldsymbol{I}}\boldsymbol{R_V}{}^{\boldsymbol{V}}\boldsymbol{r_{V,0}}) + \boldsymbol{S}({}^{\boldsymbol{I}}\boldsymbol{R_0}{}^{\boldsymbol{0}}\boldsymbol{\eta_{0,ee}})\Big){}^{\boldsymbol{I}}\boldsymbol{R_V} & {}^{\boldsymbol{I}}\boldsymbol{J_p} \end{bmatrix} \tag{2.28}$$

As concerns the orientation, let define as:
$\boldsymbol{\omega_{ee}}$: the angular velocity of the end-effector in the inertial frame $\{I\}$
$\boldsymbol{\omega_0}$: the angular velocity of the vehicle in the inertial frame $\{I\}$
${}^{\boldsymbol{0}}\boldsymbol{\omega_{0,ee}}$: the angular velocity of the manipulator with respect to the base frame expressed in the base frame $\{0\}$

$$\boldsymbol{\omega_{ee}} = \boldsymbol{\omega_0} + {}^{\boldsymbol{0}}\boldsymbol{\omega_{0,ee}} \tag{2.29}$$

From equation (2.15) we have ${}^{\boldsymbol{0}}\boldsymbol{\omega_{0,ee}} = \boldsymbol{J_o}\dot{\boldsymbol{q}}$ so by substituting to (2.29) we have:

$$\boldsymbol{\omega_{ee}} = {}^{\boldsymbol{I}}\boldsymbol{R_V}\boldsymbol{\nu_2} + {}^{\boldsymbol{I}}\boldsymbol{R_0}\boldsymbol{J_o}\dot{\boldsymbol{q}} \tag{2.30}$$

$$\boldsymbol{\omega_{ee}} = {}^{\boldsymbol{I}}\boldsymbol{R_V}\boldsymbol{\nu_2} + {}^{\boldsymbol{I}}\boldsymbol{J_o}\dot{\boldsymbol{q}} \tag{2.31}$$

$$\boldsymbol{\omega_{ee}} = \boldsymbol{J_{o,uvms}}\dot{\boldsymbol{q}} \tag{2.32}$$

where

$$\boldsymbol{J_{o,uvms}} = \begin{bmatrix} \boldsymbol{O}_{3\times 3} & {}^{\boldsymbol{I}}\boldsymbol{R_V} & {}^{\boldsymbol{I}}\boldsymbol{J_o} \end{bmatrix} \tag{2.33}$$

So the differential kinematics' equation of the UVMS is:

$$\dot{\boldsymbol{x}}_{\boldsymbol{E}} = \begin{bmatrix} \dot{\boldsymbol{\eta}}_{\boldsymbol{ee1}} \\ \boldsymbol{\omega_{ee}} \end{bmatrix} = \boldsymbol{J_{uvms}}\boldsymbol{\zeta} \tag{2.34}$$

where

$$\boldsymbol{J_{uvms}} = \begin{bmatrix} \boldsymbol{J_{p,uvms}} \\ \boldsymbol{J_{o,uvms}} \end{bmatrix} = \begin{bmatrix} {}^{\boldsymbol{I}}\boldsymbol{R_V} & -\Big(\boldsymbol{S}({}^{\boldsymbol{I}}\boldsymbol{R_V}{}^{\boldsymbol{V}}\boldsymbol{r_{V,0}}) + \boldsymbol{S}({}^{\boldsymbol{I}}\boldsymbol{R_0}{}^{\boldsymbol{0}}\boldsymbol{\eta_{0,ee}})\Big){}^{\boldsymbol{I}}\boldsymbol{R_V} & {}^{\boldsymbol{I}}\boldsymbol{J_p} \\ \boldsymbol{O}_{3\times 3} & {}^{\boldsymbol{I}}\boldsymbol{R_V} & {}^{\boldsymbol{I}}\boldsymbol{J_o} \end{bmatrix} \tag{2.35}$$

For simplicity the UVMS's geometric Jacobian will be denoted as $\boldsymbol{J}$.

2.2.4 Vehicle's Dynamics

Rigid Body Dynamics In this section, the equations of motion of the vehicle will be determined. In the following, it is considered that the origin of the body-fixed frame coincides with the vehicle's center of gravity, as it was mentioned and in previous sections.

The Newton - Euler equations of motion of a rigid body moving is space are:

$$\boldsymbol{M_{RB}}\dot{\boldsymbol{\nu}} + \boldsymbol{C_{RB}}(\boldsymbol{\nu})\boldsymbol{\nu} = \boldsymbol{\tau_{\nu}} \tag{2.36}$$

Where
$\boldsymbol{\nu}$: is the vector containing the body's translational and angular velocities.
$\boldsymbol{M_{RB}}$: is the inertia matrix
$\boldsymbol{C_{RB}}$: is the matrix contains the Coriolis and centripetal terms
$\boldsymbol{\tau_{\nu}}$: the generalized forces acting to the body

Hydrodynamic Effects While the object is moving in a fluid the hydrodynamic effects have great influence on its dynamics. The fluid surrounding the body is accelerated with the body itself. The fluid exerts a reaction force, which is equal to magnitude and opposite in direction of the force that the body exerts to the fluid that causes the fluid's acceleration. This reaction force is the added mass contribution.
Let $\boldsymbol{M_A} \in \mathbb{R}^{6\times 6}$ be the added mass matrix and $\boldsymbol{C_A}(\boldsymbol{\nu})$ be the matrix containing the added Coriolis and centripetal contribution of the added mass.

The presence of the fluid also provokes dissipative drag and lift forces on the body. Let $\boldsymbol{D_{RB}}(\boldsymbol{\nu})$ be the matrix containing the linear and quadratic damping terms that reflect the presence of dissipative drag and lift forces caused by the fluid's viscosity.

Let now consider the gravitational force acting on the body and the buoyancy. The gravity force is:

$$\boldsymbol{f_G}({}^{\boldsymbol{V}}\boldsymbol{R_I}) = {}^{\boldsymbol{V}}\boldsymbol{R_I} m \boldsymbol{g^I} \tag{2.37}$$

The buoyancy force acting in the center of buoyancy is:

$$\boldsymbol{f_B}({}^{\boldsymbol{V}}\boldsymbol{R_I}) = -{}^{\boldsymbol{V}}\boldsymbol{R_I} \rho \bigtriangledown \boldsymbol{g^I} \tag{2.38}$$

where $m \in \mathbb{R}$ is the vehicle's mass,ρ the density and $\bigtriangledown$ the volume of the body.

Let denote the vector of force/moment due to gravity and buoyancy in the body - fixed frame as:

$$\boldsymbol{g_{RB}}({}^{\boldsymbol{V}}\boldsymbol{R_I}) = -\begin{bmatrix} \boldsymbol{f_G}({}^{\boldsymbol{V}}\boldsymbol{R_I}) + \boldsymbol{f_B}({}^{\boldsymbol{V}}\boldsymbol{R_I}) \\ {}^{\boldsymbol{V}}\boldsymbol{r_G} \times \boldsymbol{f_G}({}^{\boldsymbol{V}}\boldsymbol{R_I}) + {}^{\boldsymbol{V}}\boldsymbol{r_B} \times \boldsymbol{f_B}({}^{\boldsymbol{V}}\boldsymbol{R_I}) \end{bmatrix} \tag{2.39}$$

where ${}^{\boldsymbol{V}}\boldsymbol{r_B} \in \mathbb{R}^3$ is the center buoyancy.

Considering the vehicle as a rigid body submerged into the fluid. The vehicle's equations of motion become:

$$\boldsymbol{M_v}\dot{\boldsymbol{\nu}} + \boldsymbol{C_v}(\boldsymbol{\nu})\boldsymbol{\nu} + \boldsymbol{D_{RB}}(\boldsymbol{\nu})\boldsymbol{\nu} + \boldsymbol{g_{RB}}({}^{\boldsymbol{I}}\boldsymbol{R_V}) = \boldsymbol{\tau_v} \tag{2.40}$$

where
$\boldsymbol{M_v} = \boldsymbol{M_{RB}} + \boldsymbol{M_A}$ and $\boldsymbol{C_v} = \boldsymbol{C_{RB}} + \boldsymbol{C_A}$
$\boldsymbol{\tau_v}$:the generalized forces (force and torque) acting on the vehicle

2.2.5 Manipulator's Dynamics

As concerns a manipulator moving in a fluid we have the equations of motion:

$$\boldsymbol{M_m(q)\ddot{q} + C_m(q,\dot{q})\dot{q} + D_m(q,\dot{q})\dot{q} + g_m(q) = \tau_m} \tag{2.41}$$

where
$\boldsymbol{M_m(q)}$ the manipulator's inertia matrix, including added inertia due to liquid
$\boldsymbol{C_m(q,\dot{q})}$ the matrix that contains Coriolis and centripetal terms
$\boldsymbol{D_m(q,\dot{q})}$ the hydrodynamic lift and damping matrix
$\boldsymbol{g_m(q)}$ vector of gravity and buoyancy forces
$\boldsymbol{\tau_m}$ vector of the torques acting to the manipulator's joints

2.2.6 UVMS's Dynamics

Combining vehicle's and manipulator's dynamics, equations (2.40) and (2.41) respectively, and by denoting $\boldsymbol{\zeta} = \begin{bmatrix}\boldsymbol{\nu}^T & \boldsymbol{\dot{q}}^T\end{bmatrix}^T \in \mathbb{R}^{6+n_m}$, we can derive the UVMS's equations of motion as:

$$\boldsymbol{M(q)\dot{\zeta} + C(q,\zeta)\zeta + D(q,\zeta)\zeta + g(q, {}^{I}R_B) = \tau} \tag{2.42}$$

where

$$\boldsymbol{M(q)} = \begin{bmatrix} \boldsymbol{M_v + H(q)} & \boldsymbol{M_c(q)} \\ \boldsymbol{M_c^T(q)} & \boldsymbol{M_m(q)} \end{bmatrix} \tag{2.43}$$

$$\boldsymbol{C(q,\zeta)} = \begin{bmatrix} \boldsymbol{C_v(\nu) + C_1(q,\dot{q},\nu)} & \boldsymbol{C_2(q,\dot{q})} \\ \boldsymbol{C_3(q,\dot{q},\nu)} & \boldsymbol{C_m(q,\dot{q})} \end{bmatrix} \tag{2.44}$$

$$\boldsymbol{D(q,\zeta)} = \begin{bmatrix} \boldsymbol{D_v(\nu) + D_1(q) + D_2(q,\dot{q},\nu)} & \boldsymbol{D_3(q,\dot{q},\nu)} \\ \boldsymbol{D_4(q,\dot{q},\nu)} & \boldsymbol{D_m(q) + D_5(q,\dot{q},\nu)} \end{bmatrix} \tag{2.45}$$

$$\boldsymbol{g(q, {}^{I}R_B)} = \begin{bmatrix} \boldsymbol{g_v(\eta) + g_E(q)} \\ \boldsymbol{g_m(q)} \end{bmatrix} \tag{2.46}$$

where:
$\boldsymbol{H(q)\dot{\nu}}$: is the added inertia due to the manipulator
$\boldsymbol{D_1(q)\nu}$: is the linear skin friction due to the manipulator
$\boldsymbol{C_2(q,\dot{q})\dot{q}}$: are the Coriolis and centripetal terms due to the manipulator
$\boldsymbol{M_c^T(q)\dot{\nu}}$: are the reaction forces and moments between the vehicle and the manipulator
$\boldsymbol{C_i(q,\dot{q},\nu)}$: are the Coriolis and centripetal forces due to the interaction between the vehicle and the manipulator
$\boldsymbol{D_i(q,\dot{q},\nu)}$: is the quadratic drag due to the manipulator links and vehicle
$\boldsymbol{D_m(q)}$: is the linear skin-friction affecting the manipulator
$\boldsymbol{g_E(q)}$: is the gravity force and moment vector due to the manipulator

As mentioned in [4] and [9], if the end-effector is in contact with the environment, the force/moment at the tip of the manipulator effects the whole system. In this case the equations of motion become:

$$\boldsymbol{M(q)\dot{\zeta} + C(q,\zeta)\zeta + D(q,\zeta)\zeta + g(q, {}^{I}R_B) = \tau + J^T(q, {}^{I}R_V)h} \tag{2.47}$$

In our case we are interested in the generalized forces exerted from the UVMS to its environment, so for convenience the previous equation will be rewritten as:

$$\boldsymbol{M(q)\dot{\zeta}} + \boldsymbol{C(q,\zeta)\zeta} + \boldsymbol{D(q,\zeta)\zeta} + \boldsymbol{g(q,{}^{I}R_{B})} + \boldsymbol{J}^{T}\boldsymbol{(q,{}^{I}R_{V})h} = \boldsymbol{\tau} \tag{2.48}$$

where $\boldsymbol{h} \in \mathbb{R}^{6}$ is the generalized forces vector or wrench vector (forces and moments) that the end-effector exerts to the environment, expressed in the inertial frame {I}.

As concerns the vector of the generalized forces $\boldsymbol{\tau}$, can be written as:

$$\boldsymbol{\tau} = \begin{bmatrix} \boldsymbol{\tau_{v}} \\ \boldsymbol{\tau_{man}} \end{bmatrix} \in \mathbb{R}^{(6+n_m)} \tag{2.49}$$

where $\boldsymbol{\tau_{v}} \in \mathbb{R}^{6}$ is the vector of force/moment acting on the vehicle and $\boldsymbol{\tau_{man}} \in \mathbb{R}^{n_m}$ is the vector of manipulator's joint torques. n_m is the number of manipulator's joints. For the vehicle, the forces and moments acting on it are exerted by the thrusters. The relationship between the force/moment acting on the vehicle $\boldsymbol{\tau_{v}} \in \mathbb{R}^{6}$ and the control input of the thrusters $\boldsymbol{u_{v}} \in \mathbb{R}^{n_v}$,where n_v is the number of vehicle's thrusters, is highly nonlinear. For simplicity, a linear relationship can be considered:

$$\boldsymbol{\tau_{v}} = \boldsymbol{B_{v}u_{v}} \tag{2.50}$$

where $\boldsymbol{B_{v}} \in \mathbb{R}^{6\times n_v}$ is the Thruster Control Matrix (TCM).

For the UVMS case the relationship between the generalized forces $\boldsymbol{\tau} \in \mathbb{R}^{6+n_m}$ and the control inputs is given by:

$$\boldsymbol{\tau} = \begin{bmatrix} \boldsymbol{\tau_{v}} \\ \boldsymbol{\tau_{man}} \end{bmatrix} = \begin{bmatrix} \boldsymbol{B_{v}} & \boldsymbol{O_{6\times n_m}} \\ \boldsymbol{O_{n_m\times n_v}} & \boldsymbol{I_{n_m}} \end{bmatrix} = \boldsymbol{Bu} \tag{2.51}$$

With $\boldsymbol{u}$ is denoted the vector of control inputs:

$$\boldsymbol{u} = \begin{bmatrix} \boldsymbol{u_{v}} \\ \boldsymbol{u_{m}} \end{bmatrix} \in \mathbb{R}^{n_v+n_m} \tag{2.52}$$

where $\boldsymbol{u_{v}} \in \mathbb{R}^{n_v}$ is the vector of vehicle's control inputs and $\boldsymbol{u_{m}} \in \mathbb{R}^{n_m}$ the vector of manipulator's control inputs.

By substituting equation (2.51) in UVMS's dynamics (2.48) we have:

$$\boldsymbol{M(q)\dot{\zeta}} + \boldsymbol{C(q,\zeta)\zeta} + \boldsymbol{D(q,\zeta)\zeta} + \boldsymbol{g(q,{}^{I}R_{B})} + \boldsymbol{J}^{T}\boldsymbol{(q,{}^{I}R_{V})h} = \boldsymbol{Bu} \tag{2.53}$$

2.3 Modeling of the Manipulated Object

As we mentioned before, we are interested in transferring and manipulating an object using a team of UVMSs, so it is crucial to determine the object's equations of motion. Taking into account that the object is submerged into the water, in the object's equations of motions will be incorporated the hydrodynamic effects. So the object's equations of motion become:

$$\boldsymbol{M_{o}{}^{o}\dot{\nu}_{o}} + \boldsymbol{c({}^{o}\nu_{o})} + \boldsymbol{d({}^{o}\nu_{o})} + \boldsymbol{{}^{o}G_{o}} = \boldsymbol{{}^{o}h_{o}} \tag{2.54}$$

Where
$\boldsymbol{M_o} \in \mathbb{R}^{6\times6}$ is the inertial matrix of the object containing the hydrodynamic effect, for which holds:

$$\boldsymbol{M_o} = \begin{bmatrix} m \cdot \boldsymbol{I_3} & \boldsymbol{O_3} \\ \boldsymbol{O_3} & \boldsymbol{I} \end{bmatrix} + \boldsymbol{M_{added}} \in \mathbb{R}^{6\times6} \tag{2.55}$$

where m is the object's mass, $\boldsymbol{I} \in \mathbb{R}^{3\times3}$ is the object's moment of inertia and $\boldsymbol{M_{added}} \in \mathbb{R}^{6\times6}$ the added mass matrix due to hydrodynamic effect.
$\boldsymbol{^o\dot{\nu}_o} \in \mathbb{R}^6$: is the acceleration of the object's center of gravity in the object fixed frame
$\boldsymbol{c(^o\nu_o)} \in \mathbb{R}^6$: represent the Coriolis and centripetal terms containing also the the added Coriolis and centripetal contribution of the added mass
$\boldsymbol{d(^o\nu_o)} \in \mathbb{R}^6$: the vector containing the hydrodynamic damping forces that act to the object
$\boldsymbol{^oG_o} \in \mathbb{R}^6$: the vector containing the gravity and buoyancy force acting on the object
$\boldsymbol{^oh_o} \in \mathbb{R}^6$: the vector of the generalized forces (wrench vector) exerted at the object's center of gravity.

$$\boldsymbol{^oh_o} = \begin{bmatrix} \boldsymbol{^of_o} \\ \boldsymbol{^o\mu_o} \end{bmatrix} \in \mathbb{R}^6 \tag{2.56}$$

where
$\boldsymbol{^of_o} \in \mathbb{R}^3$: the vector of the forces acting at the object's center of gravity expressed in the object frame $\{O\}$
$\boldsymbol{^o\mu_o} \in \mathbb{R}^3$: the vector of the torques acting on the object expressed at the object's frame $\{O\}$.

2.4 Cooperative System

Object's Dynamics As part of the system we will use the object's equations of motion (2.54)

$$\boldsymbol{M_o}\boldsymbol{^o\dot{\nu}_o} + \boldsymbol{c(^o\nu_o)} + \boldsymbol{d(^o\nu_o)} + \boldsymbol{^oG_o} = \boldsymbol{^oh_o} \tag{2.57}$$

Symmetric Formulation The forces and moments acting at the object's center of gravity are exerted by the generalized forces acting at the M grasp points by the UVMSs. Based on the symmetric formulation proposed at [1,10], we can express the generalized forces acting at the object's center of gravity as the sum of the generalized forces acting at the object's center of gravity by each UVMS grasped at the i-th grasp point.

$$\boldsymbol{^Ih_o} = \boldsymbol{^Ih_{S1}} + ... + \boldsymbol{^Ih_{SM}} \tag{2.58}$$

where $\boldsymbol{^Ih_o} = \begin{bmatrix} \boldsymbol{^If_o^T} & \boldsymbol{^I\mu_o^T} \end{bmatrix}^T \in \mathbb{R}^6$ with $\boldsymbol{^If_o} \in \mathbb{R}$ and $\boldsymbol{^I\mu_o^T} \in \mathbb{R}$ be the force and torque exerted to the object's center of gravity expressed in inertial frame $\{I\}$ as illustrated in Fig. 2.2. $\boldsymbol{^Ih_{Si}} \in \mathbb{R}^6$ is the vector of the generalized force provoked to the object's center of gravity from the generalized force exerted at the i-th grasp point from the i-th UVMS, ${}^{I}\boldsymbol{h_i} \in \mathbb{R}^6$. The equation connecting ${}^{I}\boldsymbol{h_i} \in \mathbb{R}^6$ with ${}^{I}\boldsymbol{h_{Si}} \in \mathbb{R}^6$ is:

$$ {}^{I}\boldsymbol{h_{Si}} = \boldsymbol{W_i}{}^{I}\boldsymbol{h_i} \tag{2.59} $$

where

$$ \boldsymbol{W_i} = \begin{bmatrix} \boldsymbol{I_3} & \boldsymbol{O_3} \\ -\boldsymbol{S}({}^{I}\boldsymbol{r_i}) & \boldsymbol{I_3} \end{bmatrix} \tag{2.60} $$

$\boldsymbol{S}({}^{I}\boldsymbol{r_i}) \in \mathbb{R}^{3\times3}$ is the skew-symmetric matrix operator performing the cross product and ${}^{I}\boldsymbol{r_i} \in \mathbb{R}^3$ the vector connecting the i-th grasp point with the object's center of gravity in the inertial frame $\{I\}$ as illustrated in Fig. 2.2.

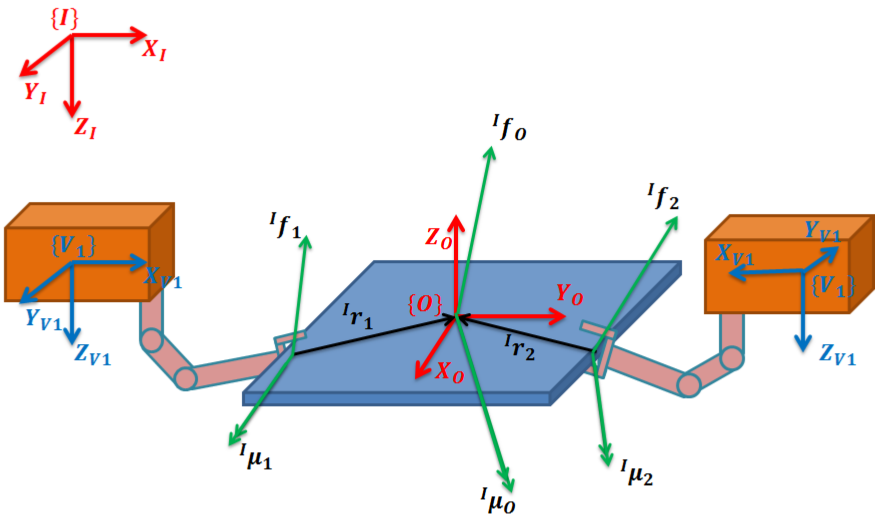

Figure 2.2: In this figure the simplified sketch of two UVMSs cooperatively grasping an object is presented. There are also illustrated the generalized forces exerted by the UVMSs at the grasp points and the generalized forces provoked to the object's center of gravity.

By substituting (2.59) in (2.58) we have:

$$ {}^{I}\boldsymbol{h_o} = \boldsymbol{W_1}{}^{I}\boldsymbol{h_1} + ... + \boldsymbol{W_M}{}^{I}\boldsymbol{h_M} = \boldsymbol{W}{}^{I}\boldsymbol{h} \tag{2.61} $$

Where $\boldsymbol{W} = \begin{bmatrix} \boldsymbol{W_1} & ... & \boldsymbol{W_M} \end{bmatrix} \in \mathbb{R}^{6\times(6\cdot M)}$ is called grasp matrix [1] and ${}^{I}\boldsymbol{h} \in \mathbb{R}^{6\cdot M}$ is the vector of the generalized forces exerted by the UVMSs at the M grasp points. For ${}^{I}\boldsymbol{h}$ we have:

$$ {}^{I}\boldsymbol{h} = \begin{bmatrix} {}^{I}\boldsymbol{h_1} \\ \vdots \\ {}^{I}\boldsymbol{h_M} \end{bmatrix} \in \mathbb{R}^{6\cdot M} \tag{2.62} $$

where ${}^{I}\boldsymbol{h_i} = \begin{bmatrix} {}^{I}\boldsymbol{f_i^T} & {}^{I}\boldsymbol{\mu_i^T} \end{bmatrix}^{\boldsymbol{T}} \in \mathbb{R}^6$ is the vector containing the generalized forces exerted by the i-th UVMS at the i-th grasp point expressed in the inertial frame

$\{I\}$, with ${}^{\boldsymbol{I}}\boldsymbol{f_i} \in \mathbb{R}^3$ and ${}^{\boldsymbol{I}}\boldsymbol{\mu_i} \in \mathbb{R}^3$ the exerted force and the torque respectively, as illustrated in Fig. 2.2.

Let ${}^{\boldsymbol{o}}\boldsymbol{R_I} \in \mathbb{R}^{3\times 3}$ be the rotation matrix from inertial $\{I\}$ to object fixed frame $\{O\}$ and let also denote the rotation matrix from inertial $\{I\}$ to object fixed frame $\{O\}$ for the wrench space as:

$$\underline{{}^{\boldsymbol{o}}\boldsymbol{R_I}} = \begin{bmatrix} {}^{\boldsymbol{o}}\boldsymbol{R_I} & \boldsymbol{O_3} \\ \boldsymbol{O_3} & {}^{\boldsymbol{o}}\boldsymbol{R_I} \end{bmatrix} \in \mathbb{R}^{6\times 6} \tag{2.63}$$

Now we can express equation (2.61) in the object fixed frame $\{O\}$ as:

$${}^{\boldsymbol{o}}\boldsymbol{h_o} = \underline{{}^{\boldsymbol{o}}\boldsymbol{R_I}} \cdot \boldsymbol{W} \cdot {}^{\boldsymbol{I}}\boldsymbol{h} \tag{2.64}$$

Let now define ${}^{\boldsymbol{I}}\boldsymbol{\nu_o} = \begin{bmatrix} {}^{\boldsymbol{I}}\boldsymbol{\nu_{1,o}^T} & {}^{\boldsymbol{I}}\boldsymbol{\nu_{2,o}^T} \end{bmatrix}^T \in \mathbb{R}^6$ as the velocity of the object's center of gravity in the inertial frame $\{I\}$ where ${}^{\boldsymbol{I}}\boldsymbol{\nu_{1,o}} \in \mathbb{R}^3$ and ${}^{\boldsymbol{I}}\boldsymbol{\nu_{2,o}} \in \mathbb{R}^3$ are the linear and angular velocities of the object's center of gravity expressed in inertial frame $\{I\}$, as illustrated in Fig. 2.3. Moreover we also define ${}^{\boldsymbol{I}}\boldsymbol{v} = \begin{bmatrix} {}^{\boldsymbol{I}}\boldsymbol{v_1^T} & \cdots & {}^{\boldsymbol{I}}\boldsymbol{v_M^T} \end{bmatrix}^T \in \mathbb{R}^{6M}$ as the vector containing the velocities of the M grasp points where ${}^{\boldsymbol{I}}\boldsymbol{v_i} = \dot{\boldsymbol{x}}_{\boldsymbol{Ei}} = \begin{bmatrix} \dot{\boldsymbol{\eta}}_{\boldsymbol{ee1,i}}{}^T & \boldsymbol{\omega_{ee,i}}{}^T \end{bmatrix}^T \in \mathbb{R}^6$ is the velocity of the i-th grasp point where $\dot{\boldsymbol{\eta}}_{\boldsymbol{ee1,i}} \in \mathbb{R}^3$ and $\boldsymbol{\omega_{ee,i}} \in \mathbb{R}^3$ are the linear and angular velocities provoked to the i-th grasp point from the i-th UVMS, as illustrated in Fig. 2.3. The relationship between them, by applying the virtual work [1] is:

$${}^{\boldsymbol{I}}\boldsymbol{v} = \boldsymbol{W}^{T\,\boldsymbol{I}}\boldsymbol{\nu_o} \tag{2.65}$$

Where $\boldsymbol{W} \in \mathbb{R}^{6\times(6\cdot M)}$ is the grasp matrix presented in (2.61).

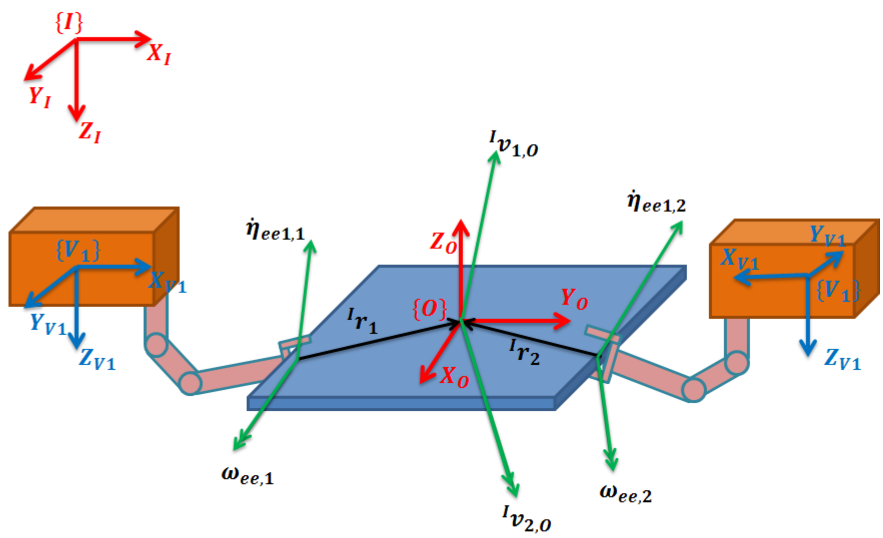

Figure 2.3: In this figure the simplified sketch of two UVMSs cooperatively grasping an object is presented. There are also illustrated the velocities at the grasp points and the velocity at the object's center of gravity

UVMS's Dynamics The equations of motion for the i-th UVMS were presented previously in equation (2.48). Let rewrite the equation as:

$$\begin{aligned}\boldsymbol{M_i}(\boldsymbol{q_i})\dot{\boldsymbol{\zeta}}_{\boldsymbol{i}} + \boldsymbol{C_i}(\boldsymbol{q_i},\boldsymbol{\zeta_i})\boldsymbol{\zeta_i} + \boldsymbol{D_i}(\boldsymbol{q_i},\boldsymbol{\zeta_i})\boldsymbol{\zeta_i} + \boldsymbol{g_i}(\boldsymbol{q_i},{}^{\boldsymbol{I}}\boldsymbol{R_B}) + \\ \boldsymbol{J_i^T}(\boldsymbol{q_i},{}^{\boldsymbol{I}}\boldsymbol{R_V})\boldsymbol{h_i} = \boldsymbol{\tau_i}\end{aligned} \tag{2.66}$$

where $i = \{1, ..., M\}$.
By substituting (2.51) in (2.66) we have:

$$\begin{aligned}\boldsymbol{M_i}(\boldsymbol{q_i})\dot{\boldsymbol{\zeta}}_{\boldsymbol{i}} + \boldsymbol{C_i}(\boldsymbol{q_i},\boldsymbol{\zeta_i})\boldsymbol{\zeta_i} + \boldsymbol{D_i}(\boldsymbol{q_i},\boldsymbol{\zeta_i})\boldsymbol{\zeta_i} + \boldsymbol{g_i}(\boldsymbol{q_i},{}^{\boldsymbol{I}}\boldsymbol{R_B}) + \\ \boldsymbol{J_i^T}(\boldsymbol{q_i},{}^{\boldsymbol{I}}\boldsymbol{R_V})\boldsymbol{h_i} = \boldsymbol{B}\boldsymbol{u_i}\end{aligned} \tag{2.67}$$

Every element of $\boldsymbol{u_i}$ has a range that depends on the corresponding motor's ability. In order to normalize the control inputs the weight factor $w_{ej} \in \mathbb{R}$ is introduced such that $u_{ij} = w_{ej}\hat{u}_{ij}$, where $u_{ij} \in \mathbb{R}$ is the j-th element of the control input vector of the i-th mobile manipulator and w_{ej} is a weighting factor such that $\hat{u}_{ij} \in [-1, 1]$. $j = \{1, ..., n_{tot}\}$. Now the control input vector of the i-th mobile manipulator becomes:

$$\boldsymbol{u_i} = \boldsymbol{W_e} \cdot \hat{\boldsymbol{u}}_{\boldsymbol{i}} \tag{2.68}$$

where $\boldsymbol{W_e} = diag(w_{e1}, ..., w_{en_{tot}}) \in \mathbb{R}^{n_{tot} \times n_{tot}}$ with $n_{tot} = n_v + n_m$.

By substituting the (2.51) and (2.68) in dynamics (2.67) we have:

$$\begin{aligned}\boldsymbol{M_i}(\boldsymbol{q_i})\dot{\boldsymbol{\zeta}}_{\boldsymbol{i}} + \boldsymbol{C_i}(\boldsymbol{q_i},\boldsymbol{\zeta_i})\boldsymbol{\zeta_i} + \boldsymbol{D_i}(\boldsymbol{q_i},\boldsymbol{\zeta_i})\boldsymbol{\zeta_i} + \boldsymbol{g_i}(\boldsymbol{q_i},{}^{\boldsymbol{I}}\boldsymbol{R_B}) + \\ \boldsymbol{J_i^T}(\boldsymbol{q_i},{}^{\boldsymbol{I}}\boldsymbol{R_V})\boldsymbol{h_i} = \boldsymbol{B}\boldsymbol{W_e}\hat{\boldsymbol{u}}_{\boldsymbol{i}}\end{aligned} \tag{2.69}$$

for simplicity let $\boldsymbol{c_i}(\boldsymbol{q_i},\boldsymbol{\zeta_i}) = \boldsymbol{C_i}(\boldsymbol{q_i},\boldsymbol{\zeta_i})\boldsymbol{\zeta_i}$ and $\boldsymbol{d_i}(\boldsymbol{q_i},\boldsymbol{\zeta_i}) = \boldsymbol{D_i}(\boldsymbol{q_i},\boldsymbol{\zeta_i})\boldsymbol{\zeta_i}$

Combining (2.69) for $i = 1, ..., M$ the equations of motion for the cooperative system of the M UVMSs are:

$$\boldsymbol{M}\dot{\boldsymbol{\zeta}} + \boldsymbol{C'}(\boldsymbol{\zeta}) + \boldsymbol{D'}(\boldsymbol{\zeta}) + \boldsymbol{G} + \boldsymbol{J}^T\boldsymbol{h} = \underline{\boldsymbol{B}\boldsymbol{W_e}}\hat{\boldsymbol{u}} \tag{2.70}$$

where

$$\boldsymbol{M} = diag(\boldsymbol{M_1}, ..., \boldsymbol{M_M}) \in \mathbb{R}^{M(6+n_m)\times M(6+n_m)} \tag{2.71}$$

$$\boldsymbol{C'} = \begin{bmatrix}\boldsymbol{c_1^T} & ... & \boldsymbol{c_M^T}\end{bmatrix}^T \in \mathbb{R}^{M(6+n_m)} \tag{2.72}$$

$$\boldsymbol{D'} = \begin{bmatrix}\boldsymbol{d_1^T} & ... & \boldsymbol{d_M^T}\end{bmatrix}^T \in \mathbb{R}^{M(6+n_m)\times M(6+n_m)} \tag{2.73}$$

$$\boldsymbol{G} = \begin{bmatrix}\boldsymbol{g_1^T} & ... & \boldsymbol{g_M^T}\end{bmatrix}^T \in \mathbb{R}^{M(6+n_m)} \tag{2.74}$$

$$\boldsymbol{J} = diag(\boldsymbol{J_1}, ..., \boldsymbol{J_M}) \in \mathbb{R}^{6M\times m(6+n_m)} \tag{2.75}$$

$$\underline{\boldsymbol{B}\boldsymbol{W_e}} = diag(\boldsymbol{B}\boldsymbol{W_e}, ..., \boldsymbol{B}\boldsymbol{W_e}) \in \mathbb{R}^{M(6+n_m)\times Mn_{tot}} \tag{2.76}$$

Accelerations By differentiating the equation (2.65) we obtain:

$$^{\boldsymbol{I}}\dot{\boldsymbol{v}} = \boldsymbol{W}^{T\boldsymbol{I}}\dot{\boldsymbol{\nu}}_{\boldsymbol{o}} + \dot{\boldsymbol{W}}^{T\boldsymbol{I}}\boldsymbol{\nu_o} \tag{2.77}$$

Defining $\boldsymbol{\zeta} = \begin{bmatrix}\boldsymbol{\zeta_1^T} & ... & \boldsymbol{\zeta_M^T}\end{bmatrix}^T \in \mathbb{R}^{M(6+n_m)}$, for the team of the UVMSs we have:

$$^{\boldsymbol{I}}\boldsymbol{v} = \boldsymbol{J}\boldsymbol{\zeta} \tag{2.78}$$

By differentiating the previous equation we have:

$$^{\boldsymbol{I}}\dot{\boldsymbol{v}} = \boldsymbol{J}\dot{\boldsymbol{\zeta}} + \dot{\boldsymbol{J}}\boldsymbol{\zeta} \tag{2.79}$$

Whole System Modeling We will regard the case that at the moment that the team of the UVMSs are exerting generalized forces on the object's grasp points in order to accelerate it, the UVMSs and the object are standing still. So we determine $\boldsymbol{\zeta} = \mathbf{0}$ and $\boldsymbol{\nu_o} = \mathbf{0}$. The equations of motion of the M UVMSs (2.70) become:

$$\boldsymbol{M\dot{\zeta}} + \boldsymbol{G} + \boldsymbol{J}^T\boldsymbol{h} = \underline{\boldsymbol{BW_e}}\boldsymbol{\hat{u}} \tag{2.80}$$

The object's equations of motion (2.57) become:

$$\boldsymbol{M_o}{}^{\boldsymbol{o}}\boldsymbol{\dot{\nu}_o} + {}^{\boldsymbol{o}}\boldsymbol{G_o} = {}^{\boldsymbol{o}}\boldsymbol{h_o} \tag{2.81}$$

As concerns the accelerations' mapping, the equation (2.77) becomes:

$${}^{\boldsymbol{I}}\boldsymbol{\dot{v}} = \boldsymbol{W}^{T\boldsymbol{I}}\boldsymbol{\dot{\nu}_o} \tag{2.82}$$

and the equation (2.79) becomes:

$${}^{\boldsymbol{I}}\boldsymbol{\dot{v}} = \boldsymbol{J\dot{\zeta}} \tag{2.83}$$

combining (2.82) and (2.83):

$$\boldsymbol{J\dot{\zeta}} = \boldsymbol{W}^{T\boldsymbol{I}}\boldsymbol{\dot{\nu}_o}\boldsymbol{\dot{\zeta}} = \boldsymbol{J}^+\boldsymbol{W}^{T\boldsymbol{I}}\boldsymbol{\dot{\nu}_o} \tag{2.84}$$

$$\boldsymbol{\dot{\zeta}} = \boldsymbol{J}^+\boldsymbol{W}^{T\boldsymbol{I}}\boldsymbol{\dot{\nu}_o} \tag{2.85}$$

and by expressing the object's acceleration on object-fixed frame:

$$\boldsymbol{\dot{\zeta}} = \boldsymbol{J}^+\boldsymbol{W}^{T\boldsymbol{I}}\underline{\boldsymbol{R_o}}{}^{\boldsymbol{o}}\boldsymbol{\dot{\nu}_o} \tag{2.86}$$

By substituting equation (2.64) in the object's equations of motion (2.81) we have:

$$\boldsymbol{M_o}{}^{\boldsymbol{o}}\boldsymbol{\dot{\nu}_o} + {}^{\boldsymbol{o}}\boldsymbol{G_o} = \underline{{}^{\boldsymbol{o}}\boldsymbol{R_I}}\boldsymbol{W}^{\boldsymbol{I}}\boldsymbol{h} \tag{2.87}$$

from the (2.87), we can determine the vector of generalized forces acting at the grasp points ${}^{\boldsymbol{I}}\boldsymbol{h} \in \mathbb{R}^{6M}$ as:

$${}^{\boldsymbol{I}}\boldsymbol{h} = \boldsymbol{W}^+\underline{{}^{\boldsymbol{o}}\boldsymbol{R_I}}^{-1}(\boldsymbol{M_o} \cdot {}^{\boldsymbol{o}}\boldsymbol{\dot{\nu}_o} + {}^{\boldsymbol{o}}\boldsymbol{G_o}) \tag{2.88}$$

By substituting (2.88) and (2.86) into (2.80) we have:

$$\boldsymbol{MJ}^+\boldsymbol{W}^{T\boldsymbol{I}}\underline{\boldsymbol{R_o}}{}^{\boldsymbol{o}}\boldsymbol{\dot{\nu}_o} + \boldsymbol{G} + \boldsymbol{J}^T\boldsymbol{W}^+\underline{{}^{\boldsymbol{o}}\boldsymbol{R_I}}^{-1}(\boldsymbol{M_o} \cdot {}^{\boldsymbol{o}}\boldsymbol{\dot{\nu}_o} + {}^{\boldsymbol{o}}\boldsymbol{G_o}) = \underline{\boldsymbol{BW_e}}\boldsymbol{\hat{u}} \tag{2.89}$$

$$\begin{aligned}(\boldsymbol{MJ}^+\boldsymbol{W}^{T\boldsymbol{I}}\underline{\boldsymbol{R_o}} + \boldsymbol{J}^T\boldsymbol{W}^+\underline{{}^{\boldsymbol{o}}\boldsymbol{R_I}}^{-1}\boldsymbol{M_o})^{\boldsymbol{o}}\boldsymbol{\dot{\nu}_o} +& \\ (\boldsymbol{G} + \boldsymbol{J}^T\boldsymbol{W}^+\underline{{}^{\boldsymbol{o}}\boldsymbol{R_I}}^{-1}{}^{\boldsymbol{o}}\boldsymbol{G_o}) &= \underline{\boldsymbol{BW_e}}\boldsymbol{\hat{u}}\end{aligned} \tag{2.90}$$

By denoting:

$$\boldsymbol{E} = (\boldsymbol{MJ}^+\boldsymbol{W}^{T\boldsymbol{I}}\underline{\boldsymbol{R_o}} + \boldsymbol{J}^T\boldsymbol{W}^+\underline{{}^{\boldsymbol{o}}\boldsymbol{R_I}}^{-1}\boldsymbol{M_o}) \tag{2.91}$$

and

$$\boldsymbol{G_{tot}} = (\boldsymbol{G} + \boldsymbol{J}^T\boldsymbol{W}^+\underline{{}^{\boldsymbol{o}}\boldsymbol{R_I}}^{-1}{}^{\boldsymbol{o}}\boldsymbol{G_o}) \tag{2.92}$$

Equation (2.90) becomes:

$$\boldsymbol{E}^{\boldsymbol{o}}\boldsymbol{\dot{\nu}_o} + \boldsymbol{G_{tot}} = \underline{\boldsymbol{BW_e}}\boldsymbol{\hat{u}} \tag{2.93}$$

The mapping from the control input space to the task space, 6-dimensional object's center of gravity acceleration space, is denoted with the following equation:

$${}^{\boldsymbol{o}}\boldsymbol{\dot{\nu}_o} + \boldsymbol{E}^+\boldsymbol{G_{tot}} = \boldsymbol{E}^+\underline{\boldsymbol{BW_e}}\boldsymbol{\hat{u}} \tag{2.94}$$

Chapter 3

Optimal Grasp Points Planning

As mentioned in the introduction, in a pick - and - place operation the robot has to reach an object, grasp it and transfer it from an initial location to a final one. The first phase of this operation, which is the reaching to grasp, includes the selection of grasp points on the transfered object, where the robot has to grasp at. In case that the object is heavy enough to be manipulated by a single robot, multiple robots have to be used in order to manipulate cooperatively the object. In this way, not only the object's transfer can be guaranteed but also better performance is possible to be achieved with lower energy consumption.

In order to exploit the benefits that the cooperative manipulation provides, it is crucial to determine the grasp points position for each robot extremely carefully. As it was mentioned, the correct selection of the grasp points could be beneficial for the rest of the operation (i.e., transportation, manipulation), by leading to lower energy consumption with higher performance of the cooperative system and as a result, to higher autonomy. On the other hand, an improper grasping could lead to inability of the team to execute the imposed operation successfully, which means system's inability to transfer the object, possible destruction of the object or of the robotic equipment and finally the failure of the whole operation.

From the above we can refer that we need a portion that will reflect our system's needs and the goals that we hope to achieve. This portion will evaluate the proposed set of grasp points in order the latter to be compared with other sets for the decision of the optimal one. These portions are the *grasp quality measures*. Two grasp quality measures are proposed in this chapter.

3.1 Related Work

The selection of grasp points on an object has already been studied by many researchers in the past and there have been presented various methods for this purpose. In [11] the MAG performance index is presented. This index is used to evaluate a grasp for a predefined trajectory-task. A method for the selection of the optimal grasp points based on the geometry of the grasp is presented in [12]. More specifically the optimal grasp position is decided such that the distance between the center of gravity and the closest edge of the triangle, consisted by the three grasping points (grasping for 3-finger hand), to be the largest possible and the loads on the robots to be as equal as possible. The optimization of load distribution is used for the grasp points selection in [13]. The initial grasp point set is decided by maximizing the probability that the center of mass exists in the conveyable area produced by a certain grasp point configuration. By measuring the real center of mass they change the grasp points based on a criterion that takes into account the load capacity of each robot and the system's energy consumption in case of re-grasping. In [14] an index is proposed for measuring the compatibility of manipulator postures for a generalized task description using manipulability ellipsoids. This can be extended in grasp points planning. Three quality measures for the evaluation of the grasp of multifinger hands are proposed in [15]. Particularly, the two measures are based on the grasp matrix properties and the third one is task - oriented but none of them are taking the system's dynamics into account. In [16] the quality of grasp is evaluated as the relation between the force to be balanced and the force applied by the griper's fingers. In [17] an optimization scheme is presented for the selection of contact points by minimizing the magnitude of the contact forces required to resist a required external force. Finally, in [18] a review of the quality measures proposed in grasp literature to quantify the grasp quality is presented. The presented measures are not taking into account the system's dynamics. Most of these works are focusing in grasping using multifinger hands, but generally, they can be extended in the cooperative grasping by multiple robots.

3.2 Proposed Approach

What we can refer from the aforementioned methods is that most of them are task specific. This means that, it is assumed an a priori knowledge of the tasks that the system has to execute during the operation. As a result, the grasp quality measure takes into account the task that has to be executed in order to provide grasp points that lead to the accomplishment of these tasks in an optimal way, based on certain criteria.

Although, this approach is desirable and more efficient when the tasks are known a priori, in many cases we are not aware of the exact path that the robots holding the manipulated object have to execute and as a result of the consecutive tasks that have to be executed. Especially, when the environment is unstructured, like an area full of ruins after an earthquake, an unexplored terrain or the deep ocean, in our case, the path has to be planned by the robots using on-line information provided by their sensory system. Even in the case that we are aware of the environment's exact structure, the system is possible to face unexpected situations like moving obstacles with unpredictable motion (e.g., a collapsing floor or a chain moved by ocean currents). In cases like these, the tasks have to be imposed during the operation and not before it.

A solution to this problem could be the re-grasping. In this case, the grasp points could be selected based on a priori defined tasks and if the system has to deal with a situation that was not predicted, then the robots will have to change grasp points during the operation, performing, as it is called, re-grasping. This is not a preferable action, because is time-consuming and demands a set of maneuvers to be executed by each robot in order to change grasp point position, which is a drawback having in mind the limited energy resources of an autonomous robot. So we have to ensure that whatever the maneuver needed for the collision avoidance with an obstacle or in order to follow a path, the system (robots and manipulated object) must be able to execute it, by also achieving the least energy consumption possible.

Consecutively, the quality measures for the evaluation of the grasp points have to provide grasp points that permit to the system to execute every possible task that might arise with the least possible energy consumption. For this purpose, non-task specific grasp quality measures are proposed to be used.

In this work, we will denote as task a desired acceleration of the grasped object's center of gravity. This direction can be translational, rotational or combination of them. As system's performance will be denoted the system's ability to accelerate in a desired direction (i.e., the acceleration's magnitude) for a given finite amount of energy.

In this chapter, two non-task specific measures are presented in order to define grasp points that by grasping them, the UVMSs holding the object will be able to execute every needed task (i.e., accelerate the object in a desired direction) with the least possible energy consumption. More specifically, the first proposed method aims at the maximization of the system's dynamic manipulability ellipsoid (DME) [8], by also guaranteeing a bound in the system's minimum performance, as concerns the provoked acceleration. As a result, this measure maximizes the system's potential acceleration in every direction of the task space (6-d acceleration space), by maximizing the volume of the system's DME, and also guarantees a lower bound at it. The second proposed method, is the minimum distance in the translational and rotational acceleration space, as arise from the decomposition of the system's DME. The maximization of this measure guarantees that the system will accelerate in the most difficult direction in the best possible way, i.e. higher magnitude with lower energy consumption.

3.3 Dynamic Manipulability Ellipsoids

As it was mentioned before we are interested to determine grasp points on the object that by grasping them the UVMSs will be able to exert at the object's center of gravity accelerations in any direction needed with high magnitude and the least possible energy consumption.

A great tool for this purpose is the Dynamic Manipulability Ellipsoids (DME). The DME provides a mapping between the space that reflect the consumed energy, which is in our case the control input space, and the space that reflects the result produced by the consumption of this energy, in our case the provoked acceleration of the object. From the system's DME we will extract the proposed measures. So in this section we will present the general concept of DME and we will build the system's (UVMSs and object) DME, in order to use it for the determination of the grasp quality measures.

3.3.1 The General Concept

The concept of manipulability ellipsoids and of the manipulability measure was first proposed by T. Yoshikawa in [8]. As concerns the manipulator case, the manipulability measure is a quantitative measure of manipulating ability of robot arms in positioning and orienting the end-effectors. This measure describes the ease of the robotic mechanism of changing arbitrarily the position and the orientation of the end - effector. The measure that Yoshikawa proposed is:

$$w = \sqrt{det(\boldsymbol{J}(\theta)\boldsymbol{J}^T(\theta))} \tag{3.1}$$

where $\boldsymbol{J}(\boldsymbol{\theta})$ is the Jacobian matrix of the manipulator at the posture $\boldsymbol{\theta}$. One of the facts that Yoshikawa mentioned was that w is equal to the volume of an ellipsoid with principal axis of size equal to the singular values of the Jacobian matrix at the determined posture. The greater the volume, the higher the degree of arbitrariness in changing the position and orientation of the end effector.

In the aforementioned, the manipulator's dynamics are not taken into account. In many cases, it is desirable to quantify the degree of arbitrariness of changing the acceleration of the end-effector under some constraints on the joint driving force. So, Yoshikawa adopt a new measure of the arm's manipulability, taking into account the arm's dynamics, the dynamic manipulability measure.

In our case, we are not only interested in the ease of the system to exert forces at the object's center of gravity, but also we are aiming to take into account the dynamic properties the manipulating object. This is important due to the fact that there are directions of the acceleration which are more difficult to implement on others due to the object's geometric characteristics. By using DMEs we can create a mapping between the control input space, that reflects the consuming energy from the system, and the task space , which is in our case the object's acceleration space. By taking advantage of these properties, we will extract the proposed grasp quality measures from the analysis of the system's Dynamic Manipulability Ellipsoid.

3.3.2 Dynamic Manipulability Ellipsoid For The Cooperative System

In order to use the system's Dynamic Manipulability Ellipsoid (DME) to extract the grasp quality measures, first we have to create it. In this section, the dynamic manipulability ellipsoid of the cooperative system, described in equation (2.93), will be built. For the following analysis we will take into account the procedure followed in [19].

Assuming that the normalized control inputs lie in a unitary sphere, let:

$$\hat{\boldsymbol{u}}^{\boldsymbol{T}}\hat{\boldsymbol{u}} = 1 \tag{3.2}$$

Solving (2.93) with respect to the control input vector $\hat{\boldsymbol{u}}$ we have:

$$\hat{\boldsymbol{u}} = \underline{\boldsymbol{BW_e}}^{+}\boldsymbol{E}({}^{\boldsymbol{o}}\dot{\boldsymbol{\nu}}_{\boldsymbol{o}} + \boldsymbol{E}^{+}\boldsymbol{G_{tot}}) \tag{3.3}$$

and by substituting (3.3) in (3.2) we have:

$$({}^{\boldsymbol{o}}\dot{\boldsymbol{\nu}}_{\boldsymbol{o}} + \boldsymbol{E}^{+}\boldsymbol{G_{tot}})^T\boldsymbol{E}^T(\underline{\boldsymbol{BW_e}}^{+})^T\underline{\boldsymbol{BW_e}}^{+}\boldsymbol{E}({}^{\boldsymbol{o}}\dot{\boldsymbol{\nu}}_{\boldsymbol{o}} + \boldsymbol{E}^{+}\boldsymbol{G_{tot}}) = 1 \tag{3.4}$$

Equation (3.4) is the equation of the system's dynamic manipulability ellipsoid in the task space.

In order to find out the ellipsoid's structure, we have to find the principal axes of the dynamic manipulability ellipsoid expressed in equation (3.4). Similar to [7] we use singular value decomposition of the mapping in (2.94), $\boldsymbol{E}^{+}\underline{\boldsymbol{BW_e}} \in \mathbb{R}^{6\times(M\cdot n_{tot})}$.

$$\boldsymbol{E}^{+}\underline{\boldsymbol{BW_e}} = \boldsymbol{U\Sigma V^T} \tag{3.5}$$

where
$\boldsymbol{\Sigma} = \begin{bmatrix} diag(\sigma_1,\ldots,\sigma_6) & \boldsymbol{O}_{6\times(M\cdot n_{tot})} \end{bmatrix} \in \mathbb{R}^{6\times(M\cdot n_{tot})}$
$\boldsymbol{U} = \begin{bmatrix} \boldsymbol{u_1} & \ldots & \boldsymbol{u_6} \end{bmatrix} \in \mathbb{R}^{6\times 6}$
$\boldsymbol{V} = \begin{bmatrix} \boldsymbol{\nu_1} & \ldots & \boldsymbol{\nu_6} \end{bmatrix} \in \mathbb{R}^{(M\cdot n_{tot})\times(M\cdot n_{tot})}$
where σ_i is the i-th singular value of the matrix $\boldsymbol{E}^{+}\underline{\boldsymbol{BW_e}} \in \mathbb{R}^{6\times(M\cdot n_{tot})}$ and it is also the size of the i-th principal axis. $\boldsymbol{u_i}$ is the unitary vector of the i-th principal axis of the ellipsoid in the object fixed frame {O}.

Let denote the vector of the ellipsoid's i-th principle axis as $\boldsymbol{u_i}\sigma_i \in \mathbb{R}^6$ as illustrated in Fig. 3.1. Let now define a 6-dimensional frame so that the origin

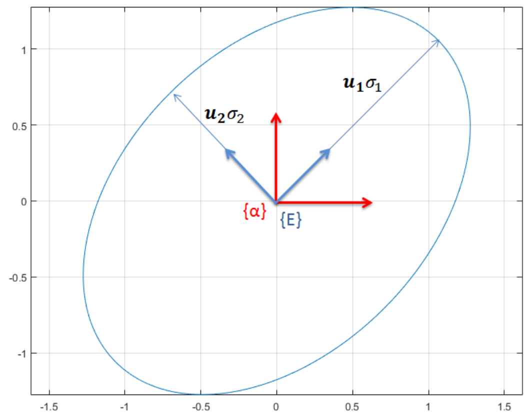

Figure 3.1: Ellipsoid's Axes

coincides with the center of the ellipsoid (and the object's center of gravity) and the axes of this frame coincide with the principal axes of the ellipsoid and let denote it as {E} as illustrated in Fig. 3.1. Let also define the 6-dimensional task space frame whose axes correspond to each element of the acceleration vector, three axes correspond to the translational acceleration and three to the rotational acceleration, and is denoted as $\{a\}$ as illustrated in Fig. 3.1.

We denote as rotation matrix from frame $\{E\}$ to frame $\{a\}$ the matrix:

$$^{\boldsymbol{a}}\boldsymbol{R_E} = \boldsymbol{U} = \begin{bmatrix} \boldsymbol{u_1} & \ldots & \boldsymbol{u_6} \end{bmatrix} \in \mathbb{R}^{6\times 6} \tag{3.6}$$

With the dynamic manipulability ellipsoid, presented in this section, we are able to determine the potential magnitude of the acceleration in any direction for a control input vector of unitary magnitude. In this way we are able to detect the directions that the acceleration has potentially higher magnitude and the directions with lower ones.

3.4 Proposed Quality Measures

In this section the quality measures for the evaluation and the selection of the grasp points, will be presented. As it was mentioned before, the presented quality measures are base on the system's dynamic manipulability ellipsoid. It was, also, highlighted that by maximizing the size of the system's DME, the magnitude of the potential acceleration of the object's center of gravity is also maximized, for a finite amount of consumed energy (control inputs) by the UVMSs. The following presented measures aim at the maximization of the DME's size by treating it in different ways.

The assumptions that have been made for the selection of the quality measures are:

- We are aware of the object's exact shape.
- We are aware of the exact position of the object's center of gravity.
- The end-effectors of the UVMSs are performing rigid grasp at the grasp points on the object.
- The UVMSs used for the pick and place operation are identical.
- During the selection of the grasp points, each robot is aware of the grasp points that corresponds to each one of the other robots of the team.

3.4.1 1st Measure: Dynamic Manipulability Ellipsoid's Volume

The first proposed measure that will be presented aims in the maximization of the DME's volume with a lower bound in the minimum performance, as concerns the acceleration produced.

According to [8] the volume of the dynamic manipulability ellipsoid is:

$$w = d \cdot \sigma_1 \cdot ... \cdot \sigma_6 \tag{3.7}$$

where $\sigma_i \in \mathbb{R}$ is the i-th singular value of the transformation (3.5) and $d \in \mathbb{R}$ is a constant value for which holds:

$$d = \begin{cases} (2\pi)^{(m/2)}/(2 \cdot 4 \cdot 6... \cdot (m-2) \cdot m) \text{when m is even} \\ 2(2\pi)^{(m-1)/2}/(1 \cdot 3 \cdot 5 \cdot ... \cdot (m-2) \cdot m) \text{when m is odd} \end{cases} \tag{3.8}$$

where m is the size of the task space. In our application $m = 6$.

As it was mentioned before, our goal is to achieve the highest possible acceleration norm in any direction in the task space (not only in any acceleration's direction but also in any combination of translational and rotational acceleration). In order to do so, we have to maximize the volume of DME or the function:

$$f(\boldsymbol{x}) = w = d \cdot \sigma_1 \cdot ... \cdot \sigma_6 \tag{3.9}$$

where $\boldsymbol{x} \in \mathbb{R}^{3M}$ encloses the position of the grasp points on the object.

As can be seen in (3.4) the DME illustrates the system's "generalized acceleration" produced by the given set of control inputs. This acceleration incorporates the "net acceleration" ${}^{\boldsymbol{o}}\dot{\boldsymbol{\nu}}_{\boldsymbol{o}} \in \mathbb{R}^6$ that is applied to the object's center of gravity, and the acceleration produced by the system's weight $\boldsymbol{E}^{+}\boldsymbol{G_{tot}} \in \mathbb{R}^6$. The latter portion facilitates the acceleration to certain directions and resists to others. As mentioned in [20] this acceleration produces an equal translation of the ellipsoid with respect to object fixed frame. To illustrate this point, in

Fig. 3.2a the ellipsoid before and after its translation due to weight is presented, with segmented and continuous line respectively. With the red arrow the desired direction along which we want to accelerate the system is presented. Moreover, an undesirable situation in which the ellipsoid does not contains the origin of the reference frame is illustrated in Fig. 3.2b. Obviously, in this case the previously desired direction can not be achieved.

Although that we are maximizing the ellipsoid's volume, this does not guarantee that the acceleration's norm is maximized in every direction. As can be seen in Fig. 3.3 the volume of the ellipsoid with the dotted line is greater than the one with the continuous line, even if in some directions the distance between the center of the ellipsoid and the surface is greater at the ellipsoid with the continuous line. From the above we can refer the possibility of the system's inability to lift its own weight.

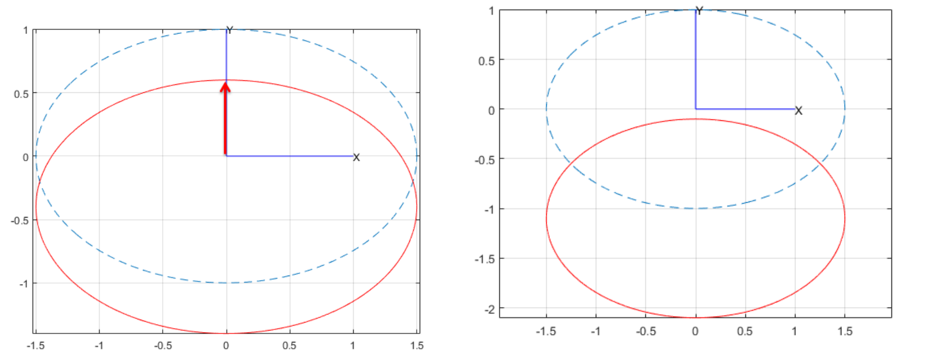

(a) The desired acceleration can be achieved.

(b) The desired acceleration can not be achieved.

Figure 3.2: Translated ellipsoid due to weight: the ellipsoid before and after its translation is indicated with segmented and continuous line respectively. The red arrow illustrates the desired direction of the acceleration.

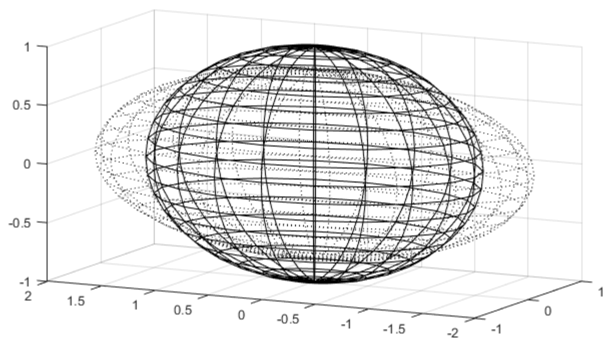

Figure 3.3: Comparison of ellipsoids with different volumes

In order to avoid this situation, a constraint will accompany the proposed measure. As it is known, the minimum principal axis is the smallest distance between a point of the ellipsoid's surface and its center. We have to guarantee that this distance $min(\sigma_i) \in \mathbb{R}$, will be greater than the euclidean norm of the acceleration produced by the system's weight $\|\boldsymbol{E}^{+}\boldsymbol{G_{tot}}\| \in \mathbb{R}$ or in inequality form:

$$min(\sigma_i) \geq \|\boldsymbol{E}^{+}\boldsymbol{G_{tot}}\| \tag{3.10}$$

Assuming now that the equality in (3.10) exists, we are facing the danger of the system to be able to lift the object without the ability of performing any other maneuver. In order to avoid this situation a safety factor which guarantees that the system in combination with the object's lift will be able to be accelerated in other directions is presented. Let this safety factor be $a > 1$. So the proposed constraint becomes:

$$min(\sigma_i) \geq a \cdot \|\boldsymbol{E}^{+}\boldsymbol{G_{tot}}\|, \quad a > 1 \tag{3.11}$$

3.4.2 2nd Measure: Minimum Distance in Translational and Rotational Acceleration Space

The previous method uses as measure the volume of dynamic manipulability ellipsoid. But the task space is constituted by translational and rotational accelerations, which are of different units and, consequently, of different order of magnitude. More specifically the magnitude of the rotational acceleration depends on the distance between the grasp points and the object's center of gravity in a way that the longer this distance, the higher the rotational acceleration's magnitude. As a result, the solution is dominated by the accelerations with the highest magnitude. In order to overcome this situation, the following measure is presented.

The second proposed quality measure, aims at the maximization of the minimum distance in the translational and rotational acceleration space, as results from the decomposition of the DME (3.4).

The task space is constituted by the object's translational and rotational accelerations, or in other words by two subspaces, the translational and the rotational acceleration space, which are of different order of magnitude that depends on the object's size. Due to that fact the results of the previous method are dominated by the acceleration with the highest magnitude. In order to overcome this situation, it is proposed to confront separately the two acceleration spaces, i.e. the translational and the rotational.

For the DME, is known that the distance between the ellipsoid's reference frame's origin and a point of its surface, in a given direction, expresses the ease of the system to accelerate in this direction. As a result, our goal is to maximize this distance in the direction that takes its minimum value. As concerns the two acceleration spaces, it is desired to maximize the minimum distance between the center of each subspace and its boundary.

The task space decomposition With $\{a\}$, is denoted the frame of the task space as mentioned in previous sections and with $\{E\}$ the ellipsoid's frame, also mentioned in previous sections. In order to take into account the system's weight, the ellipsoid's center has to be translated with respect to the task space reference frame in direction and measure equal to $\boldsymbol{E}^{+}\boldsymbol{G_{tot}} \in \mathbb{R}^6$. For convenience we will translate the frame of the task space in direction and measure equal to $-\boldsymbol{E}^{+}\boldsymbol{G_{tot}} \in \mathbb{R}^{6}$. Let $\{a'\}$ be the translated frame due to the system's weight and the vector connecting the frames $\{a\}$ and $\{a'\}$ is:

$$^{\boldsymbol{a}}\boldsymbol{r_{a'}} = -\boldsymbol{E}^{+}\boldsymbol{G_{tot}} \tag{3.12}$$

This vector is illustrated in Fig. 3.4. In equation (3.6) the rotation matrix from the ellipsoid's frame $\{E\}$ to the task space frame $\{a\}$ has been denoted as $^{\boldsymbol{a}}\boldsymbol{R_E} = \boldsymbol{U} = \begin{bmatrix}\boldsymbol{u_1} & \dots & \boldsymbol{u_6}\end{bmatrix} \in \mathbb{R}^{6\times 6}$. So expressing the vector in (3.12) in ellipsoid's frame we have:

$$^{\boldsymbol{E}}\boldsymbol{r_{a'}} = {}^{\boldsymbol{E}}\boldsymbol{R_a}{}^{\boldsymbol{a}}\boldsymbol{r_{a'}} \tag{3.13}$$

Let $^{\boldsymbol{a'}}\dot{\boldsymbol{\nu}} \in \mathbb{R}^{6}$ be the vector connecting the origin of the new task space frame $\{a'\}$ with a point of the ellipsoid's surface in the new object fixed frame as illustrated in Fig. 3.4. The homogeneous transformation from the new object fixed frame $\{a'\}$ to the ellipsoid's frame {E} is:

$$^{\boldsymbol{E}}\boldsymbol{T_{a'}} = \begin{bmatrix} ^{\boldsymbol{E}}\boldsymbol{R_a} & ^{\boldsymbol{E}}\boldsymbol{r_{a'}} \\ \boldsymbol{O_{1\times 6}} & 1 \end{bmatrix} = \begin{bmatrix} ^{\boldsymbol{E}}\boldsymbol{R_a} & ^{\boldsymbol{E}}\boldsymbol{R_a}{}^{\boldsymbol{a}}\boldsymbol{r_{a'}} \\ \boldsymbol{O_{1\times 6}} & 1 \end{bmatrix} \in \mathbb{R}^{7\times 7} \tag{3.14}$$

In this way, the vector connecting a point on the surface of the ellipsoid with the origin of $\{a'\}$ in the ellipsoid frame is:

$$^{\boldsymbol{E}}\dot{\boldsymbol{\nu}} = {}^{\boldsymbol{E}}\boldsymbol{T_{a'}}{}^{\boldsymbol{a'}}\dot{\boldsymbol{\nu}} \tag{3.15}$$

Let $^{\boldsymbol{E}}\boldsymbol{l} \in \mathbb{R}^{6}$ be the vector connecting the same point of the ellipsoid's surface with the origin of the ellipsoid's frame, as illustrated in Fig. 3.4, for which holds:

$$^{\boldsymbol{E}}\boldsymbol{l} = {}^{\boldsymbol{E}}\boldsymbol{r_{a'}} + {}^{\boldsymbol{E}}\dot{\boldsymbol{\nu}} = {}^{\boldsymbol{E}}\boldsymbol{R_a}{}^{\boldsymbol{a}}\boldsymbol{r_{a'}} + {}^{\boldsymbol{E}}\boldsymbol{T_{a'}}{}^{\boldsymbol{a'}}\dot{\boldsymbol{\nu}} \tag{3.16}$$

The elements of $^{\boldsymbol{E}}\boldsymbol{l} \in \mathbb{R}^{6}$ are satisfying the ellipsoid's equation:

$$\frac{{}^{E}l_1{}^{2}}{\sigma_1^2} + \frac{{}^{E}l_2{}^{2}}{\sigma_2^2} + \dots + \frac{{}^{E}l_6{}^{2}}{\sigma_6^2} = 1 \tag{3.17}$$

where $^{E}l_i \in \mathbb{R}$ is the i-th element of the vector $^{\boldsymbol{E}}\boldsymbol{l} \in \mathbb{R}^{6}$ with $i = \{1, \dots, 6\}$.

Let us now write the ellipsoid surface point position expressed in $\{a'\}$ as:

$$^{\boldsymbol{a'}}\dot{\boldsymbol{\nu}} = \|^{\boldsymbol{a'}}\dot{\boldsymbol{\nu}}\|^{\boldsymbol{a'}}\hat{\dot{\boldsymbol{\nu}}} \tag{3.18}$$

where $\|^{\boldsymbol{a'}}\dot{\boldsymbol{\nu}}\| \in \mathbb{R}$ is the euclidean norm of the vector $^{\boldsymbol{a'}}\dot{\boldsymbol{\nu}} \in \mathbb{R}^{6}$. By substituting (3.18) in (3.16), the latter becomes:

$$^{\boldsymbol{E}}\boldsymbol{l} = {}^{\boldsymbol{E}}\boldsymbol{r_{a'}} + {}^{\boldsymbol{E}}\dot{\boldsymbol{\nu}} = {}^{\boldsymbol{E}}\boldsymbol{R_a}{}^{\boldsymbol{a}}\boldsymbol{r_{a'}} + {}^{\boldsymbol{E}}\boldsymbol{T_{a'}}\|^{\boldsymbol{a'}}\dot{\boldsymbol{\nu}}\|^{\boldsymbol{a'}}\hat{\dot{\boldsymbol{\nu}}} \tag{3.19}$$

Given now, a desired direction of acceleration in the new task space frame $\{a'\}$, $^{\boldsymbol{a'}}\hat{\dot{\boldsymbol{\nu}}} \in \mathbb{R}^{6}$, and by solving (3.19) and (3.17) we are able to determine the distance between the frame's origin and the ellipsoid's surface in the given directions, which is also the potential magnitude of the acceleration in this direction, i.e. $\|^{\boldsymbol{a'}}\dot{\boldsymbol{\nu}}\| \in \mathbb{R}$. Let $^{\boldsymbol{a'}}\hat{\dot{\boldsymbol{\nu}}}_{\boldsymbol{tr}} \in \mathbb{R}^{3}$ be the desired direction in the translational space, for which we are interested. Following the previous procedure, the magnitude of the acceleration in the desired direction, translational in this case, depends on the desired direction in the task space, i.e. on the desired rotational direction. This fact is illustrated in Fig. 3.5. In case 1 the

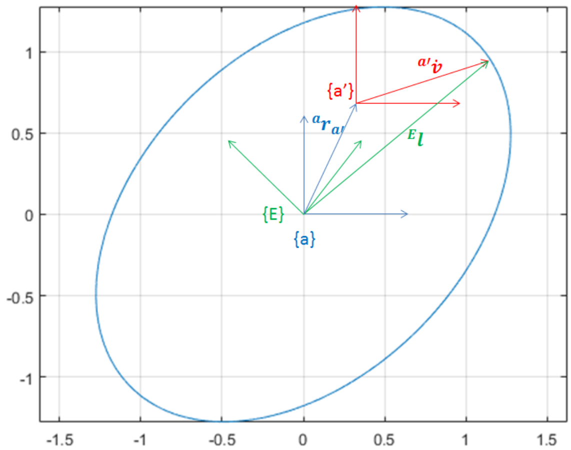

Figure 3.4: Translated frame due to weight

green arrow represents the case that the rotational direction is equal to zero $^{a'}\hat{\boldsymbol{\nu}} = \begin{bmatrix} ^{a'}\hat{\boldsymbol{\nu}}_{\boldsymbol{tr}}^{T} & \boldsymbol{O}_{\boldsymbol{1\times3}}^{T} \end{bmatrix}^{T} \in \mathbb{R}^{6}$. In case 2, with the orange arrow, the desired direction is a combination of a desired translational and a rotational direction $^{a'}\hat{\boldsymbol{\nu}} = \left[(^{a'}\hat{\boldsymbol{\nu}}_{\boldsymbol{tr}} cos(\theta))^{T} \quad (^{a'}\hat{\boldsymbol{\nu}}_{\boldsymbol{rot}} sin(\theta))^{T} \right]^{T} \in \mathbb{R}^{6}$. From the Fig. 3.5 we can refer that the projection in the translational subspace is greater in case 2 comparing to the case 1.

Therefore, in order to create an acceleration subspace, for any given direction, we are using the measure with the higher projected magnitude in this subspace.

Proposed Measure After the decomposition of the task space and the creation of the translational and rotational spaces, we are able to determine the minimum distances in these two resulted acceleration spaces. Let $d_{mintr} \in \mathbb{R}$ and $d_{minrot} \in \mathbb{R}$ be the minimum distance in the translational and rotational acceleration spaces respectively. In order to ensure that at least at the worst direction the acceleration is the highest possible, we have to maximize these quantities.

Let $f(\boldsymbol{x}) = f(d_{mintr}, d_{minrot}) \in \mathbb{R}$ be a function that depends on the way that we want to treat the two quantities. For the maximization of this function we have to solve a multi-objective optimization problem. There are many methods of multi-objective optimization as mentioned in [21] depending on the hierarchy between the analyst and the decision maker. For our application we will use the weighting method [21]. If $we \in [0, 1]$ is a weighting factor, the function that has to be maximized is:

$$f(\boldsymbol{x}) = (1 - we) \cdot d_{mintr} + we \cdot d_{minrot} \tag{3.20}$$

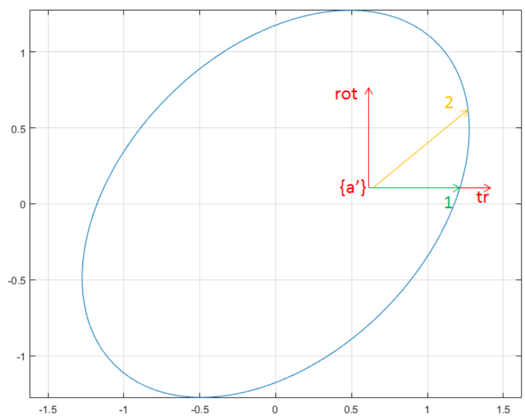

Figure 3.5: Acceleration's desired direction: The green arrow represents the case 1 where the rotational direction is equal to zero. The case 2, where the desired direction is a combination of a desired translational and a rotational direction is denoted by the orange arrow. The projection in the translational subspace is greater in case 2 comparing to the case 1.

Chapter 4

Optimization Schemes

Generally, on an object there might be numerous of potential grasp points. Especially in the case that the object is thin enough, like a plate, so that the end-effector can grasp at any point of its periphery, the potential grasp points are infinite.

In order to select the grasp points, we have to use an optimization scheme. As it was mentioned before, we are looking forward in maximizing the system's DME. In the case that is examined, the cooperative manipulation of an object by a number of UVMSs, not only the position of the grasp points affects the size of the DME, but also each of the UVMSs' configuration. Our main goal is to find the grasp points' position, but for each set of grasp points there is a UVMS's configuration that maximizes the grasp quality measure. So the UVMSs' configuration must be taken into account. As a result, the decision variables are the position of the grasp points and the configuration of each UVMS (vehicle's and joint's position).

As concerns the grasp points' position, generally, we need a three-variables representation in the 3-dimensional space. If we are aware of the object's shape and of its pose with respect to the inertial frame, as it is assumed in our case, we are able to determine the position of a point on the object's periphery by only using one variable. Let this variable for the i-th grasp point denoted as $r_i \in \mathbb{R}$, where $i = \{1, ..., M\}$. So let $\boldsymbol{x}$ be the vector of the decision variables:

$$\boldsymbol{x} = \begin{bmatrix} r_1 & ... & r_M & \boldsymbol{q_1^T} & ... & \boldsymbol{q_M^T} \end{bmatrix}^{\boldsymbol{T}} \in \mathbb{R}^{(M+n_{tot} \cdot M)} \tag{4.1}$$

4.1 1st Measure: Dynamic Manipulability Ellipsoid's Volume

In this section, the optimization scheme for the selection of the grasp points by maximizing the volume of the system's DME, will be presented.

4.1.1 Objective Function

As objective function, the function presented in equation (3.9) will be used. As it was mentioned, we are interested in maximizing this function or to minimize the function:

$$f(\boldsymbol{x}) = -d \cdot \sigma_1 \cdot ... \cdot \sigma_6 \tag{4.2}$$

4.1.2 Constraints

The constraints that have to be satisfied when we decide grasp points, will be introduced.

Configuration's Limits Let for simplicity denote as $\boldsymbol{q_i} \in \mathbb{R}^{6+n_m}$ the vector containing the pose of the i-th UVMS (i.e., its position in the inertial frame $\{I\}$ and its attitude (roll, pitch, yaw angles)) and the n_m manipulator's joints' position.

$$\boldsymbol{q_i} = \begin{bmatrix} \boldsymbol{\eta_{1i}} \\ \boldsymbol{\eta_{2i}} \\ \boldsymbol{q_{mi}} \end{bmatrix} \in \mathbb{R}^{6+n_m} \tag{4.3}$$

As concerns the joints' position, each joint has an angle range in which it can move. Let $q_{ij,min}$ be the lower bound as concern the angle that the j-th manipulator's joint of the i-th UVMS can reach and $q_{ij,max}$ be the upper bound as concern the angle that the j-th manipulator's joint of the i-th UVMS can reach. So we have:

$$\boldsymbol{q_{mi,min}} = \begin{bmatrix} q_{i1,min} & \cdots & q_{iM,min} \end{bmatrix}^T \in \mathbb{R}^{n_m} \tag{4.4}$$

and

$$\boldsymbol{q_{mi,max}} = \begin{bmatrix} q_{i1,max} & \cdots & q_{iM,max} \end{bmatrix}^T \in \mathbb{R}^{n_m} \tag{4.5}$$

for which holds:

$$\boldsymbol{q_{mi,min}} \leq \boldsymbol{q_{mi}} \leq \boldsymbol{q_{mi,max}} \tag{4.6}$$

Let now conciser that each UVMS is able to, or it is desirable to, move in a predefined area. We define as $\boldsymbol{\eta_{1i,min}} \in \mathbb{R}^3$ and $\boldsymbol{\eta_{1i,max}} \in \mathbb{R}^3$ the limits of this area (a sphere around a reference frame). So we also have:

$$\boldsymbol{\eta_{1i,min}} \leq \boldsymbol{\eta_{1i}} \leq \boldsymbol{\eta_{1i,max}} \tag{4.7}$$

For the UVMS's attitude we also can consider bounds. Let $\boldsymbol{\eta_{2i,min}} \in \mathbb{R}^3$ and $\boldsymbol{\eta_{2i,max}} \in \mathbb{R}^3$ be the lower and the upper bound respectively.

$$\boldsymbol{\eta_{2i,min}} \leq \boldsymbol{\eta_{2i}} \leq \boldsymbol{\eta_{2i,max}} \tag{4.8}$$

Combining all the previous bounds we can define for the i-th UVMS the lower and the upper configuration bound as $\boldsymbol{q_{i,min}} = \begin{bmatrix} \boldsymbol{\eta^T_{1i,min}} & \boldsymbol{\eta^T_{2i,min}} & \boldsymbol{q^T_{mi,min}} \end{bmatrix}^T \in \mathbb{R}^{6+n_m}$ and $\boldsymbol{q_{i,max}} = \begin{bmatrix} \boldsymbol{\eta^T_{1i,max}} & \boldsymbol{\eta^T_{2i,max}} & \boldsymbol{q^T_{mi,max}} \end{bmatrix}^T \in \mathbb{R}^{6+n_m}$ respectively. So we have the contraint for the UVMS's configuration:

$$\boldsymbol{q_{i,min}} \leq \boldsymbol{q_i} \leq \boldsymbol{q_{i,max}} \tag{4.9}$$

There are also some equality constraints as concerns the UVMS's configuration. These constraints can be represented for the i-th UVMS as:

$$\boldsymbol{A_i q_i} = \boldsymbol{b_{eq,i}} \tag{4.10}$$

Let $\boldsymbol{q} \in \mathbb{R}^{M\cdot(6+n_m)}$ be the vector containing the configuration vectors $\boldsymbol{q_i} \in \mathbb{R}^{6+n_m}$ for the M UVMSs such that:

$$\boldsymbol{q} = \begin{bmatrix} \boldsymbol{q_1} \\ \vdots \\ \boldsymbol{q_M} \end{bmatrix} \in \mathbb{R}^{M\cdot(6+n_m)} \tag{4.11}$$

then from (4.9) and (4.10) and for $i = \{1, ..., M\}$, we have the constraints:

$$\boldsymbol{q_{min}} \leq \boldsymbol{q} \leq \boldsymbol{q_{max}} \tag{4.12}$$

and

$$\boldsymbol{Aq} = \boldsymbol{b_{eq}} \tag{4.13}$$

End-Effector's Position As long as we are using as decision variables both the UVMSs configuration and the grasp points' position, it is crucial to ensure that the point at which the i-th UVMS grasps, coincides with the i-th grasp point. In order to determine the end-effector's position of the i-th UVMS, its direct kinematics will be used. From equation (2.14) we have

$$\boldsymbol{\eta_{ee,i}} = \boldsymbol{k}(\boldsymbol{\eta_{1i}}, \boldsymbol{\eta_{2i}}, \boldsymbol{q_{mi}}) \tag{4.14}$$

or using the notation (4.3):

$$\boldsymbol{\eta_{ee,i}} = \begin{bmatrix} \boldsymbol{\eta_{ee1,i}} \\ \boldsymbol{\eta_{ee2,i}} \end{bmatrix} = \boldsymbol{k}(\boldsymbol{q_i}) \tag{4.15}$$

For the grasp points' position, as it was mentioned before, the variable $r_i \in \mathbb{R}$ is used. For the mapping from the 1-dimensional to the 3-dimensional representation the function $\boldsymbol{P_1}(\cdot)$ is used. This function depends on the object and its pose with respect to the inertial frame $\{I\}$. So the i-th grasp point position in the inertial frame is:

$$\boldsymbol{p_{1i}} = \boldsymbol{P_1}(r_i) \tag{4.16}$$

In order to guarantee that the point at which the i-th UVMS grasps, coincides with the i-th grasp point, the following equation must be satisfied:

$$\boldsymbol{p_{1i}} = \boldsymbol{\eta_{ee1,i}} \tag{4.17}$$

End-Effector's Orientation As concerns the orientation, it is obvious that the end-effector can not grasp the object arbitrarily. The permitted orientation depends on the object's shape. By using the variable $r_i \in \mathbb{R}$ again, the function that gives this orientation for any value of this variable is denoted as $\boldsymbol{P_2}(\cdot)$. So the orientation that the end-effector must have in order to grasp at the i-th grasp point is given as:

$$\boldsymbol{p_{2i}} = \boldsymbol{P_2}(r_i) \tag{4.18}$$

In order to guarantee that the end-effector's orientation is the permitted for the certain grasp point, the following equation must be satisfied

$$\boldsymbol{p_{2i}} = \boldsymbol{\eta_{ee2i}} \tag{4.19}$$

Collision Avoidance In order to decide the optimal grasp points we have to guarantee that the UVMSs will not collide to each other. Let assume that the AUVs body fixed frame has its origin at the center of gravity and we will determine as r_{safe} the distance of the most remote point on the surface of the AUV with respect to the center of gravity. In this way we create a sphere that totally contains the AUV. Assuming that we have identical UVMSs, the distance that the two AUVs' center of gravity have to keep in order the two vehicles not to collide to each other is $d_{safe} = 2 \cdot r_{safe}$. So we have the constraint:

$$d_i^{i'} \geq 2 \cdot r_{safe} \tag{4.20}$$

where

$$d_i^{i'} = \|\boldsymbol{\eta_{ee1}}(\boldsymbol{q_i}) - \boldsymbol{\eta_{ee1}}(\boldsymbol{q_{i'}})\| \tag{4.21}$$

and

$$i, i' \in \{1, ..., M\}, \quad i \neq i' \tag{4.22}$$

This constrain has to be repeated for every possible combination between the UVMSs of the team.

Minimum Performance Constraint As it was mentioned at the definition of the 1st measure, we are looking forward to maximize the volume of the DME by also guaranteeing a lower bound as concerns the system's performance. This will be achieved by using the constraint proposed in (3.11).

$$min(\sigma_i) \geq a \cdot \|\boldsymbol{E}^{+}\boldsymbol{G_{tot}}\|, \quad a > 1 \tag{4.23}$$

4.1.3 Optimization Scheme

Combining the objective function and the aforementioned constraints, the optimization scheme for the selection of grasp points by using as quality measure the volume of DME is:

$$\begin{aligned}
\min_{\boldsymbol{x}} & f = -d \cdot \sigma_1 \cdot ... \cdot \sigma_6 \\
\text{s.t. } & \boldsymbol{q_{min}} \leq \boldsymbol{q} \leq \boldsymbol{q_{max}} \\
& \boldsymbol{P_1}(r_i) = \boldsymbol{\eta_{ee1}}(\boldsymbol{q_i}) \\
& \boldsymbol{P_2}(r_i) = \boldsymbol{\eta_{ee2}}(\boldsymbol{q_i}) \\
& \boldsymbol{A}\boldsymbol{q} = \boldsymbol{b_{eq}} \\
& d_i^{i'} \geq 2 \cdot r_{safe} \\
& min(\sigma_i) \geq \alpha \cdot \|\boldsymbol{E}^{+}\boldsymbol{G_{tot}}\|
\end{aligned}$$

4.2 2nd Measure: Minimum Distance in Translational and Rotational Acceleration Space

In this section, the optimization scheme for the selection of grasp points by maximizing the minimum distances in the translational and rotational acceleration space, will be presented.

4.2.1 Objective Function

As objective function, the function presented in equation (3.20) will be used. As it was mentioned we are interested in maximizing this function or to minimize the function:

$$f(\boldsymbol{x}) = -((1 - we) \cdot d_{mintr} \cdot \gamma + we \cdot d_{minrot}) \tag{4.24}$$

where $\gamma \in \mathbb{R}$ is used in order to compensate the difference in the order of magnitude which is due to the different units of the two accelerations.

4.2.2 Constraints

The constraint that will be used in this optimization scheme are the same to those presented for the 1st measure excluding the one for the minimum performance.

4.2.3 Optimization Scheme

Combining the objective function and the aforementioned constraints, the optimization scheme for the selection of grasp points by using as quality measure the minimum distance in translational and rotational acceleration spaces is:

$$\min_{\boldsymbol{x}} f(\boldsymbol{x}) = -((1 - we) \cdot \gamma \cdot d_{mintr} + we \cdot d_{minrot}) \tag{4.25}$$

$$\text{s.t.} \quad \boldsymbol{q_{min}} \leq \boldsymbol{q} \leq \boldsymbol{q_{max}} \tag{4.26}$$

$$\boldsymbol{P_1}(r_i) = \boldsymbol{\eta_{ee1}}(\boldsymbol{q_i}) \tag{4.27}$$

$$\boldsymbol{P_2}(r_i) = \boldsymbol{\eta_{ee2}}(\boldsymbol{q_i}) \tag{4.28}$$

$$\boldsymbol{Aq} = \boldsymbol{b_{eq}} \tag{4.29}$$

$$d_i^{i'} \geq 2 \cdot r_{safe} \tag{4.30}$$

Chapter 5

Simulations

In the previous chapters, two measures for the grasp point evaluation were presented. These measures aim at the determination of the grasp points on an object, where M UVMS have to grasp at during a pick-and-place operation. In this chapter the previously presented measures will be tested by applying the optimization schemes presented in Chapter 4 in different case studies. These optimization schemes are written in MATLAB code, which is presented in the appendix.

Various scenarios were tested, including the cases where 2, 3 and 4 UVMSs are used in order to grasp a rod and a plate of square, rectangle, circular and elliptical face. Based on these results we will examine the appropriateness of each measure's use.

5.1 1st Measure: Dynamic Manipulability Ellipsoid's Volume

In this section, the grasp points that resulted by the use of the 1st grasp quality measure, will be presented. The following results emerged from the solution of the optimization scheme presented in Section 4.1.3. The code of this optimization scheme, written in MATLAB, is listed in the Appendix. The results for the rod are presented in figures 5.1a, 5.1c and 5.1e.For the square in figures 5.2a, 5.2c and 5.2e. For the rectangle in figures 5.3a, 5.3c and 5.3e. Finally, for the circle and the ellipse the results are presented in figures 5.4a, 5.4c ,5.4e and 5.5a, 5.5c, 5.5e respectively.

As a first comment on the result it is mentioned that, intuitively in the rod's case we would expect the grasp point to be located at the rod's extremes. As can be seen in figures 5.1a, 5.1c and 5.1e two of the grasp points are located at the extremes of the rod irrespective of the number of the mobile manipulators. This fact could be a first verification for the presented methods.

Generally, we can refer that this method gives results in a short time. The decision of the grasp points is taken in time that ranges between 0.5 min and 1 min depending on the object's shape and the initial grasp points. This performance makes this method suitable in cases that the decision have to be taken fast. A case like this is when we are not aware of the exact shape of the object or we are not aware of obstacles that might prevent the robot from grasping certain areas of the object's surface. In this case, the object identification have to be done during the operation by the robots. As a result, the grasp points decision must not last long, guaranteeing that the robots will not consume excessive energy resources in this phase.

As concerns general comments about the proposed measure, this measure is used for the maximization of the volume of the system's DME. In this way, the DME is magnified in any direction and consequently the translational and rotational potential acceleration and their combination do so. The way that this volume is maximized is arbitrary, so it does not guarantees that the magnitude of the acceleration in any direction is maximized. Furthermore, the method does not separates the two acceleration subspaces, the translational and the rotational, which are of different units and as a result of different order of magnitude. So the acceleration space with the higher order of magnitude, or at least the one that by changing the grasp points has the greater influence in the DME's volume change, dominates the solution. Another remark is that this measure does not take into account the influence of the gravitational forces exerted to the UVMSs and the object, but is protected from the undesirable situations (system's inability to lift and manipulate the object due to the weight's influence) that this fact could lead, by the use of the proposed constraint (3.11). Finally, it is important to be mentioned that by using as decision variables the UVMSs' configuration (4.1), a change in this configuration is possible to lead to greater change of the DME's volume, than a change in the grasp points position. As a result, the final solution, it is possible to reflect the optimal UVMSs' configuration and not the optimal grasp points' position.

5.2 2nd Measure: Minimum Distance in Translational and Rotational Acceleration Space

In this section the grasp point resulted by the use of the 2nd grasp quality measure will be presented. The following results emerged from the solution of the optimization scheme presented in Section 4.2.3. The code of this optimization scheme, written in MATLAB, is introduced in the Appendix. The results for the rod are presented in figures 5.1b, 5.1d and 5.1f. For the square in figures 5.2b, 5.2d and 5.2f. For the rectangle in figures 5.3b, 5.3d and 5.3f. Finally, for the circle and the ellipse the results are presented in figures 5.4b, 5.4d ,5.4f and 5.5b, 5.5d, 5.5f respectively.

Firstly, for this measure also, the intuitive verification of the results will be used. As it was mentioned before, in the rod's case we would expect, intuitively, the grasp point to be located at the rod's extremes. As can be seen in figures 5.1b, 5.1d and 5.1f, two of the grasp points are located at the extremes of the rod, irrespective of the number of the mobile manipulators.

Generally, this measure aims at the maximization of the system's worst performance. A great advantage of this measure is that decomposes the 6-dimensional task space into two spaces, the translational and the rotational acceleration space, and treats them separately. In this way, the different order of magnitude between the two accelerations does not affect the result as does in the previous method, where the acceleration with the higher order of magnitude dominates the solution. On the other hand, the decomposition of the task space deals with the difficult situation of how the accelerations' combination will be reflected to the two new spaces. This situation is treated with the projection of the combined acceleration to the two spaces as was explained in Section 3.4.2. The decomposition and the treatment of the combined accelerations lead to the measures great disadvantage, which is the decision time. This time ranges from 30 min to 50 min depending on the number of the UVMSs, the object's shape and the initial grasp points. This time makes this method unsuitable for on-line grasp point selection. This is due to the fact that during the operation the robots are consuming their own energy resources, so such a long decision time would not be desirable. Consequently, this method is suitable for the selection of grasp points, before the start of the operation in cases where the object's shape and position are already known.

A great advantage, on the other hand, is that this method takes into account the effect of the systems weight, so the danger of the system's inability to lift its own weight is vanished, if the robots have the performance to do so. This measure's characteristic, also ensures that the expected system's performance will not change due to the weight's effect, as happens in the 1st proposed measure.

5.3 Comparison

Comparing the results, the two measures give different grasp points for the same number of robots. This is due to the fact that the two measures maximize in a different way the system's DME. In order to illustrate this difference, the proposed measures are compared with a third one which is the volume of the DME without the proposed constraint. The three methods tested in the case that 4 UVMSs grasp a rod. After the selection, for each set of grasp points, the task space is scanned and for every direction in the acceleration space the maximum magnitude is given using as decision variables the UVMSs' configuration. For each grasp points set, we are searching for the maximum and the minimum magnitude of the acceleration. In Fig. 5.6 these results are presented. The bar-1 corresponds to the volume maximization with the constraint, the bar-2 to the minimum distance maximization and the bar-3 to the volume maximization without the constraint. As can be seen in Fig. 5.6a the first measure provides the larger maximum magnitude while the 2nd method the minimum. On the other hand in Fig. 5.6b the second method has the best minimum performance. What can we also refer from the Fig. 5.6b is that the minimum magnitude overcomes the constraint for the minimum performance which has been set to $a \cdot \|\boldsymbol{E}^{+}\boldsymbol{G_{tot}}\| = 1.5355$ for all the measures. This means that the constraint did not affect the selection of the grasp points in this case study.

From the above we can refer that as concerns the 1st proposed measure, the grasp points guarantee the maximization of the DME with a bound in the minimum performance, as concerns the provoked acceleration. On the other, hand the 2nd proposed measure maximizes the magnitude of the accelerations' directions with the minimum magnitude and as a result maximizes the systems worst performance, as concerns the provoked acceleration.

As concerns the duration of the decision time, for the first measure this time ranges from 0.5 min to 1 min depending on the object's shape and the initial grasp points. On the other hand, for the second measure, the time ranges from 30 min to 50 min. Having in mind that at the time of the decision the UVMSs consume energy resources the first measure is acceptable while the second is not. As a result, the two measures have to be used in different cases. For instance, the first one is suitable to be used during real time operations, where the exact object's shape has not to be known a priori and is figured by robot onboard sensor system. On the other hand, the second measure is suitable for more demanding operations, only in the special case that the decision can be taken beforehand.

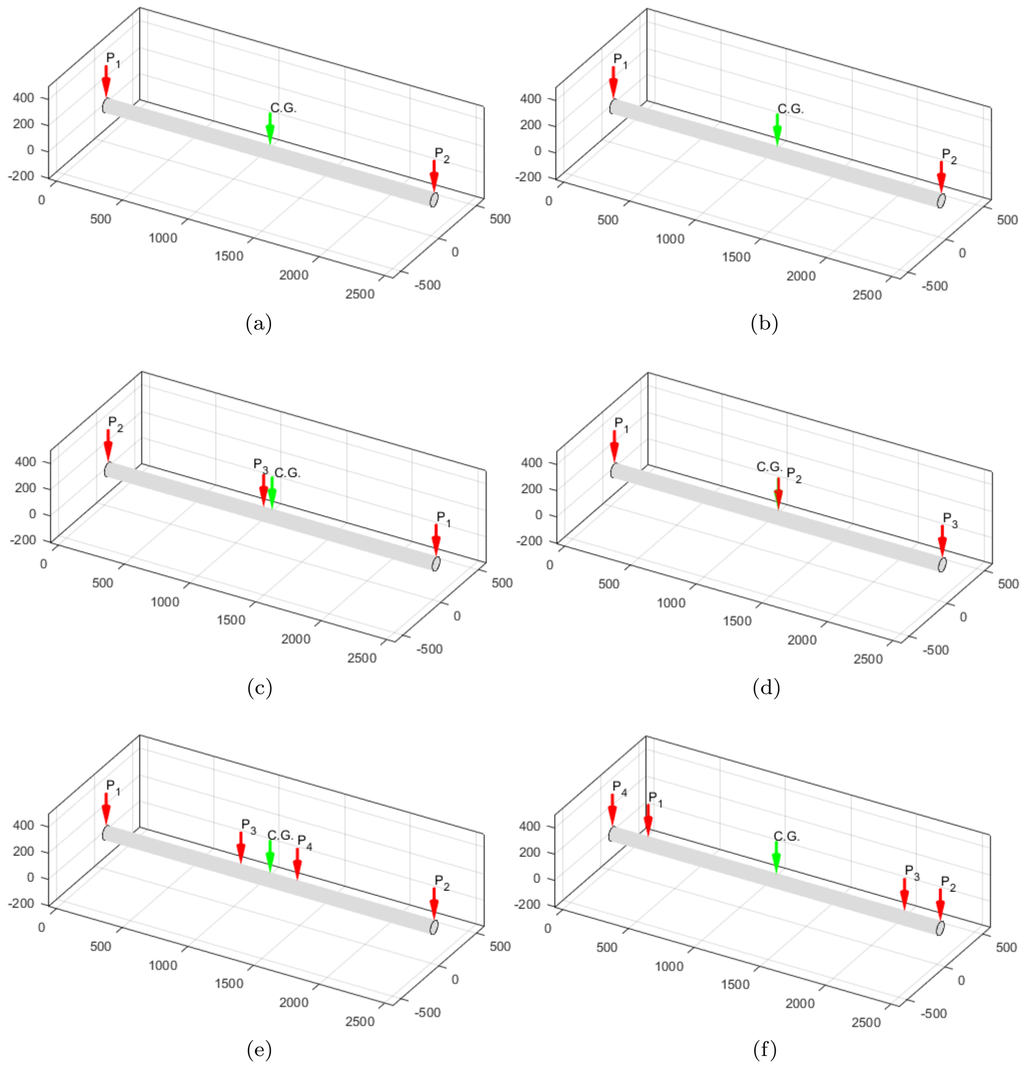

Figure 5.1: Grasp points positions on a rod: the results (a), (c) and (e) correspond to the volume maximization for 2, 3 and 4 robots respectively and the results (b), (d) and (f) to the minimum distance maximization for 2, 3 and 4 robots respectively.

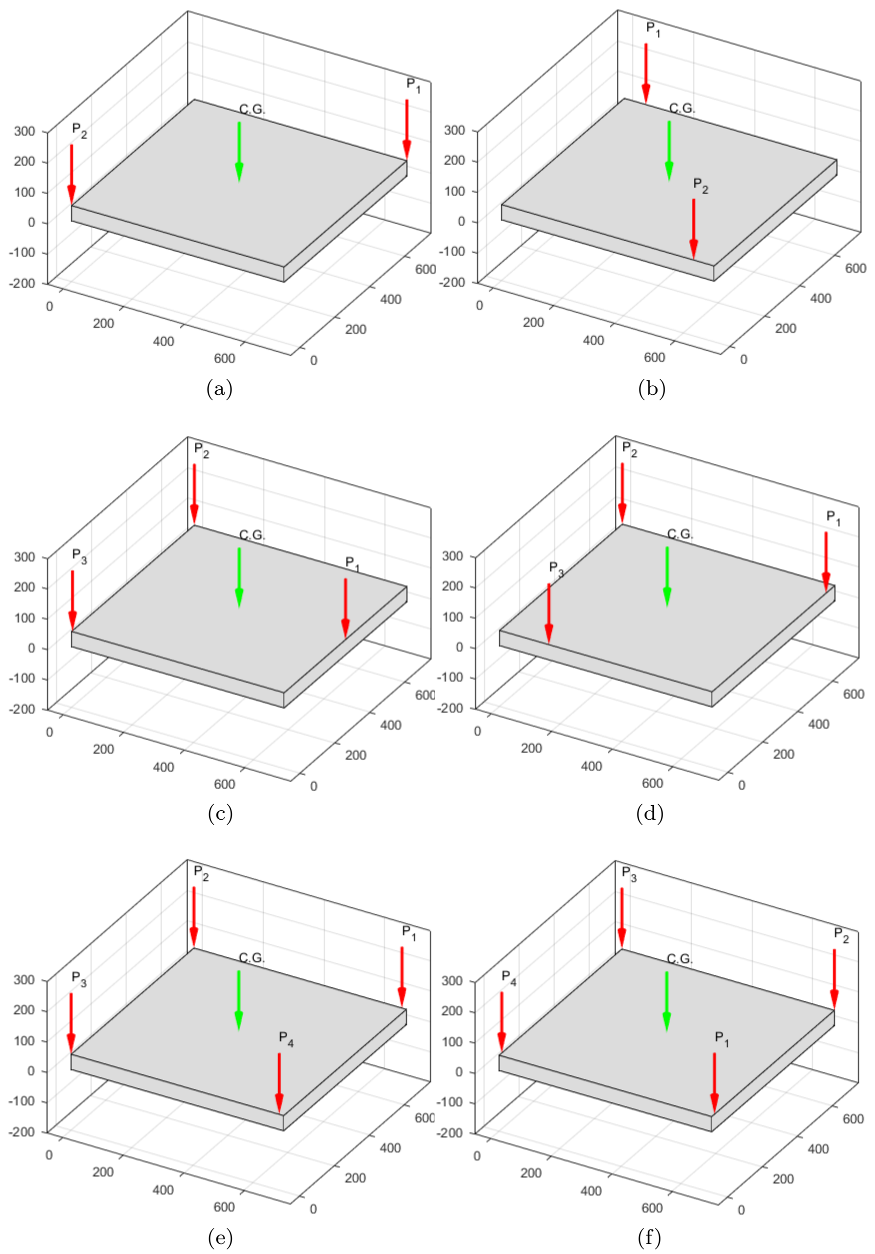

Figure 5.2: Grasp points positions on a square: the results (a), (c) and (e) correspond to the volume maximization for 2, 3 and 4 robots respectively and the results (b), (d) and (f) to the minimum distance maximization for 2, 3 and 4 robots respectively.

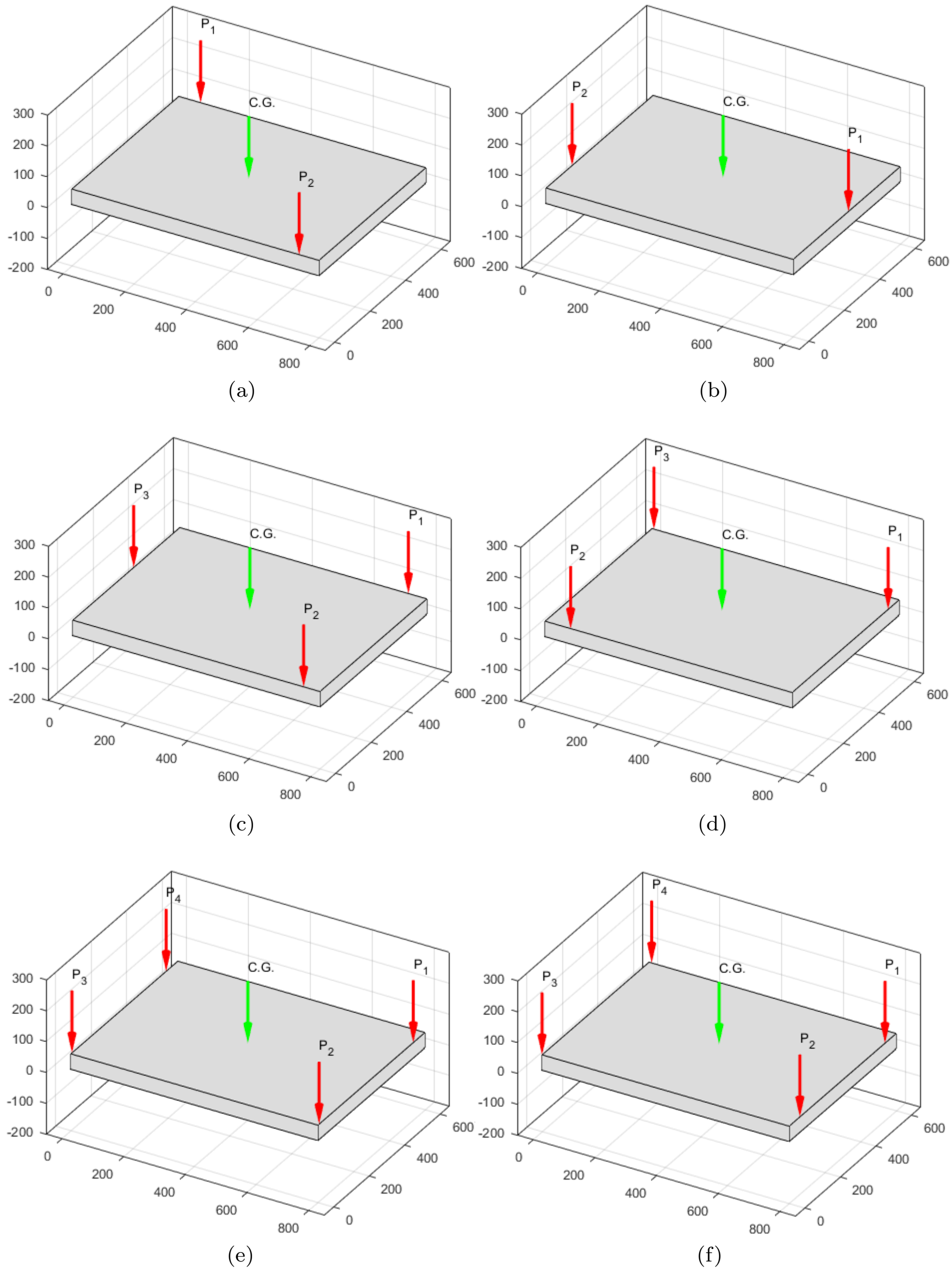

Figure 5.3: Grasp points positions on a rectangle: the results (a), (c) and (e) correspond to the volume maximization for 2, 3 and 4 robots respectively and the results (b), (d) and (f) to the minimum distance maximization for 2, 3 and 4 robots respectively.

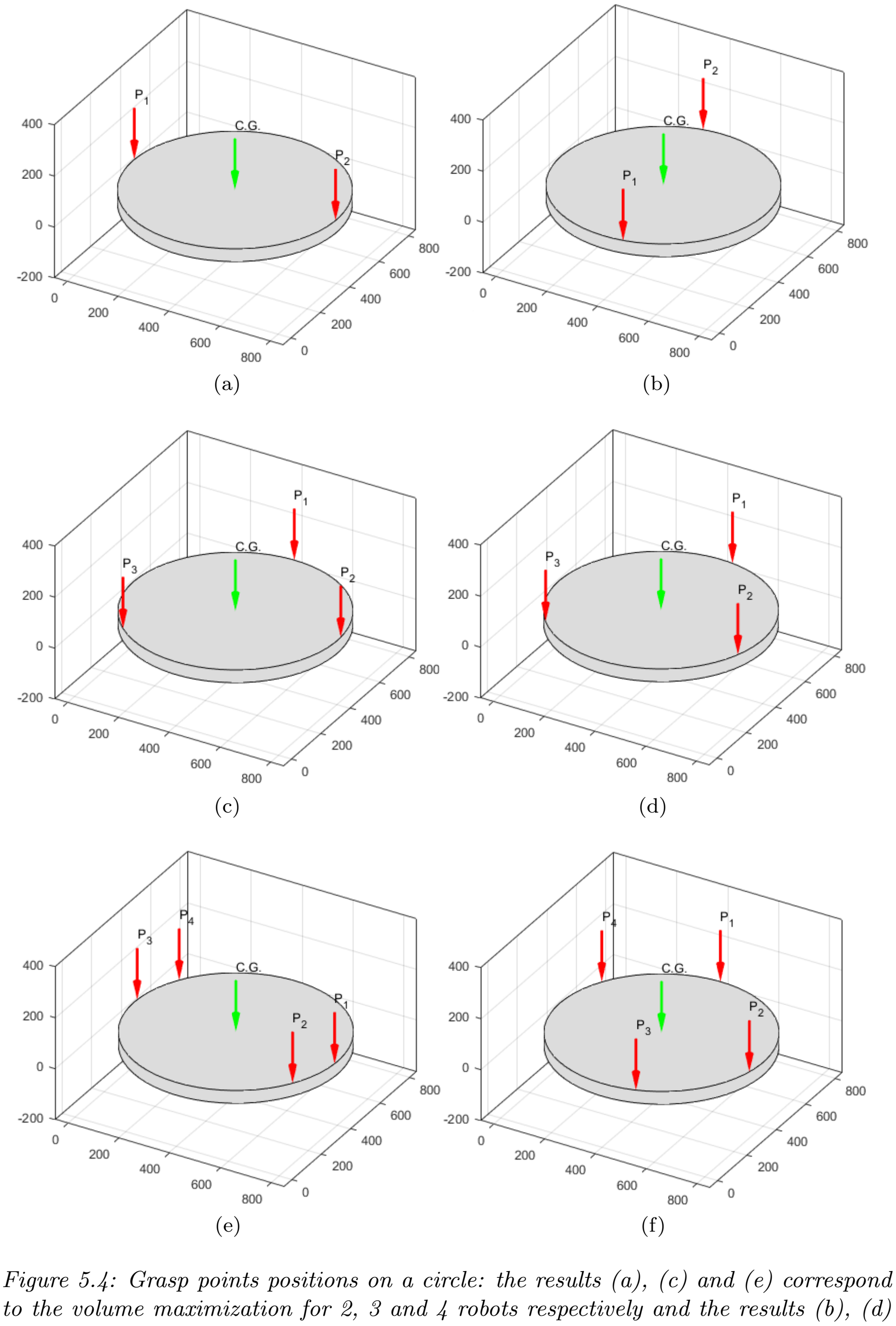

(a) (b) (c) (d) (e) (f)

Figure 5.4: Grasp points positions on a circle: the results (a), (c) and (e) correspond to the volume maximization for 2, 3 and 4 robots respectively and the results (b), (d) and (f) to the minimum distance maximization for 2, 3 and 4 robots respectively.

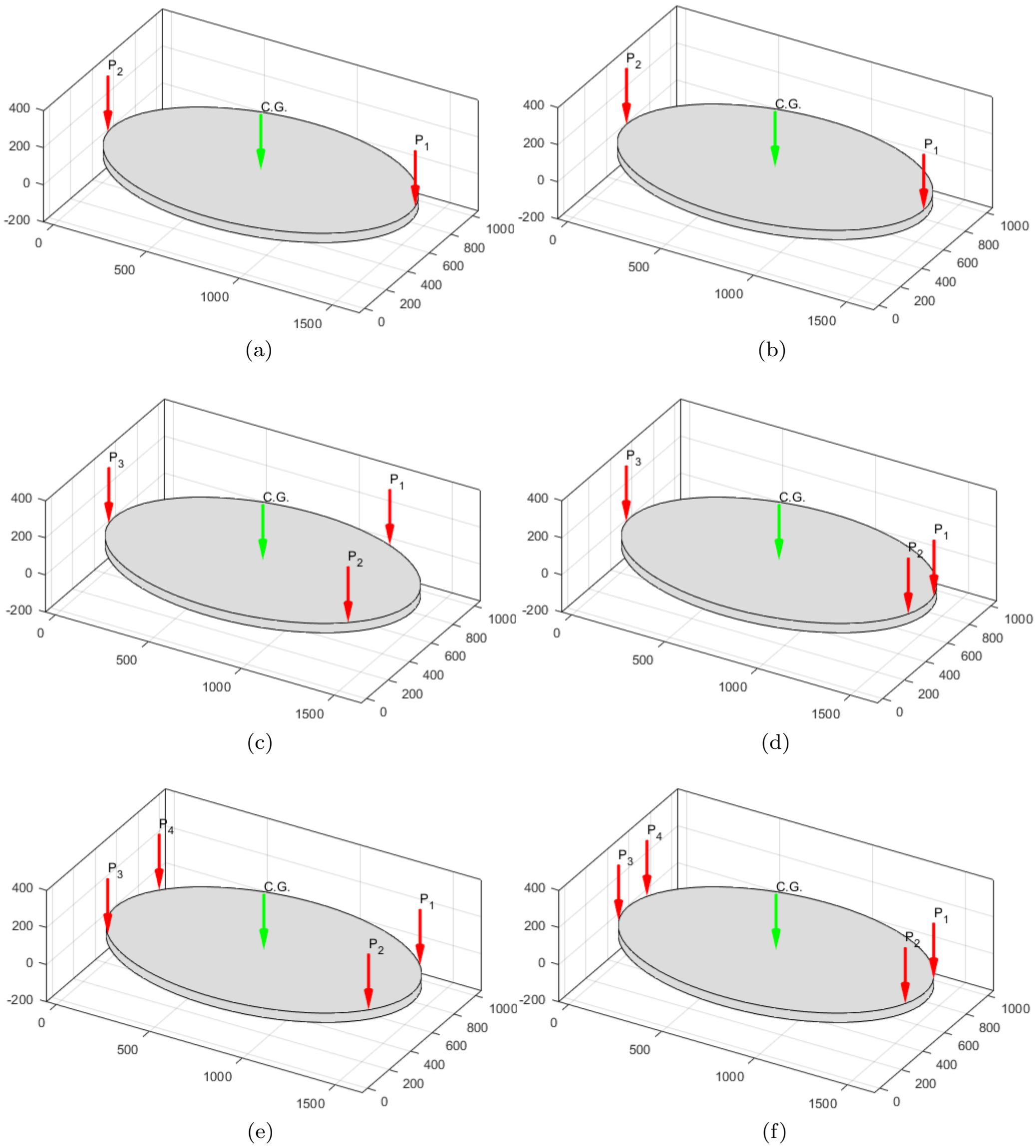

Figure 5.5: Grasp points positions on an ellipse: the results (a), (c) and (e) correspond to the volume maximization for 2, 3 and 4 robots respectively and the results (b), (d) and (f) to the minimum distance maximization for 2, 3 and 4 robots respectively.

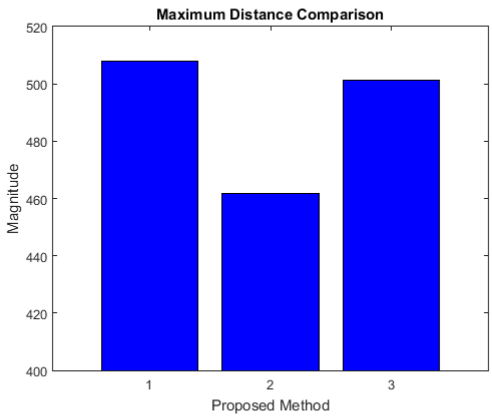

(a) Maximum acceleratin magnitide

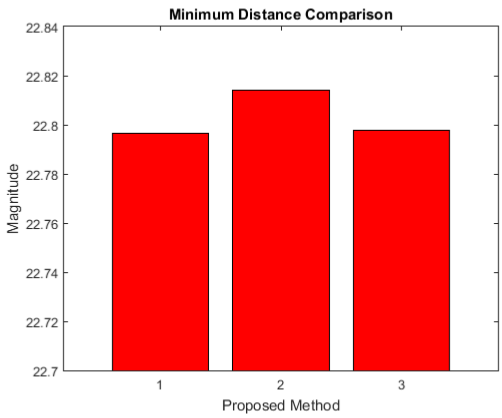

(b) Minimum acceleration magnitude

Figure 5.6: Methods Comparison: Bar-1, Bar-2 and Bar-3 corresponds to the 1st proposed measure, the 2nd proposed measure and to the volume of DME without the proposed constraint respectively.

Chapter 6

Concluding Remarks

6.1 Conclusions

In this work two non-task specific measures for the selection of grasp points on an object are proposed. From the analysis and the simulations presented above we can refer that:

As concerns the 1st proposed measure, which is the maximization of DME's volume with lower performance bound:

- Maximizes the DME in any direction.
- Provides greater highest potential accelerations.
- Short decision time. Suitable for decisions during the operation.
- Guarantees a lower bound in system's performance as concerns the provoked acceleration.
- The results are affected of the different accelerations' orders of magnitude.
- The directions in which the DME is maximized can not be controlled.
- Does not take into account the effect system's weight. As a result the expected results, as concern the potential acceleration, may change.

As concerns the 2nd proposed measure, which is the maximization of the minimum distances in translational and rotational acceleration spaces):

- Guarantees the highest possible worst performance,i.e. high acceleration magnitude and lean energy consumption in the most difficult directions, as concern the translational and rotational acceleration.
- The results are not affected by the different acceleration's order of magnitude.
- More conservative results. Focuses only to the maximization of the worst directions.
- Does not guarantees the maximization of the accelerations with the higher magnitudes.

- Long decision time, suitable for operations that the object's shape is known a priori and the decision can be taken before the operation's beginning.

- The directions that combine translational and rotational part, are not treated in a clear way.

6.2 Issues for Further Research

Generally, the field of grasp planning is offered for further research. As concerns the proposed measures, there are also some issues that are susceptible of improvement, which was not possible in the limited time of this thesis. Firstly, as concerns the assumptions that have been made, it was mentioned that the object is rigidly grasped by each end-effector. An improvement to the presented measures would be the incorporation of the contact modeling [1], which would lead to more reliable results. Another assumption was that the UVMSs used are identical, so the proposed measures should be extended for the case that the UVMSs are of different ability. Finally, in this work it is assumed that each UVMS is aware of the grasp point position that the rest of the UVMSs are intended to grasp (centralized). This is a convenient issue and absolutely realistic when the grasp point selection is done in advance. On the other hand, if the decision is taken during the phase of reaching to grasp, communication issues have to be addressed, so the knowledge of the exact potential grasp point position between the UVMSs might be difficult.

As concerns the proposed measures, for the 1st measure, the effect of the system's weight should be incorporated, so that the ellipsoid, whose volume is maximized, to be the translated one due to the weight. As concerns the 2nd measure, a faster way for the task space decomposition should be implemented by also incorporating the combination of the transnational and rotational acceleration in a clearer way. Another point that can be improved is the way that the two minimum distances, $d_{mintr} \in \mathbb{R}$ and $d_{minrot} \in \mathbb{R}$, are maximized. The weighting method is suggested to be replaced by a no-preference method [21] so that the difference of order of magnitude between the two distances to not affect the result at all.

As concern the decision variables that are used in the proposed optimization schemes, both the grasp point position and the UVMSs' configuration participated. In this way, the solution is affected from the changes in the UVMSs' configuration. This issue could possibly lead to results that reflect the optimal configuration and not the optimal grasp points' position. In order to resolve this problem, it is proposed the configuration to be excluded from the decision variables and for every proposed grasp point set, the optimal configuration to be taken into account for the evaluation of the set. This approach demands the use of enfolded optimizations.

Finally, as concerns the general operation, in this thesis the pick-and-place operation is studied and we dealt with its first phase, the selection of the grasp points. The next step that has to be done is the investigation of the way that the team of the UVMSs will reach the object in order to grasp at the selected grasp points. This could be done in a centralized or in a decentralized way depending on the ease of the communication between the robots.

Appendix A

MATLAB Code

A.1 1st Proposed Measure: Optimization Scheme

In this section of the appendix, the code used for the implementation of the 1st optimization scheme, presented in section 4.1, that corresponds to the 1st proposed measure, is listed.

Let first explain the way that this code works. The code takes as an input the number of the UVMSs that participate in the operation. It also takes as an input the shape and all the geometric and dynamic characteristics of the object as well as its position and orientation with respect to the inertial frame. As it was mentioned in previous chapter, in order to decide the optimal grasp points we do not only use as decision variables the variables concerning the position of the grasp points, but we also have to use the variables correspond to the configuration of each UVMS. The code places the initial grasp points on the object and using the inverse kinematics of the UVMSs, initializes their configuration. In this way we have the optimization's initial point.

As concern the objective function *obj_volume.m*, it takes as input the decision variables. By taking the 1-d variable that corresponds to the i-th grasp point, the function determines the point's position in the 3-d space. This is repeated for all the grasp points. Then the function determines the grasp matrix, the geometric Jacobian of the UVMSs' team and their inertial matrix and consequently the matrix (2.91). Then singular value decomposition is applied as determined in (3.5). Finally, the function computes the volume of the system's DME for the current value of the decision variables.

As concerns the constraints *const_volume.m*, this function takes also as an input the decision variables. By taking the 1-d variable that corresponds to the i-th grasp point, determines the point's position in the 3-d space and the orientation that the end-effector must have in order to grasp at that point. This function also determines the position and the orientation of the end-effector by using the UVMS's forward dynamics. As equality constraints are determined the equality between the position of the grasp point and the permitted orientation at it and the position and the orientation of the end-effector for each grasp point and each corresponding UVMS. In this way, it is guaranteed that the end-effector's position and the grasp point will be identical. After that, the function computes the matrices (2.91) and (2.92) and then sets the inequality constraint concerning the minimum performance (3.11). For the collision avoidance, the function guarantees that each vehicle will not approach each other more a specified distance.

The main code *main.m* and the functions *obj_volume.m* and *const_volume.m* are presented bellow.

```
%% main.m
% selection of grasp points using as grasp quality measure the volume of
% the system's Dynamic Manipulability Ellipsoid
clear all
clc
global gplim_lb gplim_ub
global x_d_first object
global M  R_O2I_wrench R_O2I  di_I
global  T_O2I Po_1 Po_2
global plot_var_fitness plot_obj_tr plot_obj_rot check_vals_mat percent
plot_var_fitness=[];
plot_obj_tr=[];
plot_obj_rot=[];
check_vals_mat=[];
percent=1.1;%
%% Number of UVMSs
M=4;
%% Object's Frame wrt Inertial Frame
Po_1=[0;0;0]; % position of object's frame origin
Po_2=[0;pi;pi/2];% orientation wrt inertial frame
%% Transformations form {O} to {I} frames
R_O2I=eulertoR(Po_2);% rotation matrix from object to inertial frame
T_O2I=Homogen_transf([Po_1;Po_2]);
R_O2I_wrench=[R_O2I zeros(3);zeros(3) R_O2I]; % rotation in wrench space
%% Geometry Recognition
object='rod'; %object's shape
if strcmp(object,'rod')
    rod_geometry;
elseif strcmp(object,'rectangle')
    rect_geometry;
elseif strcmp(object,'circle')
    circle_geometry;
elseif strcmp(object,'ellipse')
    ellipse_geometry;
else
end
%% UVMSs Characteristics
uvms_parameters;
%% Optimal Position and Configuration Search
% grasp points' configuration limits
theta_lb=ones(M,1)*theta_min;
theta_ub=ones(M,1)*theta_max;
%UVMS's configuration limits
q_ub=[];%upper Bound
q_lb=[];%Lower Bound
for i=1:M
    q_ub=[q_ub;gplim_ub];
    q_lb=[q_lb;gplim_lb];
end
%the bounds of the decision variables
ub=[theta_ub;q_ub];
lb=[theta_lb;q_lb];

q_init=[]; % UVMSs' initial configuration
```

```
di_I=[]; % Initial end-effector positions
phi_i=[];% Initial end-effector configuration
for i=1:M
    if strcmp(object,'rod')
        [ P ] = Position_ypol_rod( theta_in(i) );%position
        [ phi ] = Orientation_ypol_rod( theta_in(i) );%orientation
    elseif strcmp(object,'rectangle')
        [ P ] = Position_ypol_rect( theta_in(i) );
        [ phi ] = Orientation_ypol_rect( theta_in(i) );
    elseif strcmp(object,'circle')
        [ P ] = Position_ypol_circle( theta_in(i) );
        [ phi ] = Orientation_ypol_circle( theta_in(i) );
    elseif strcmp(object,'ellipse')
        [ P ] = Position_ypol_ellipse( theta_in(i) );
        [ phi ] = Orientation_ypol_ellipse( theta_in(i) );
    else
    end
    Pi_O=P;
    Pi_I=T_O2I*[Pi_O;0];
    Pi_I=Pi_I(1:3);
    di_I=[di_I Po_1+Pi_I];% position of i-th grasp point from inertial...
    %frame expressed in inertial frame
    phi_i=[phi_i phi];
end

%UVMSs' initial configuration
for i=1:M
    nee1_i=di_I(:,i);
    Ree_o=eulertoR(phi_i(:,i));
    [nee2_i(1,1),nee2_i(2,1),nee2_i(3,1)]=GetEulerAngles_tar(R_O2I*Ree_o);
    x_d_first=[nee1_i;nee2_i];
    q_start=[0;0;0;0;0;0;0;0;pi/3;0];
    q_initial_i=inverse_kinematic_UVMS(q_start);
    q_init=[q_init;q_initial_i];
end

des_var_init=[theta_in;q_init];% initial decision variables

Aeq=[];% linear equality constraints
for i=1:M
    aeq=[0 0 0 1 0 0 0 0 0 0;0 0 0 0 1 0 0 0 0 0];
    Aeq_in=[zeros(2,10*(i-1)) aeq zeros(2,10*(M-i))];
    Aeq=[Aeq;Aeq_in];
end
Aeq=[zeros(2*M,M) Aeq];
beq=zeros(2*M,1);

% optimization
options=optimoptions('fmincon','Display','iter',...
    'Algorithm','sqp','MaxFunEvals',100000000,...
    'MaxIter',1000000,'TolFun',1e-6,'TolX',1e-6,'TolCon',1e-4);
[des_var,fval_tr]=fmincon(@obj_volume,des_var_init,[],[],...
    Aeq,beq,lb,ub,@const_volume,options);
%% Results
if strcmp(object,'rod')
    rod_plots;
elseif strcmp(object,'rectangle')
    rectangle_plots;
elseif strcmp(object,'circle')
    circle_plots;
elseif strcmp(object,'ellipse')
    ellipse_plots;
```

```
else
end
```

```
function [ f ] = obj_volume( des_var )
% The objective function of the proposed optimization scheme that uses as
% grasp quality measure the volume of the Dynamic Manipulability
% Ellipsoid
global T_O2I Po_1 ME R_O2I M Beta weight_mat_torq Gforce
global U S metatopish_tot
global plot_var_fitness  check_vals_mat percent object
R_O2I_big=[R_O2I zeros(3,3);zeros(3,3) R_O2I];
%% Computation of W
ri_I=[];% vector that connects the i-th grasp point with...
        % the center of gravity
di_I=[];% end-effector's position in inertial frame
for i=1:M
    if strcmp(object,'rod')
        [ P ] = Position_ypol_rod( des_var(i) );
    elseif strcmp(object,'rectangle')
        [ P ] = Position_ypol_rect( des_var(i) );
    elseif strcmp(object,'circle')
        [ P ] = Position_ypol_circle( des_var(i) );
    elseif strcmp(object,'ellipse')
        [ P ] = Position_ypol_ellipse( des_var(i) );
    else
    end
    Pi_O=P;
    Pi_I=T_O2I*[Pi_O;0];
    Pi_I=Pi_I(1:3);
    ri_I=[ri_I -Pi_I];% position of object frame from i-th...
    %grasp point expresed in inertial frame
    di_I=[di_I Po_1+Pi_I];% position of i-th grasp point from...
    %inertial frame expressed in inertial frame
end
WW=[];% Grasp Matrix
for i=1:M
    sm=[0 -ri_I(3,i) ri_I(2,i);ri_I(3,i) 0 -ri_I(1,i);...
        -ri_I(2,i)...
        ri_I(1,i) 0];
    W=[eye(3) zeros(3);-sm eye(3)];
    WW=[WW W];
end
%% Configuration
q_i_all=des_var(M+1:size(des_var,1));
BWs=[];
J=[];
M_mat=[];
for i=1:M
    q_i=q_i_all((i-1)*10+1:(i-1)*10+10);% configuration of the i-th UVMS
    [Jg, Ja] = JacUvms_down(q_i);% Jg the geometric Jacobian...
                                 % of the i-th UVMS
    M_i=Mi(q_i);% Inertia matrix of the i-th UVMS
    % The inertia matrix of the cooperative UVMSs
    M_mat=[M_mat zeros(size(M_mat,1),size(M_i,2));...
        zeros(size(M_i,1),size(M_mat,2)) M_i];
    % The Jacobian of the cooperative UVMSs
    J=[J zeros(size(J,1),size(Jg,2));zeros(size(Jg,1),size(J,2)) Jg];

    BWs=[BWs zeros(size(BWs,1),size(Beta*weight_mat_torq,2));...
        zeros(size(Beta*weight_mat_torq,1),size(BWs,2))...
        Beta*weight_mat_torq];
```

```
end
EE=M_mat*pinv(J)*WW'*R_O2I_big+J'*pinv(WW)*inv(R_O2I_big)*ME;
metasx=pinv(EE)*BWs;% the mapping between the control input space...
                    % and the acceleration space
[U,S,V]=svd(metasx);% Singular Value Decomposition
%% Ellispoid's Translation due to Weight
Guvms=[];% Gravitational forces of the cooperative system
for i=1:M
    q_i=q_i_all((i-1)*10+1:(i-1)*10+10);
    [G]= Gi(q_i);% i-th UVMS's gravitational Forces
    Guvms=[Guvms;G];
end
GG=J'*pinv(WW)*inv(R_O2I_big)*Gforce+Guvms;
metatopish_tot=-pinv(EE)*GG; % the translation vector
%% Objective function
d=(2*pi)^3/(2*4*6);
volume=d*S(1,1)*S(2,2)*S(3,3)*S(4,4)*S(5,5)*S(6,6);% Ellipsoid's Volume
f=-volume;
sing_vals=[S(1,1);S(2,2);S(3,3);S(4,4);S(5,5);S(6,6)];
check_vals_mat=[check_vals_mat [sing_vals;min(sing_vals);...
    norm(metatopish_tot)*percent]];
plot_var_fitness=[plot_var_fitness des_var];
end
```

```
function [ c,ceq ] = const_volume( des_var )
% The constraints of the proposed optimization scheme that uses as
% grasp quality measure the volume of the Dynamic Manipulability
% Ellipsoid.
global M T_O2I Po_1 R_O2I equalities r_safe  Gforce
global object percent Beta weight_mat_torq ME
R_O2I_big=[R_O2I zeros(3,3);zeros(3,3) R_O2I];
equalities=zeros(M*6,1);
q_i_all=des_var(M+1:size(des_var,1));
%% Constraints In Position
ri_I=[];% vector that connects the i-th grasp point with...
        % the center of gravity
di_I=[];% end-effector's position in inertial frame
phi_i=[];% end-effector's orientation
safe_ineq=[];
for i=1:M
    if strcmp(object,'rod')
        [ P ] = Position_ypol_rod( des_var(i) );
        [ phi ] = Orientation_ypol_rod( des_var(i) );
    elseif strcmp(object,'rectangle')
        [ P ] = Position_ypol_rect( des_var(i) );
        [ phi ] = Orientation_ypol( des_var(i) );
    elseif strcmp(object,'circle')
        [ P ] = Position_ypol_circle( des_var(i) );
        [ phi ] = Orientation_ypol_circle( des_var(i) );
    elseif strcmp(object,'ellipse')
        [ P ] = Position_ypol_ellipse( des_var(i) );
        [ phi ] = Orientation_ypol_ellipse( des_var(i) );
    else
    end
    Pi_O=P;
    Pi_I=T_O2I*[Pi_O;0];
    Pi_I=Pi_I(1:3);
    ri_I=[ri_I -Pi_I];% position of object frame from i-th grasp
                      % point expresed in inertial frame
    di_I=[di_I Po_1+Pi_I];% position of i-th grasp point from
                          % inertial frame expressed in inertial frame
```

```
    phi_i=[phi_i phi];
end
for i=1:M
    % the following equality constraints guarantee that the position
    % of the i-th end-effector coincides with the i-th grasp point
    % and the orientation of the i-th end-effector's frame is the
    % allowed one depending on the position of the grasp point and
    % the object's shape

    q_i=q_i_all((i-1)*10+1:(i-1)*10+10);% configuration of the i-th UVMS
    [ p_i] = Forward_kin_UVMS( q_i);% corresponding end-effector's
                                    % position
    nee1_i=di_I(:,i);
    Ree2o=eulertoR(phi_i(:,i));
    [nee22(1,1),nee22(2,1),nee22(3,1)]=GetEulerAngles_tar(R_O2I*Ree2o);
    equalities((i-1)*6+1:(i-1)*6+6)=[p_i(1:3)-nee1_i;p_i(4:6)-nee22];

    % collision avoidance between the UVMSs
    pos_veh_i=q_i(1:3);
    for j=i+1:M
        q_j=q_i_all((j-1)*10+1:(j-1)*10+10);
        pos_veh_j=q_j(1:3);
        safe_ineq=[safe_ineq;2*r_safe-norm(pos_veh_i-pos_veh_j)];
    end
end
%% Constraint for the lower bound of the system's performance
%computation of Wi
WW=[];% Grasp matrix
for i=1:M
    sm=[0 -ri_I(3,i) ri_I(2,i);ri_I(3,i) 0 -ri_I(1,i);...
        -ri_I(2,i)...
        ri_I(1,i) 0];
    W=[eye(3) zeros(3);-sm eye(3)];
    WW=[WW W];
end
BWs=[];
J=[];
M_mat=[];
for i=1:M
    q_i=q_i_all((i-1)*10+1:(i-1)*10+10);% configuration of the i-th UVMS
    [Jg, Ja] = JacUvms_down(q_i);% Jg the geometric Jacobian
                                 % of the i-th UVMS
    M_i=Mi(q_i);% Inertia matrix of the i-th UVMS
    % The inertia matrix of the cooperative UVMSs
    M_mat=[M_mat zeros(size(M_mat,1),size(M_i,2));zeros(size(M_i,1),...
        size(M_mat,2)) M_i];
    % The Jacobian of the cooperative UVMSs
    J=[J zeros(size(J,1),size(Jg,2));zeros(size(Jg,1),size(J,2)) Jg];
    BWs=[BWs zeros(size(BWs,1),size(Beta*weight_mat_torq,2));...
        zeros(size(Beta*weight_mat_torq,1),size(BWs,2))...
        Beta*weight_mat_torq];
end
EE=M_mat*pinv(J)*WW'*R_O2I_big+J'*pinv(WW)*inv(R_O2I_big)*ME;
metasx=pinv(EE)*BWs;% the mapping between the control input space
                    % and the acceleration space
[U,S,V]=svd(metasx);

% Ellispoid's Translation due to Weight
Guvms=[];
for i=1:M
    q_i=q_i_all((i-1)*10+1:(i-1)*10+10);
    [G]= Gi(q_i);% i-th UVMS's gravitational Forces
```

```
    Guvms=[Guvms;G];
end
GG=J'*pinv(WW)*inv(R_O2I_big)*Gforce+Guvms;
metatopish_tot=-pinv(EE)*GG;% the translation vector
sing_vals=[S(1,1);S(2,2);S(3,3);S(4,4);S(5,5);S(6,6)];

% inequality constraints for the lower performance bound. The minimum
% singular value must be greater equal to the norm of the vector of the
% ellipsoid's translation multiplied with a safety factor guaranteeing
% higher minimum performance
grav_ineq=percent*norm(metatopish_tot)-min(sing_vals);
%% output
c=[safe_ineq;grav_ineq];
ceq=equalities;
end
```

A.2 2nd Proposed Measure: Optimization Scheme

In this section of the appendix the code used for the 2nd optimization scheme, presented in section 4.2, that corresponds to the 2nd proposed measure, is listed.

The main code *main.m* has more or less the same structure with the one presented for the 1st optimization scheme. The main difference between the two codes is detected in the objective function *obj_min_dist.m* since they refer to different grasp quality measures. The function takes as an input the decision variables. By taking the 1-d variable that corresponds to the i-th grasp point, the function determines the point's position in the 3-d space. This is repeated for all the grasp points. Then the function determines the grasp matrix, the geometric Jacobian of the UVMSs' team and their inertial matrix and consequently the matrix (2.91). Then singular value decomposition is applied as determined in (3.5). In the sequel, the function determines the position vector of the translated frame due to the system's weight, $\{a'\}$, with respect to the frame $\{a\}$ (3.12). After that, the function decomposes the system's DME in order to create the translational and the rotational acceleration space. Assuming that we are interested in the creation of the translational acceleration space. Let a direction of the translational acceleration in the 3d space. The function creates the 6d acceleration combining the desired translational acceleration and a rotational acceleration creating the desired acceleration in the 6-d task space. In this direction calculates the distance between the translated, due to weight, DME's center and the ellipsoid's surface. This distance is projected in the translational acceleration space. The same procedure for the desired translational acceleration is repeated for every possible rotational acceleration direction. The maximum value of the projection is saved. This is repeated for every direction of the translational acceleration. In this way, the translational acceleration space is created. The same procedure is followed for the rotational acceleration space. Then the minimum distance in these two spaces is determined. Finally, the two resulting values, multiplied with a weighting factor, are added. The resulting quantity is the one that the optimization maximizes.

As concerns the constraints of the optimization scheme *const_min_dist.m*, they are the same with the constraints presented for the 1st measure, excluding the one concerning the bound in the minimum performance (3.11) which is not required.

The aforementioned main code *main.m* and the functions *obj_min_dist.m* and *const_min_dist.m* are presented bellow.

```
%% main.m
% selection of grasp points using as grasp quality measure the minimum
% distance in the translational and rotational acceleration space as
% exerted from the system's Dynamic Manipulability Ellipsoid
clear all
clc
global gplim_lb gplim_ub
global x_d_first object
global M  R_O2I_wrench R_O2I  di_I
global  T_O2I Po_1 Po_2 direction_matrix
global plot_var_fitness plot_obj_tr plot_obj_rot check_vals_mat percent
plot_var_fitness=[];
plot_obj_tr=[];
plot_obj_rot=[];
check_vals_mat=[];
percent=1.1;%
%% Number of UVMSs
M=4;
%% Object's Frame wrt Inertial Frame
Po_1=[0;0;0]; % position of object's frame origin
Po_2=[0;pi;pi/2];% orientation wrt inertial frame
%% Transformations form {O} to {I} frames
R_O2I=eulertoR(Po_2);% rotation matrix from object to inertial frame
T_O2I=Homogen_transf([Po_1;Po_2]);
R_O2I_wrench=[R_O2I zeros(3);zeros(3) R_O2I]; % rotation in wrench space
%% Acceleration space
% the 6-d acceleration space is created by unitary acceleration vectors
% translational rotational or combination of them
diakr=pi/4;% sparcity of the acceleration space
[ space_mat ] = space_constr_3d( diakr );
direction_matrix=space_mat;
%% Geometry Recognition
object='rod'; %object's shape
if strcmp(object,'rod')
    rod_geometry;
elseif strcmp(object,'rectangle')
    rect_geometry;
elseif strcmp(object,'circle')
    circle_geometry;
elseif strcmp(object,'ellipse')
    ellipse_geometry;
else
end
%% UVMSs Characteristics
uvms_parameters;
%% Optimal Position and Configuration Search
% grasp points' configuration limits
theta_lb=ones(M,1)*theta_min;
theta_ub=ones(M,1)*theta_max;
%UVMS's configuration limits
q_ub=[];%upper Bound
q_lb=[];%Lower Bound
for i=1:M
    q_ub=[q_ub;gplim_ub];
    q_lb=[q_lb;gplim_lb];
end
%the bounds of the decision variables
ub=[theta_ub;q_ub];
```

```
lb=[theta_lb;q_lb];

q_init=[]; % UVMSs' initial configuration
di_I=[]; % Initial end—effector positions
phi_i=[];% Initial end—effector configuration
for i=1:M
    if strcmp(object,'rod')
        [ P ] = Position_ypol_rod( theta_in(i) );%position
        [ phi ] = Orientation_ypol_rod( theta_in(i) );%orientation
    elseif strcmp(object,'rectangle')
        [ P ] = Position_ypol_rect( theta_in(i) );
        [ phi ] = Orientation_ypol_rect( theta_in(i) );
    elseif strcmp(object,'circle')
        [ P ] = Position_ypol_circle( theta_in(i) );
        [ phi ] = Orientation_ypol_circle( theta_in(i) );
    elseif strcmp(object,'ellipse')
        [ P ] = Position_ypol_ellipse( theta_in(i) );
        [ phi ] = Orientation_ypol_ellipse( theta_in(i) );
    else
    end
    Pi_O=P;
    Pi_I=T_O2I*[Pi_O;0];
    Pi_I=Pi_I(1:3);
    di_I=[di_I Po_1+Pi_I];% position of i—th grasp point from inertial...
    %frame expressed in inertial frame
    phi_i=[phi_i phi];
end

%UVMSs' initial configuration
for i=1:M
    nee1_i=di_I(:,i);
    Ree_o=eulertoR(phi_i(:,i));
    [nee2_i(1,1),nee2_i(2,1),nee2_i(3,1)]=GetEulerAngles_tar(R_O2I*Ree_o);
    x_d_first=[nee1_i;nee2_i];
    q_start=[0;0;0;0;0;0;0;0;pi/3;0];
    q_initial_i=inverse_kinematic_UVMS(q_start);
    q_init=[q_init;q_initial_i];
end

des_var_init=[theta_in;q_init];% initial decision variables

Aeq=[];% linear equality constraints
for i=1:M
    aeq=[0 0 0 1 0 0 0 0 0 0;0 0 0 0 1 0 0 0 0 0];
    Aeq_in=[zeros(2,10*(i—1)) aeq zeros(2,10*(M—i))];
    Aeq=[Aeq;Aeq_in];
end
Aeq=[zeros(2*M,M) Aeq];
beq=zeros(2*M,1);

% optimization
    options=optimoptions('fmincon','Display','iter',...
        'Algorithm','sqp','MaxFunEvals',100000000,...
        'MaxIter',1000000,'TolFun',1e—6,'TolX',1e—6,'TolCon',1e—4);
    [des_var,fval_tr]=fmincon(@obj_min_dist,des_var_init,[],[],...
        Aeq,beq,lb,ub,@const_min_dist,options);
%% Results
if strcmp(object,'rod')
    rod_min_dist_plots;
elseif strcmp(object,'rectangle')
    rectangle_min_dist_plots;
elseif strcmp(object,'circle')
```

```
    circle_min_dist_plots;
elseif strcmp(object,'ellipse')
    ellipse_min_dist_plots;
else
end
```

```
function [ f ] = obj_min_dist( des_var )
% The objective function of the proposed optimization scheme that uses as
% grasp quality measure the minimum distance in the translational and
% rotational acceleration space as exerted from the system's
% Dynamic Manipulability Ellipsoid
global T_O2I Po_1 ME R_O2I M Beta weight_mat_torq Gforce
global direction_matrix object
global U S metatopish_tot
global plot_var_fitness plot_obj_tr plot_obj_rot
R_O2I_big=[R_O2I zeros(3,3);zeros(3,3) R_O2I];
%% Computation of W
ri_I=[];% vector that connects the i-th grasp point with...
% the center of gravity
di_I=[];% end-effector's position in inertial frame
for i=1:M
    if strcmp(object,'rod')
        [ P ] = Position_ypol_rod( des_var(i) );
    elseif strcmp(object,'rectangle')
        [ P ] = Position_ypol_rect( des_var(i) );
    elseif strcmp(object,'circle')
        [ P ] = Position_ypol_circle( des_var(i) );
    elseif strcmp(object,'ellipse')
        [ P ] = Position_ypol_ellipse( des_var(i) );
    else
    end
    Pi_O=P;
    Pi_I=T_O2I*[Pi_O;0];
    Pi_I=Pi_I(1:3);
    ri_I=[ri_I -Pi_I];% position of object frame from i-th...
    %grasp point expresed in inertial frame
    di_I=[di_I Po_1+Pi_I];% position of i-th grasp point from...
    %inertial frame expressed in inertial frame
end
WW=[];% Grasp Matrix
for i=1:M
    sm=[0 -ri_I(3,i) ri_I(2,i);ri_I(3,i) 0 -ri_I(1,i);...
        -ri_I(2,i)...
        ri_I(1,i) 0];
    W=[eye(3) zeros(3);-sm eye(3)];
    WW=[WW W];
end
%% Configuration
q_i_all=des_var(M+1:size(des_var,1));
BWs=[];
J=[];
M_mat=[];
for i=1:M
    q_i=q_i_all((i-1)*10+1:(i-1)*10+10);% configuration of the i-th UVMS
    [Jg, Ja] = JacUvms_down(q_i);% Jg the geometric Jacobian...
    % of the i-th UVMS
    M_i=Mi(q_i);% Inertia matrix of the i-th UVMS
    % The inertia matrix of the cooperative UVMSs
    M_mat=[M_mat zeros(size(M_mat,1),size(M_i,2));...
        zeros(size(M_i,1),size(M_mat,2)) M_i];
    % The Jacobian of the cooperative UVMSs
```

```
    J=[J zeros(size(J,1),size(Jg,2));zeros(size(Jg,1),size(J,2)) Jg];

    BWs=[BWs zeros(size(BWs,1),size(Beta*weight_mat_torq,2));...
        zeros(size(Beta*weight_mat_torq,1),size(BWs,2))...
        Beta*weight_mat_torq];
end
EE=M_mat*pinv(J)*WW'*R_O2I_big+J'*pinv(WW)*inv(R_O2I_big)*ME;
metasx=pinv(EE)*BWs;% the mapping between the control input space...
% and the acceleration space
[U,S,V]=svd(metasx);% Singular Value Decomposition
%% Ellispoid's Translation due to Weight
Guvms=[];% Gravitational forces of the cooperative system
for i=1:M
    q_i=q_i_all((i-1)*10+1:(i-1)*10+10);
    [G]= Gi(q_i);% i-th UVMS's gravitational Forces
    Guvms=[Guvms;G];
end
GG=J'*pinv(WW)*inv(R_O2I_big)*Gforce+Guvms;
metatopish_tot=-pinv(EE)*GG; % the translation vector
%% Acceleration space
% The Dynamic Manipulability Ellipsoid is decomposed into translational
% and rotational acceleration spaces

feasible_space_transl=zeros(size(direction_matrix,1),3);
feasible_space_rot=zeros(size(direction_matrix,1),3);
direct=direction_matrix;% the directions of the task space which are
                        % identical to the 6-d acceleration space
SSconv=zeros(6,1);
for ii=1:6
    SSconv(ii,1)=S(ii,ii);
end
UUconv=U';
UUconv=UUconv(:);
priv=[UUconv;SSconv;metatopish_tot];
dist_transl=zeros(size(direction_matrix,1),1);
dist_rot=zeros(size(direction_matrix,1),1);

parfor(i=1:size(direct,1),4)
% the direction of interest in translational space
translational_direction=direct(i,:)';
% the direction of interest in rotational space
rotational_direction=direct(i,:)';
max_transl_proj=0;
max_rot_proj=0;
for j=1:size(direct,1)
    % the direction in rotational space to be combined with
    % the translational
    rotational_direction_for_tr=direct(j,:)';
    % h ypopsifia pio epibaryntikh translational thn rotational
    translational_direction_for_rot=direct(j,:)';
    for theta_comb=0:pi/16:pi/2
        % Projection on the translational acceleration space
        direction_6d_for_tr=[translational_direction*...
            cos(theta_comb);rotational_direction_for_tr*...
            sin(theta_comb)];% The direction of interest in the 6-d
                             % space
        P_odot_dist_tr=[direction_6d_for_tr;priv];
        % The distance from the center to the surface is
        [ P_dist ] = distance_from_weighted_point_par( P_odot_dist_tr);
        % The projection in the translational acceleration space
        projection2transl_dir=dot(P_dist*direction_6d_for_tr,...
            [translational_direction;0;0;0])/...
```

```
            norm(translational_direction);
        % Search for the maximum projection
        if max_transl_proj<=projection2transl_dir
            max_transl_proj=projection2transl_dir;
        end

        % projection on the rotational acceleration space
        direction_6d_for_rot=[translational_direction_for_rot*...
            sin(theta_comb);...
            rotational_direction*cos(theta_comb)];% The direction of
                                                 % interest in the 6-d
                                                 % space
        P_odot_dist_rot=[direction_6d_for_rot;priv];
        % The distance from the center to the surface in the desired
        % direction is:
        [ P_dist ] = distance_from_weighted_point_par( P_odot_dist_rot);
        projection2rot_dir=dot(P_dist*direction_6d_for_rot,...
            [0;0;0;rotational_direction])/norm(rotational_direction);
        % Search for the maximum projection
        if max_rot_proj<=projection2rot_dir
            max_rot_proj=projection2rot_dir;
        end
    end
end
dist_transl(i)=max_transl_proj;
dist_rot(i)=max_rot_proj;
end

%% Minimum distance in translational acceleration space
norm_tr_min=min(dist_transl);%
f_tr=-norm_tr_min;

%%  Minimum distance in rotational acceleration space
norm_rot_min=min(dist_rot);
f_rot=-norm_rot_min;
%% Weighted sum objective function
w=0.5;
f=(1-w)*f_tr+w*f_rot;% the objective function
plot_var_fitness=[plot_var_fitness des_var];
plot_obj_tr=[plot_obj_tr;-f_tr];
plot_obj_rot=[plot_obj_rot;-f_rot];

end
```

```
function [ c,ceq ] = const_min_dist( des_var )
% The constraints of the proposed optimization scheme that uses as
% grasp quality measure the minimum distance in the translational
% and rotational acceleration space as exerted from the system's
% Dynamic Manipulability Ellipsoid
global M T_O2I Po_1 R_O2I equalities r_safe
global object
R_O2I_big=[R_O2I zeros(3,3);zeros(3,3) R_O2I];
equalities=zeros(M*6,1);
q_i_all=des_var(M+1:size(des_var,1));
%% Constraints In Position
ri_I=[];% vector that connects the i-th grasp point with...
        % the center of gravity
di_I=[];% end-effector's position in inertial frame
phi_i=[];% end-effector's orientation
safe_ineq=[];
for i=1:M
```

```
    if strcmp(object,'rod')
        [ P ] = Position_ypol_rod( des_var(i) );
        [ phi ] = Orientation_ypol_rod( des_var(i) );
    elseif strcmp(object,'rectangle')
        [ P ] = Position_ypol_rect( des_var(i) );
        [ phi ] = Orientation_ypol( des_var(i) );
    elseif strcmp(object,'circle')
        [ P ] = Position_ypol_circle( des_var(i) );
        [ phi ] = Orientation_ypol_circle( des_var(i) );
    elseif strcmp(object,'ellipse')
        [ P ] = Position_ypol_ellipse( des_var(i) );
        [ phi ] = Orientation_ypol_ellipse( des_var(i) );
    else
    end
    Pi_O=P;
    Pi_I=T_O2I*[Pi_O;0];
    Pi_I=Pi_I(1:3);
    ri_I=[ri_I -Pi_I];% position of object frame from i-th grasp...
                      % point expresed in inertial frame
    di_I=[di_I Po_1+Pi_I];% position of i-th grasp point from...
                          % inertial frame expressed in inertial frame
    phi_i=[phi_i phi];
end
for i=1:M
    % the following equality constraints guarantee that the position
    % of the i-th end-effector coincides with the i-th grasp point
    % and the orientation of the i-th end-effector's frame is the
    % allowed one depending on the position of the grasp point and
    % the object's shape

    q_i=q_i_all((i-1)*10+1:(i-1)*10+10);% configuration of the i-th UVMS
    [ p_i] = Forward_kin_UVMS( q_i);% corresponding end-effector's
                                    % position
    nee1_i=di_I(:,i);
    Ree2o=eulertoR(phi_i(:,i));
    [nee22(1,1),nee22(2,1),nee22(3,1)]=GetEulerAngles_tar(R_O2I*Ree2o);
    equalities((i-1)*6+1:(i-1)*6+6)=[p_i(1:3)-nee1_i;p_i(4:6)-nee22];

    % collision avoidance between the UVMSs
    pos_veh_i=q_i(1:3);
    for j=i+1:M
        q_j=q_i_all((j-1)*10+1:(j-1)*10+10);
        pos_veh_j=q_j(1:3);
        safe_ineq=[safe_ineq;2*r_safe-norm(pos_veh_i-pos_veh_j)];
    end
end
c=safe_ineq;
ceq=equalities;
end
```

A.3 Shared Code

In this section of the appendix, the scripts of code that the two previously presented schemes share, are presented. As it was mentioned before, for the grasp points' position a one-variable representation is used. In order to transform the one-variable representation into a point in 3d space, a proper function for each object shape is used. The functions *Position_ypol_rod.m*, *Position_ypol_rect.m*, *Position_ypol_circle.m* and *Position_ypol_ellipse.m* are used in order to transform the 1d variable into 3d point on a rod, a rectangle, a circle and an ellipse respectively. As concern the permitted orientation that the end-effector must have in order to grasp a certain grasp point, the following functions are used in order to transform the variable that refers to the grasp point in the end-effector's permitted orientation. These functions are *Orientation_ypol_rod.m*, *Orientation_ypol_rect.m*, *Orientation_ypol_circle.m* and *Orientation_ypol_ellipse.m* and correspond to the permitted orientations on a rod, a rectangle, a circle and an ellipse respectively.

Finally in the script *uvms_parameters.m*, the UVMS's characteristics, as concern the position of the manipulator on the vehicle, the length of the manipulator's links, the configuration limits and the torque limits, are determined.

The aforementioned functions are presented bellow:

```
function [ P ] = Position_ypol_rod( lamda )
% Takes as an input the 1-d variable that determines the position on the
% object and gives the actual position of the grasp point in the 3d space
global rod_d L
Pref=rod_d*L*lamda;
P=Pref-[0;L/2;0];
end
```

```
function [ P ] = Position_ypol_rect( theta )
% Takes as an input the 1-d variable that determines the position on the
% object and gives the actual position of the grasp point in the 3d space
global thetaA thetaB thetaC thetaD H L
if theta>=thetaD ||theta<=thetaA
    x=H/2;
    y=tan(theta)*x;
    P=[x;y;0];
elseif theta>=thetaA && theta<=thetaB
    y=L/2;
    x=-tan(theta-pi/2)*y;
    P=[x;y;0];
elseif theta>=thetaB && theta<=thetaC
    x=-H/2;
    y=tan(theta-pi)*x;
    P=[x;y;0];
else
    y=-L/2;
    x=-tan(theta-3*pi/2)*y;
    P=[x;y;0];
end
end
```

```
function [ P ] = Position_ypol_circle( theta )
% Takes as an input the 1-d variable that determines the position on the
% object and gives the actual position of the grasp point in the 3d space
global Rakt
x=Rakt*cos(theta);
y=Rakt*sin(theta);
P=[x;y;0];
end
```

```
function [ P ] = Position_ypol_ellipse( theta )
% Takes as an input the 1-d variable that determines the position on the
% object and gives the actual position of the grasp point in the 3d space
global alpha be
x=alpha*cos(theta);
y=be*sin(theta);
P=[x;y;0];
end
```

```
function [ phi ] = Orientation_ypol_rod( lamda )
% Takes as an input the variable that determines the position on the
% object and gives the orientation that the end-effector of the UVMS
% must have in order to grasp at that position
phi=[0;-pi/2;0];
end
```

```
function [ phi ] = Orientation_ypol_rect( theta )
% Takes as an input the variable that determines the position on the
% object and gives the orientation that the end-effector of the UVMS
% must have in order to grasp at that position
global thetaA_b thetaA_a thetaB_b thetaB_a thetaC_b thetaC_a thetaD_b
global thetaD_a
phiDA=[0 3*pi/2 0]';
phiAB=[0 3*pi/2 pi/2]';
phiBC=[0 3*pi/2 pi]';
phiCD=[0 3*pi/2 3*pi/2]';
if theta>=thetaD_a || theta<=thetaA_b
    phi=phiDA;
elseif theta>=thetaA_b && theta<=thetaA_a
    phi=phiDA+(phiAB-phiDA)/(thetaA_a-thetaA_b)*(theta-thetaA_b);
elseif theta>=thetaA_a && theta<=thetaB_b
    phi=phiAB;
elseif theta>=thetaB_b && theta<=thetaB_a
    phi=phiAB+(phiBC-phiAB)/(thetaB_a-thetaB_b)*(theta-thetaB_b);
elseif theta>=thetaB_a && theta<=thetaC_b
    phi=phiBC;
elseif theta>=thetaC_b && theta<=thetaC_a
    phi=phiBC+(phiCD-phiBC)/(thetaC_a-thetaC_b)*(theta-thetaC_b);
elseif theta>=thetaC_a && theta<=thetaD_b
    phi=phiCD;
else
    phiCD=[0 3*pi/2 -pi/2]';
    phi=phiCD+(phiDA-phiCD)/(thetaD_a-thetaD_b)*(theta-thetaD_b);
end
end
```

```
function [ phi ] = Orientation_ypol_circle( theta )
% Takes as an input the variable that determines the position on the
% object and gives the orientation that the end-effector of the UVMS
% must have in order to grasp at that position
phi=[0;3*pi/2;theta];
end
```

```
function [ phi ] = Orientation_ypol_ellipse( theta )
```

```
% Takes as an input the variable that determines the position on the
% object and gives the orientation that the end-effector of the UVMS
% must have in order to grasp at that position
global alpha be
x_T=-(alpha*sin(theta))/sqrt(be^2*(cos(theta))^2+alpha^2*(sin(theta))^2);
y_T=(be*cos(theta))/sqrt(be^2*(cos(theta))^2+alpha^2*(sin(theta))^2);
tangent=[x_T;y_T;0];
strof=atan2(tangent(2),tangent(1));
if strof<0
    strof=2*pi+strof;
end
phi=[0;3*pi/2;strof-pi/2];
end
```

```
%% uvms_parameters.m
% contains the characteristics of the UVMS
global x_v y_v z_v phi_v th_v psi_v L1 L2 L3 L4 L5
global u_lim_lb u_lim_ub gplim_lb gplim_ub
global Beta weight_mat_torq r_safe
% position and orientation of the manipulator base frame(0) relative
% to vehicle body-fixed frame(B)
x_v = 0.16; y_v = 0; z_v = 0.09;
phi_v = 0; th_v = 0; psi_v = 0;

L1 = 77.8*10^-3; %meter
L2 = 2.2*10^-3;
L3 = 147.69*10^-3;
L4 = 28*10^-3;
L5 = 75.4*10^-3;
% actuators' limits
u_lim_lb=[-15;-15;-15;-15;-5;-5;-5;-5];
u_lim_ub=[15;15;15;15;5;5;5;5];
%joints position limits
gplim_lb = [ -30 , -30 , -30 , -pi/18 , -pi/18 , -2*pi ,...
    -2*pi , -2*pi, -2*pi , -2*pi]';   % lower bounds of q
gplim_ub = [ 30 , 30 , 30 , pi/18 , pi/18 , 2*pi , 2*pi ,...
    2*pi , 2*pi , 2*pi]';   % upper bounds of q
% Thruster Control Matrix
Bv=[1 1 0 0;0 0 1 0;0 0 0 1;0 0 0 0;0 0 0 0;0.0475 -0.0475 -0.05 0];
Beta=[Bv zeros(6,4);zeros(4,4) eye(4)];
weight_mat_torq=100*diag([10 10 10 10 5 5 5 5]);
% radius of a sphere containing the vehicle used for collision avoidance
r_safe=0.2;
```

Bibliography

[1] B. Siciliano and O. Khatib, *Springer Handbook of Robotics.*

[2] E. Papadopoulos and J. Poulakakis, “Trajectory planning and control for mobile manipulator systems,”

[3] T. Fossen, *Guidance and Control of Ocean Vehicles.* New York, NY: Wiley, 1995.

[4] G. Antonelli, *Underwater Robots*, vol. 96 of *Springer Tracts in Advanced Robotics.* Springer, 2014.

[5] I. Schjølberg and T. I. Fossen, “Modelling and control of underwater vehicle-manipulator systems,” pp. 45–57, 1994.

[6] C. I. G. Chinelato and L. D. S. Martins-Filho, “Cooperative multiple mobile manipulators transporting a common payload: an integrated approach,” 2013.

[7] T. Yoshikawa, *Foundations of Robotics: Analysis and Control.* East European Monographs; 279, MIT Press, 1990.

[8] T. Yoshikawa, “Manipulability of robotic mechanisms,” *The International Journal of Robotics Research*, vol. 4, no. 2, pp. 3–9, 1985.

[9] B. Siciliano, L. Sciavicco, L. Villani, and G. Oriolo, “Robotics: modelling, planning and control,” 2010.

[10] M. Uchiyama and P. Dauchez, “Symmetric kinematic formulation and non-master/slave coordinated control of two-arm robots,” *Advanced Robotics*, vol. 7, no. 4, pp. 361–383, 1992.

[11] F. Cheraghpour, S. A. A. Moosavian, and A. Nahvi, “Multiple aspect grasp performance index for cooperative object manipulation tasks,” pp. 386–391, 2009.

[12] T. Yoshikawa, M. Kurisu, and T. Kozuka, “Deciding grasping positions and regrasping action by cooperating multiple mobile robots,”

[13] J. Sasaki, J. Ota, E. Yoshida, D. Kurabayashi, and T. Arai, “Cooperating grasping of a large object by multiple mobile robots,” vol. 1, 1995.

[14] S. L. Chiu, “Task compatibility of manipulator postures,” *The International Journal of Robotics Research*, vol. 7, no. 5, pp. 13–21, 1988.

[15] Z. Li and S. S. Sastry, "Task-oriented optimal grasping by multifingered robot hands," *IEEE Journal on Robotics and Automation*, vol. 4, no. 1, 1988.

[16] C. Ferrari and J. Canny, "Planning optimal grasps," *Proceedings 1992 IEEE International Conference on Robotics and Automation*, 1992.

[17] T. Watanabe and T. Yoshikawa, "Grasping optimization using a required external force set," *IEEE Transactions on Automation Science and Engineering*, vol. 4, 2007.

[18] M. R. Raul Suarez and J. Cornella, "Grasp quality measures," 2006.

[19] P. Chiacchio, S. Chiaverini, L. Sciavicco, and B. Siciliano, "Reformulation of dynamic manipulability ellipsoid for robotic manipulators," pp. 2192–2197 vol.3, 1991.

[20] P. Chiacchio, S. Chiaverini, L. Sciavicco, and B. Siciliano, "Reformulation of dynamic manipulability ellipsoid for robotic manipulators,"

[21] K. Miettinen, *Nonlinear Multiobjective Optimization.* Springer US, 1998.